

HILLSLOPE HYDROLOGICAL PROCESSES IN A COSTA RICAN RAINFOREST:  
WATER SUPPLY PARTITIONING USING ISOTOPE TRACERS

A Thesis

by

ANDREA LYN DUMONT

Submitted to the Office of Graduate and Professional Studies of  
Texas A&M University  
in partial fulfillment of the requirements for the degree of

MASTER OF SCIENCE

Chair of Committee,	Gretchen Miller
Committee Members,	Anthony Cahill
	Brendan Roark
Head of Department,	Robin Autenrieth

May 2014

Major Subject: Civil Engineering

Copyright 2014 Andrea Lyn DuMont

## ABSTRACT

Costa Rican tropical premontane rainforests are among the world's most valuable ecosystems in terms of diversity of animals, plants, and natural resources. These environments are dependent on water resources which fluctuate in quantity during the dry and wet seasons and which are significantly influenced by vegetation feedbacks. Currently, tropical premontane forest watersheds are insufficiently characterized in terms of groundwater and stream water interactions due to their limited accessibility and complex geological conditions. However, water produced from these watersheds is a critical renewable resource in Costa Rica. It plays a significant role in the production of downstream hydropower and acts as a supply for water distribution systems in many rural areas.

In this study, stable isotope tracing of  $\delta^{18}\text{O}$  and  $\delta\text{D}$  was used to determine the source of water in a stream, and the relative contributions of water budget components (e.g., groundwater, soil water). Samples were collected beginning in the dry season and continuing through the wet season from 2013-2014 as the soil became progressively wetter. The  $\delta^{18}\text{O}$  and  $\delta\text{D}$  samples represent precipitation in the tropical forest, as well as groundwater, soil water, and stream water at several locations. This data is important to understanding the influence of vegetation and hydrogeological properties on groundwater and stream water in tropical headwater catchments.

Streamflow averaged  $0.06 \text{ m}^3/\text{min}$  in baseflow and greater than  $0.10 \text{ m}^3/\text{min}$  during storms. Groundwater was seen to contribute to 80% of streamflow and was the

main stream component even during storm events. A small proportion of the total amount of streamflow came from interflow and soil water (1%).

Additional findings indicated that precipitation, about 4200 mm/yr, in the rainforest can be recycled source water. Storm tracks alternate from distribution starting in the Pacific Ocean to the Caribbean Sea over the course of the wet season. Overall precipitation was seen to be dominated by deep convection and enhanced during the wet season due to the North American Monsoon and the Intertropical Convergence Zone.

## DEDICATION

I dedicate this thesis to my family: Mom, Dad, Brianna, Devin, and Zela (my cat) who faithfully slept through the entire writing of my thesis.

## ACKNOWLEDGEMENTS

I would like to give my appreciation to my committee chair, Dr. Gretchen Miller, my committee members, Dr. Tony Cahill and Dr. Brendan Roark, as well as Dr. Kelly Brumbelow, Dr. Chris Houser, Dr. Oliver Frauenfeld, Dr. Steven Quiring, and Leland Cohen for their direction, assistance and enthusiasm throughout the course of this research and my time at Texas A&M and the Soltis Center.

I would also like to thank Eugenio Gonzalez and staff at the Soltis Center for their support of this work and continued efforts in keeping the research equipment running and functional at the center. I extend my thanks to the students of the 2013 Research Experience for Undergraduates (REU) in Costa Rica for helping to collect samples and keeping me company in the field, along with previous work done by REU students Nathan Tourtellotte, Olivia Dodge, and Esther Buckwalter.

Finally, thanks to the National Ground Water Research and Education Foundation for funding a grant given to Dr. Miller which supported travel and lab samples.

## NOMENCLATURE

Soltis	Texas A&M University Soltis Center for Research and Education
TF	Throughfall
SF	Stemflow
masl	Meters above sea level
VSMOW	Vienna Standard Mean Ocean Water
Picarro	Picarro Cavity Ring-Down Spectroscopy L2130-i
CS	Campbell Scientific
ITCZ	Intertropical Convergence Zone
$\delta^{18}\text{O}$	Oxygen-18 isotope ratio
$\delta\text{D}$	Hydrogen-2 isotope ratio known as Deuterium

## TABLE OF CONTENTS

	Page
ABSTRACT .....	ii
DEDICATION .....	iv
ACKNOWLEDGEMENTS .....	v
NOMENCLATURE .....	vi
TABLE OF CONTENTS .....	vii
LIST OF FIGURES .....	ix
CHAPTER I INTRODUCTION AND STUDY SITE BACKGROUND .....	1
Costa Rica .....	1
Study Watershed .....	2
CHAPTER II USING STABLE ISOTOPE TRACERS TO QUANTIFY BASEFLOW IN A COSTA RICAN PREMONTANE RAINFOREST .....	11
Introduction .....	11
Methods .....	14
Results .....	18
Discussion .....	30
Conclusion .....	34
CHAPTER III TROPICAL PRECIPITATION INFLUENCE ON HYDROLOGICAL CONDITIONS IN A COSTA RICAN WATERSHED .....	36
Introduction .....	36
Methods .....	39
Results and Discussion .....	43
Conclusion .....	54
CHAPTER IV CONCLUSION .....	55
Further Studies .....	55
Closing Remarks .....	56

REFERENCES .....	60
APPENDIX A .....	67
APPENDIX B .....	88
APPENDIX C .....	94



## LIST OF FIGURES

	Page
Figure 1. View of Costa Rica with Soltis Center marker north of 10° latitude and topography ~400-800 meters above sea level .....	3
Figure 2. Monthly climate and hydrology data since 2010 show variability with wet and dry seasons but no major temperature shifts .....	7
Figure 3. Design storm on October 21, 2012 shows shows high intensity (>6 mm/5 min) and long duration (3.5 hours) response to rain event.....	8
Figure 4. Gauged locations and daily sampling where elevation gradient is relative to stream outlet at weir .....	10
Figure 5. Illustration of gauged rainforest watershed showing weir for gauging streamflow (center), piezometer (right), heterogeneous geological conditions including perched aquifers, meteorological tower (back), and native vegetation and animals .....	15
Figure 6. Hydrograph with baseflow separation using local minimum method shows 50% groundwater during design storm on October 21, 2012 .....	19
Figure 7. Baseflow separation using a two component, one tracer mass balance method for events 2-5 where events 3 and 5 were high intensity collections .....	21
Figure 8. Soil water contribution is minimal during storm events possibility due to low hydraulic conductivity or vertical aging of water, rather than interflow hydrological processes.....	23
Figure 9. Seasonal water isotope trends show a distinct seasonal pattern changing from enriched to depleted sources as values move towards the lower quadrant.....	25
Figure 10. O-D relationship describes evaporation of surface samples with green arrow.....	26
Figure 11. Box and whisker plot shows median and upper/lower quartiles of sample distribution .....	27
Figure 12. Lysimeter sample results divided up by position in the watershed show similar enrichment across the site and variable precipitation during June and July .....	28

Figure 13. Scatter plot comparison for electrical conductivity ( $\mu\text{S}$ ) and baseflow percentage of total flow from the one isotopic tracer, two component model .....	29
Figure 14. Elapsed time series-EC ( $\mu\text{S}$ ) plot of events 2-5 with trendlines described by a 4th order polynomial .....	30
Figure 15. Gauged locations and daily sampling where elevation gradient is relative to stream outlet at weir .....	41
Figure 16. Annual water isotope trends including precipitation which varies seasonally and streamflow which has less variation .....	44
Figure 17. Event 1 plotted as a $\delta$ -plot shows stream values (groundwater + event flow) are consistent with the GMWL while the precipitation has an evaporated signature .....	46
Figure 18. Event 2 shows an isotopic rain signature which is depleted in heavy isotopes due to rain-out .....	47
Figure 19. Event 3 was a deep, fast convection event with heavy isotopic values and a short intensity and duration; precipitation types are similar proving little to no canopy evaporation on site .....	48
Figure 20. Event 4, which occurred on July 12, 2013, is shown with the HYSPLIT model to see the trajectory backcasted to the Caribbean ocean .....	49
Figure 21. Relationship between O-D for event 4 shows that precipitation has an evaporated trend which may occur at a regional scale .....	50
Figure 22. The rain-out and amount effect is seen at a local scale during event 5 .....	51
Figure 23. Event 5 was a slightly slower event where rain-out and a lengthened collection period contributed to the light isotopic values.....	52
Figure 24. Comparison of events with a time-series plot shows the localized amount effects during storms 4 and 5 and a rain-out effect during storm 2.....	53
Figure 15. Model shows a yearly time scale for d-excess values of different sources of water within the watershed as well as the finalized conceptual model.....	58

## CHAPTER I

### INTRODUCTION AND STUDY SITE BACKGROUND

In Costa Rica, the combination of surface and groundwater sources downstream of mountainous hillslope terrains provides for rural drinking water and energy which is produced at hydropower plants, particularly in the Guanacaste region (ICE 2002). However, our understanding of groundwater-surface water interactions in the mountainous terrain is limited, particularly for those areas in northwestern Costa Rica where water availability is limited during the dry season relative to the rest of the year (Coen 1983, Bachmair and Weiler 2011). Furthermore, the ability to gather data in these type of environments is constrained by their accessibility, dense vegetation, and complex subsurface features (McDonnell et al. 2007, Sivapalan 2003, Bachmair and Weiler 2011, USACE 1996).

#### **Costa Rica**

In a report on Costa Rica and its water resources produced by the Army Corps of Engineers (1996), Costa Rica occupies 50,895 km<sup>2</sup> of land, just shy of the size of West Virginia, with coastal areas adjacent to the Caribbean Sea (east) and Pacific Ocean (west). Geographically, the country is separated by a mountain chain formed by tectonic uplift in the western side of the country extending from the northwest to Panama. The population of over 3 million people grows at an annual rate of 2.7%; major economic sectors include agriculture-bananas, coffee, sugar, beef- and tourism (USACE 1996).

Additionally, hydroelectric power generation is vital to Costa Rica because it supplies 75% (1,228 MW) of the country's energy needs (ICE 2002).

Sources of water in Costa Rica are surface and groundwater with most of the precipitation falling seasonally between May and December. Storms, which are most abundant during the wet season, may dismantle civil infrastructure by raising swift currents with high sediment load and causing slope failures. Furthermore, water quality may be compromised in rural areas due to quick recharge rates and biological waste in the shallow subsurface zone (USACE 1996).

Improving our scientific understanding of the hydrogeological and ecological processes unique to the premontane tropical forests will be fundamental to limiting the damage done to these areas; some of the damage relevant in tropical montane forested watersheds includes threats from land-use and climate change (Toledo-Aceves et al. 2011, Jarvis and Mulligan 2011). Scientific understanding of these regions is also important for the continued implementation of hydropower, like the Peñas Blancas Hydroelectric Project, and for improved predictions in similar, ungauged watersheds (ICE 2002).

### **Study Watershed**

The study watershed is located in San Juan de Peñas Blancas, east of the Cordillera de Tilarán mountain range backing up to the Monteverde Cloud Forest Reserve (Figure 1). The mountainous forest is considered a lower montane forest due to elevation ranges from 450 meters above sea level (masl) to 1,800 masl (González 2013,

Bruijnzeel and Scatena 2011). The wildlife, which is important to the ecosystem in this watershed, is extremely diverse with estimates of over 350 bird species and 70 reptile and amphibian species (Soltis Center 2014). Biodiversity of the plant species are immense with estimates of over 2,000 vascular species (Soltis Center 2014). The area has previously been selectively logged resulting in some primary and some secondary forest.



**Figure 1. View of Costa Rica with Soltis Center marker north of 10° latitude and topography ~400-800 meters above sea level (ESRI 2014).**

## *Geology*

González (2013), who previously studied this watershed and surrounding areas, reports that the local geology is abundant in continuous lava flows which are andesitic basalts to andesites in composition (formerly known as the Monteverde Formation) with breccias, tuffs, and laterite soils from the Pleistocene epoch (Quaternary Period). He classified this formation as Catarata Andesitic Basalt (Q<sub>1-ct</sub>) with several identifying characteristics:

1. Presence of olivine, augite, hypersthene, and pyrite;
2. Degree of weathering;
3. Aphanitic to porphyritic texture;
4. Plagioclases with millimeter sizes;
5. Deep gray matrix; and
6. Lava flow direction of N35°E with an inclination of 18°.

González also reports that slopes range from 10-50°, however steep inclines are present only at elevations above 530 masl. The unconsolidated layer is breccia tuff with a thickness of up to 28 m. Drainage is dendritic but poorly developed due to topography.

## *Soil Matrix*

Soils in this watershed are the conduit for water flow in the vadose (unsaturated) zone. The geological characteristics in this zone are heterogeneous and complex with igneous rock erratics spread throughout the zone. Erratics range from the parent andesitic rock to weathered saprolitic tuff. Some perched aquifers can be found along

with macropores from animal burrows and roots. Andisol clays show a typical soil horizon: O horizon is top soil with vegetation, A horizon is the zone of accumulation of clays and includes roots, Bw horizon is the next subsurface clay zone with weathering and includes roots, and the B/Cr horizon is a root limited horizon and transitions into the parent rock.

The study site has developed a foundation of water budget knowledge with continued scientific gauging of streamflow, groundwater, precipitation, and transpiration (Cohen et al. 2013, Buckwalter et al. 2012, Miller et al. 2013). All data collection techniques can be found in Chapter II.

### *Precipitation*

Rainfall exhibits a distinct annual trend associated with the seasons, however the dry season still receives up to 350 mm of rainfall per month (Figure 2). Total rainfall collected at the center is 4,200 mm/yr (Soltis Center 2014). Some fog is common but it is not persistent enough to be considered a cloud forest (Bruijnzeel and Scatena 2011). Air temperature fluctuates between 20-25°C year-round. Solar radiation is a function of sunlight that is able to penetrate the cloud layer; it is limited in the dry season and ranges from 80-180 Watts/m<sup>2</sup>. Vapor pressure deficit (VPD) is a calculated value using relative humidity (RH) and temperature. It directly correlates to transpiration which increases in the wet season. Transpiration rates have been measured at 1.2 mm/day with sapflow sensor technology using the Granier and Burgess methods (Miller et al. 2013). At an average of 438 mm/yr, transpiration is a relatively minor component of the water budget, but essential for the ecological processes in the rainforest.

## *Surface Water*

The main stream in the watershed was equipped with a V-notch weir in 2012 to measure streamflow rates. The stream is a gaining stream; this means that when it is not immediately raining, all the water in the stream is groundwater fed (baseflow).

Baseflow averages  $0.06 \text{ m}^3/\text{min}$  and represents the biggest contribution to the water budget. Any event with streamflow rates above  $0.10 \text{ m}^3/\text{min}$  was notated as 'peak flow' and considered a storm event. Stream values found in Figure 2 are monthly mean harmonic stream values.

Hydrographs (time-series of streamflow during storms) were separated for their event (rainfall and runoff) and pre-event (groundwater and interflow) contributions to streamflow during this study. Based on a design storm from 2012 (high intensity, long duration), streamflow was seen to respond the event water within 5-10 minutes (Figure 3). This event occurred during October, one of the rainiest months at the Soltis Center with high antecedent moisture conditions.

During long duration or high intensity events, direct runoff will occur through filling up of pore water capacity. Excess water will drain down the hillslope in thin sheets known as Hortonian Overland flow or infiltration excess flow (Bachmair and Weiler 2011). This flow will contribute to the stream as event water.



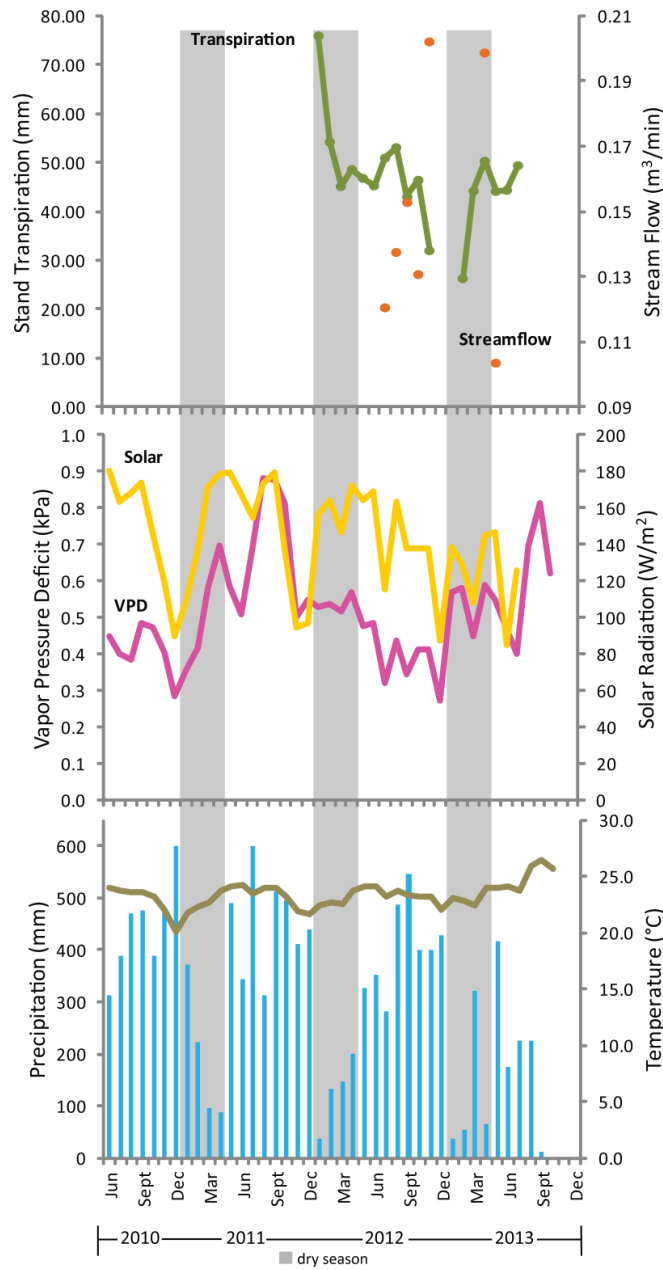


**Figure 2. Monthly climate and hydrology data since 2010 show variability with wet and dry seasons but no major temperature shifts. Shading refers to dry season months.**

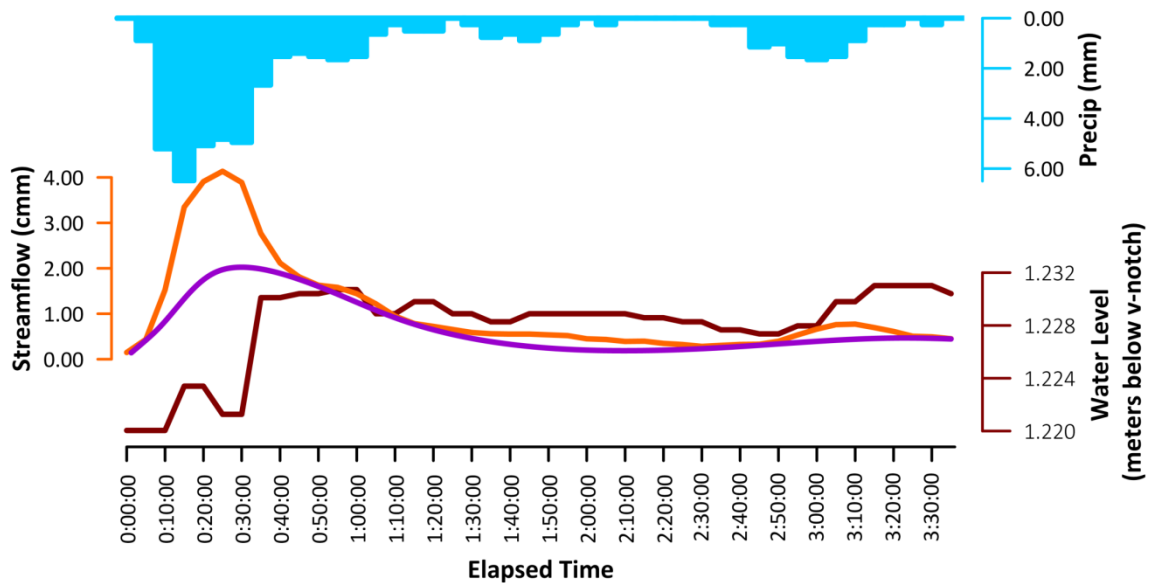


**Figure 3. Design storm on October 21, 2012 shows high intensity (>6 mm/5 min) and long duration (3.5 hours) response to rain event. There is rapid response of streamflow (5-10 minutes) and relatively rapid groundwater response (30 minutes). Purple flow line indicates local minimum baseflow response (~50% of streamflow).**

### *Groundwater*

Between 2012 and 2013, nineteen piezometers were installed around the watershed and arranged with design to transect the stream and vary by depth. Groundwater level values have been collected since 2013 in one well at five minute intervals. According to hillslope hydrology, shallow subsurface flow will occur due to the steep mountainous topography of the watershed. Water movement is a product of pressure differentials in the unsaturated subsurface (vadose zone) and will contribute to streamflow during rain events; this contribution is known as interflow.

In the October 2012 design storm (Figure 3), groundwater was seen to respond 30 minutes into the rain event and then stay constant throughout the remainder of the

storm. The fast response time can be attributed to groundwater ridging (interflow through the vadose zone towards the groundwater table at particular points) or high infiltration rates vertically into the groundwater table.

The local minimum technique is a conventional method for identifying baseflow; it connects a smoothed line between the rising and falling limbs of the hydrograph (Hooper and Shoemaker 1986). This technique has been added to Figure 3 to show that around 50% of streamflow could be baseflow during the storm. This value is consistent with other methods which have shown that in tropical environments around 30 to 80% of flow is baseflow (Lachneit and Patterson 2002, Goller et al. 2005, Weiler and McDonnell 2004).

#### *Sample Collection*

The collection period for water samples spanned 4 events with 55 days of daily samples; high frequency samples were collected during major storm events in June and July 2013 at five minute frequencies. All samples were analyzed for  $\delta^{18}\text{O}$  and  $\delta^2\text{H}$ . These were analyzed at the Stable Isotope Geosciences Facilities at Texas A&M University. Samples collected included net precipitation, throughfall, stemflow, xylem water, soil water, seep water, stream water, and groundwater.

Samples for isotopic analysis were collected with respect to the nearest physical data collection points previously established at the site (Figure 4). When possible, field parameters such as temperature and electrical conductivity were measured during collection with a YSI 85 meter. A mass balance calculation using a one-tracer, two-component baseflow separation model was conducted along with a two-tracer, three-

component separation model for soil and groundwater during the five storm events.

Additional information was collected on transport times through the vadose zone for soil water.

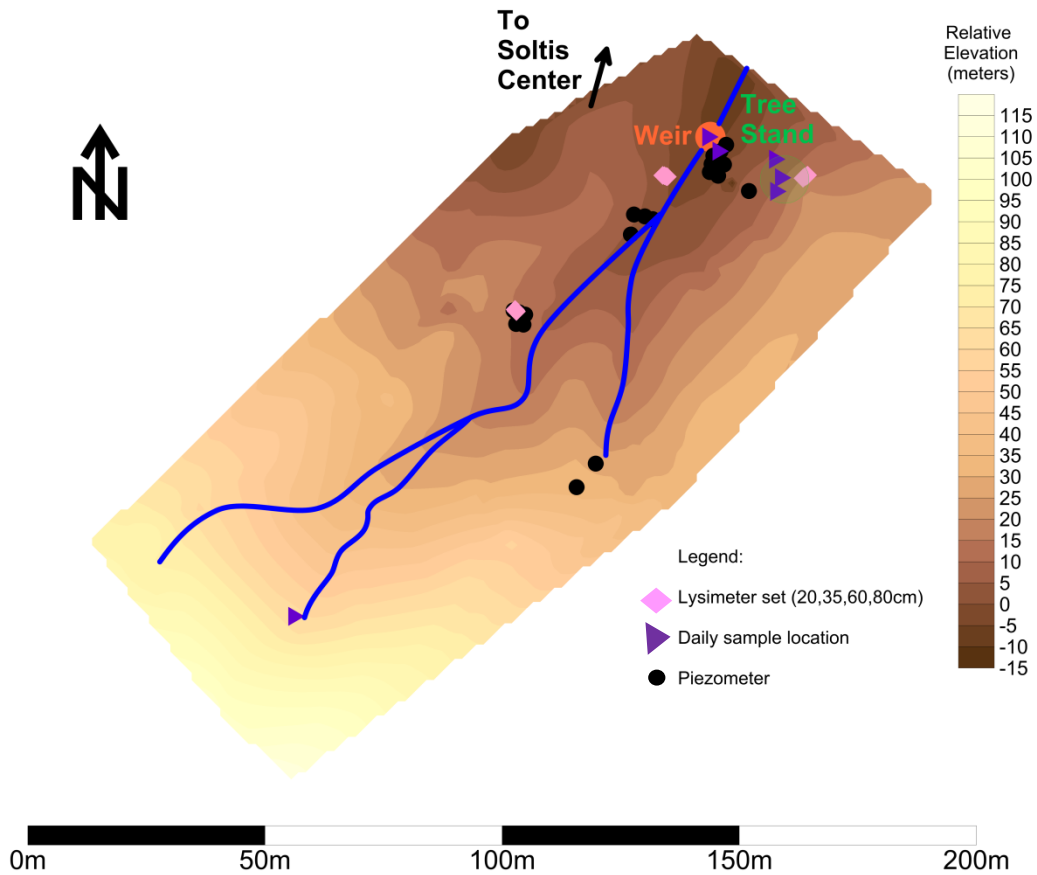


**Figure 4. Gauged locations and daily sampling where elevation gradient is relative to stream outlet at weir. Major elevation changes are located at the S-SW sector and between the weir and tree stand.**

CHAPTER II  
USING STABLE ISOTOPE TRACERS TO QUANTIFY BASEFLOW IN A COSTA  
RICAN PRE-MONTANE RAINFOREST

**Introduction**

In order to sustain their high demand for water, ecosystems in tropical rainforests rely on the abundant rainfall during the wet season and more continuous sources, like surface and groundwater, during the drier periods. The year-round availability of these flows is dependent on geology and climate conditions in the mountainous region of Costa Rica. In this area, groundwater subsists in shallow aquifers and aquitards in relatively complex geological conditions. Surface soils are high in macropores due to abundant roots and animal burrows, while deeper materials can be erratic originating from landslides over lava flows.

Isotopic analysis can be effectively used to quantify precipitation differences by isotope signatures as well as contributions to streamflow as seen in several notable studies like Goller et al. (2005), Rhodes et al. (2006), and Hooper and Shoemaker (1986). However, literature on groundwater recharge in these areas is lacking, especially that from sources such as throughfall and stemflow (Goldsmith et al. 2012, Muñoz-Villers and McDonnell 2012, Holwerda et al. 2010, Goller et al. 2005, etc.) Additionally, groundwater's interaction with streamflow is even less understood in small, tropical rainforest catchments. Oxygen and hydrogen isotopes are commonly

used because they have the widest utility: tracing origin of water, determining age, and finding the mode of recharge for groundwater (Mook 2000).

### *Surface Water*

Surface water is composed of both continuous groundwater flows and event precipitation from runoff and direct entrance to the stream. Hortonian overland (infiltration excess) flow occurs when rainfall amount exceeds the capacity of the soil to infiltrate water due to antecedent moisture conditions or prolonged rain events (Brutsaert 2005); it is typical of Andic clays which dominate the soil texture at the site (Burns et al. 2012). By looking at isotopic signals of surface water, runoff can be compared to event (rain) and pre-event (soil) water because it transmits relatively similar signals to the rainfall: some differences occur when there is localized evaporation which creates an isotopic ratio that is more enriched in heavy isotopes (Gat 2010).

### *Groundwater*

Groundwater dynamics in these environments are less understood than surface water due to major data gaps (Gonfiantini et al. 1998). In hillslope catchments, baseflow originates from preferential flow networks including fractures in parent rock material and shallow subsurface flow in unsaturated volcanic substrate (Gabielli et al. 2012, Weiler and McDonnell 2004, Bonnell 2005, Tobon et al. 2010, Anderson et al. 2009). Additionally, Buttle (1998) describes very small temporal variation in groundwater isotopic signatures associated with long residence times and diffusivities with previous water in the phreatic (saturated) zone. Previous studies report that under tropical conditions, groundwater can account for between 30 to 80% of total streamflow during

rain events (Lachneit and Patterson 2002, Goller et al. 2005, Weiler and McDonnell 2004).

### *Soil Water*

Interflow can be a significant contribution to streamflow, as pre-event water which has not percolated to the water table becomes flushed out of pore spaces during heavy precipitation events (Anderson et al. 2009, Ridolfi et al. 2003). This movement is due to pressure changes in the soil structure and can move water to the surface in hillslope environments or rapidly to the groundwater table known as groundwater ridging (Brutsaert 2005, Buttle 2006). In isotopic composition studies, shallow soil water signatures will show evaporation by an increase in the ratio of heavy isotopes; however, as depth increases through the vadose zone a dilution of the variable signatures occurs known as the “percolation flux” (Goldsmith et al. 2012, Gat 2010). The percolation effect displaces changes in the input waters (due to seasonal variations) vertically and can be seen in a smoothing of the isotopic abundance differences at progressive depths as it mixes with antecedent waters left in the pore spaces (Gat 2010).

The goals of this project were to effectively determine which subsurface pathways are conduits to water flow through the subsurface and out of the watershed. Initial data from the watershed suggested that there was a relatively short lag time between start of a rain event and groundwater level response indicative of baseflow processes dominating the hillslope. I hypothesized that flow direction followed classic hillslope hydrologic behavior which assumes flowpaths parallel to the surface through macropores and infiltration excess overland flow (Bonell and Bruijnzeel 2005). Our

objective was to test the hypothesis: by describing different forms of tropical precipitation and transit through the subsurface, precipitation will illustrate the contribution of macropore flow by a lag time of <1 hour between precipitation and weir flow peaks. These goals were accomplished by supplementing hydraulic and physical data already available at the site with use of isotope tracers.

## **Methods**

### *Study Site*

The 2.2 ha watershed used in this research is located in Peñas Blancas, Costa Rica at the Texas A&M Soltis Center for Research and Education. Complex geology due to Pleistocene epoch lava flows and lahars with breccia tuff and saprolite erratics exists alongside a thick andisol clay substrate and dense vegetation. Predominant biota in the area ranges from primary forest trees to grasses in selectively logged areas (Figure 5). The site has been gauged for streamflow with a V-notch weir and Campbell Scientific (CS) pressure transducer, stemflow and throughfall monitoring with tipping buckets, and piezometers including one piezometer with a CS transducer for groundwater level measurements. A meteorological station was installed in an open area near the center building; it has measured humidity and temperature at 10 ft and 30 ft, as well as precipitation, wind speed, and solar radiation since 2010.



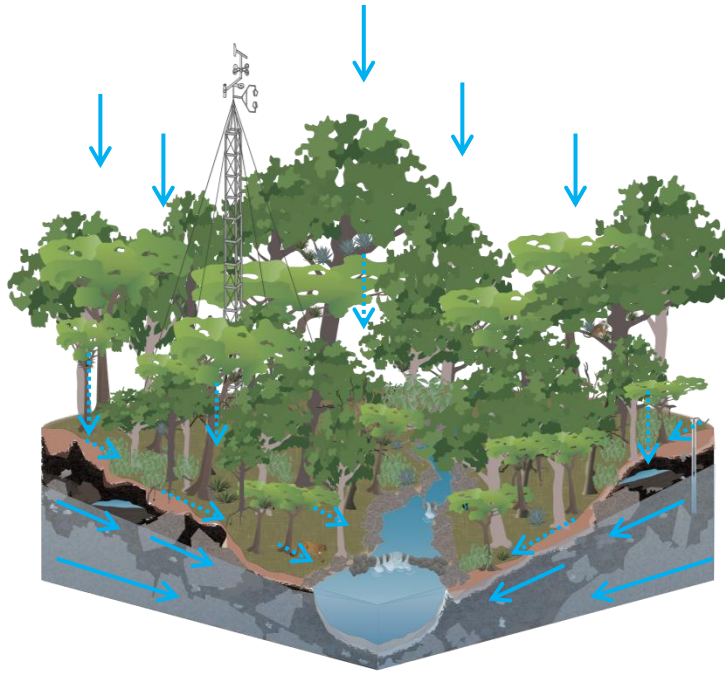


**Figure 5. Illustration of gauged rainforest watershed showing weir for gauging streamflow (center), piezometer (right), heterogeneous geological conditions including perched aquifers, meteorological tower (back), and native vegetation and animals. As indicated by the arrows we hypothesized flow pathways following the hillslope; interflow, shallow subsurface flow, stemflow, throughfall, and lateral movement along water table have dashed arrows representing smaller amounts of flow.**

### *Sample Collection and Analysis*

A Picarro Cavity Ring-Down Spectrometer L2120-i was used to determine  $\delta^{18}\text{O}$  and  $\delta\text{D}$  values in the water samples (Picarro Inc. 2012, Shuss and Seibold 2010). The ring-down spectroscopy works by illuminating the cavity and gaseous material ( $\text{H}_2\text{O}$ ) up to 20 km in length using a single-frequency laser diode and three high precision mirrors (Picarro 2012). Once the laser is switched off (in a few tens of microseconds), light decays from the cavity due to optical loss and resonant absorption by the gas (Picarro 2012). The identification of concentrations is evident because the strength of the absorption peak can be recognized with a long effective pathlength (Picarro 2012).

Light abundance can then be calculated using the Beer-Lambert Law:  $I(t, \lambda) = I_0 e^{-t/\tau(\lambda)}$

where  $I_0$  is the initial transmitted light intensity and  $\tau(\lambda)$  is the ring down time constant; for a given wavelength, the decay rate,  $R$ , is known for an empty cavity and from that concentration,  $C$ , can be identified using  $R(\lambda, C) = 1/(\lambda) = R(\lambda, O) + c\varepsilon(\lambda)C$  where  $c$  is the speed of light and  $\varepsilon$  is the extinction coefficient (Picarro 2012). The isotope concentration over the abundant isotope concentration gives a ratio that is expressed as a ‰ value and is labeled with a  $\delta$  (delta, Dansgaard 1964, Kendall and McDonnell 1998). Samples were calibrated against an existing international standard VSMOW (NIST RM#8535) and an internal standard SIGF2013 (working lab standard). External precision of the analyzed were  $\pm 0.3\text{‰}$  for  $\delta D$  and  $\pm 0.12$  for  $\delta^{18}O$ . D-excess, a measure of both  $\delta^{18}O$  and  $\delta D$ , was calculated using Dansgaard (1964):  $d = \delta D - 8 \cdot \delta^{18}O$ .

#### *Baseflow Separation*

For determining the baseflow contribution during these storms, a one tracer, two component method was used (Hinton et al. 1994, Buttle 2006, Pinder and Jones 1969, Sklash et al. 1976):

$$Q_b = Q_s \left( \frac{C_s - C_p}{C_{GW} - C_p} \right)$$

where  $C_p$  is the concentration of the new event water,  $C_{GW}$  is the concentration of the older groundwater, and  $C_s$  is water concentration from the stream;  $Q_s$  is the total volumetric streamflow, as measured at the weir, and  $Q_b$  is the resultant portion of the flow attributable to baseflow.

### *Soil Water Analysis*

Soil water isotopic composition was determined in order to identify the soil water component of baseflow. Suction lysimeters (UMS 2013) were custom manufactured to access different horizons of the substrate: organic soil layer (horizon O), andisol clay (A), weathered saprolitic tuff cobbles within andisol clay (Bw), and root-limiting basaltic parent rock erratics (B/Cr). All lysimeters were purged with deionized water before installation, and the first collection of soil water was discarded. Subsequent collections occurred weekly at each of the three sites. A two tracer, three component mass balance equation was used to determine the influence of interflow to the stream during storms (Hinton et al 1994, Ogunkoya and Jenkins 1993):

$$Q_r = \frac{Q_t \cdot (\delta^{18}O_t - \delta^{18}O_{GW}) - Q_s \cdot (\delta^{18}O_s - \delta^{18}O_{GW})}{\delta^{18}O_r - \delta^{18}O_{GW}},$$

$$Q_{GW} = \frac{Q_t \cdot (\delta D_t - \delta D_r) - Q_s \cdot (\delta D_s - \delta D_r)}{\delta D_{GW} - \delta D_r}, \text{ and}$$

$$Q_t = Q_r + Q_{GW} + Q_s$$

where the subscript r represents the runoff component, GW the groundwater component, s the soil water component, and t the total streamflow.

## **Results**

### *Preliminary Findings*

Baseflow separation was completed on a long duration, high intensity storm on October 21, 2012 to represent a point of departure for the groundwater interaction hypothesis. Figure 6 shows that during this storm, the rising limb of the hydrograph begins within 10 minutes from the beginning of the rain event. Within 30 minutes, the groundwater rises rapidly and remains constant throughout the rest of the event. By connecting the rising and falling limbs of the hydrograph (local minimum technique), baseflow is seen to contribute roughly 50% of the storm during peak flow. The response times indicate that there is fast movement through the subsurface which can be attributed to several possibilities: vertical flow straight to water table (total depth of 2.173 meters to water table from top of casing) and conduits for water by-pass (macropores, animal burrows, etc.) or high antecedent moisture conditions near the end of the wet season in October.

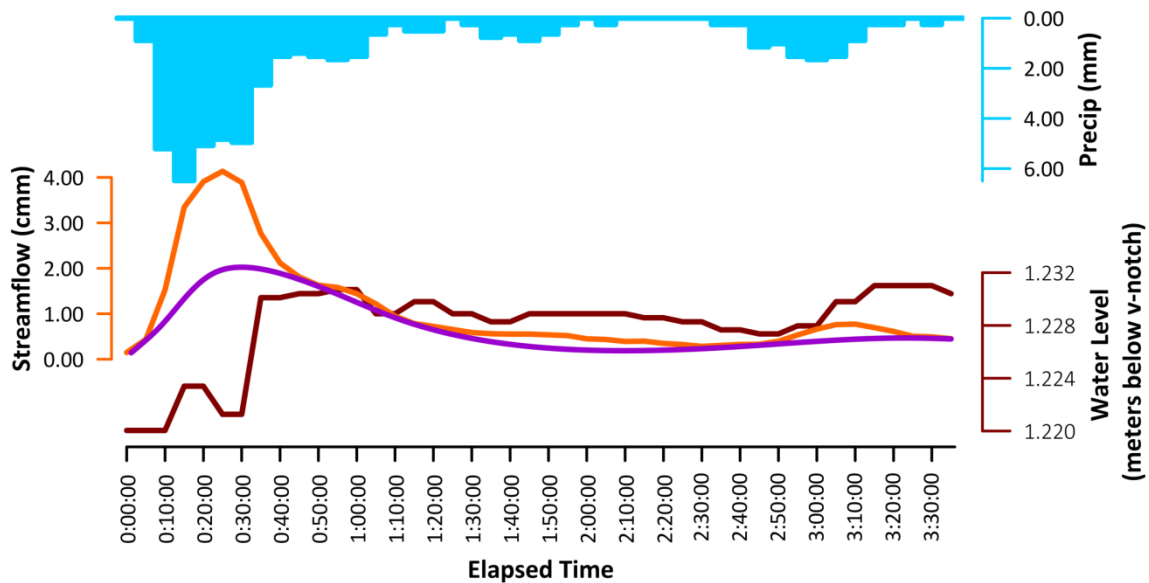


**Figure 6: Hydrograph with baseflow separation using local minimum method shows 50% groundwater during design storm on October 21, 2012. Precipitation values reached 6 mm/5 min and the groundwater table rose 1.2 cm. Baseflow is considered at 0.06 m<sup>3</sup>/min on a year-round scale with this event rising above 4.00 m<sup>3</sup>/min.**

### *Hydraulic Conductivities*

A major influence on the amount of interflow is the relatively slow hydraulic conductivity of the thick andisol clay soils ( $K_{sat} \sim 1 \times 10^{-9}$  to  $1 \times 10^{-12}$  m/s, Freeze and Cherry 1979) interspersed with cobbles of saprolitic tuff and inconsistencies due to macropores from roots and animal burrows. Slug testing was used as an in-situ test to further characterize permeability at specific locations in the watershed. Slug testing of three wells were chosen due to their constant saturation and calculations were made using the Hvorslev method (Butler 1997, Cohen et al. 2013). The value found ( $K \sim 1.3 \times 10^{-6}$  m/s) is consistent with the value derived from soil analysis and the Rosetta

database (Schaap et al. 2001); Rosetta values suggested a range from 1.4 to  $3.2 \times 10^{-6}$  m/s which corresponds to that of fractured igneous rock (Freeze and Cherry 1979).

### *Baseflow Separation*

During major rain events in the wet season of 2013, streamflow was considered peak flow at values which surpassed  $0.10 \text{ m}^3/\text{min}$ . As seen below (Figure 7), baseflow consisted of  $49.5 \pm 21.5\%$  of total flow in the stream during storm events, averaged over 3 events during peak flows ( $>0.10 \text{ m}^3/\text{min}$ ). When averaged over the full, 1.5-2 hour collection periods (peak flows, rising limb, and receding limb of hydrograph), baseflow accounted for  $80\% \pm 20\%$  of the total streamflow. Event 1 was discarded due to weir maintenance which restricted the corresponding streamflow data; event 4 did not reach peak flow and was not considered in baseflow averages.

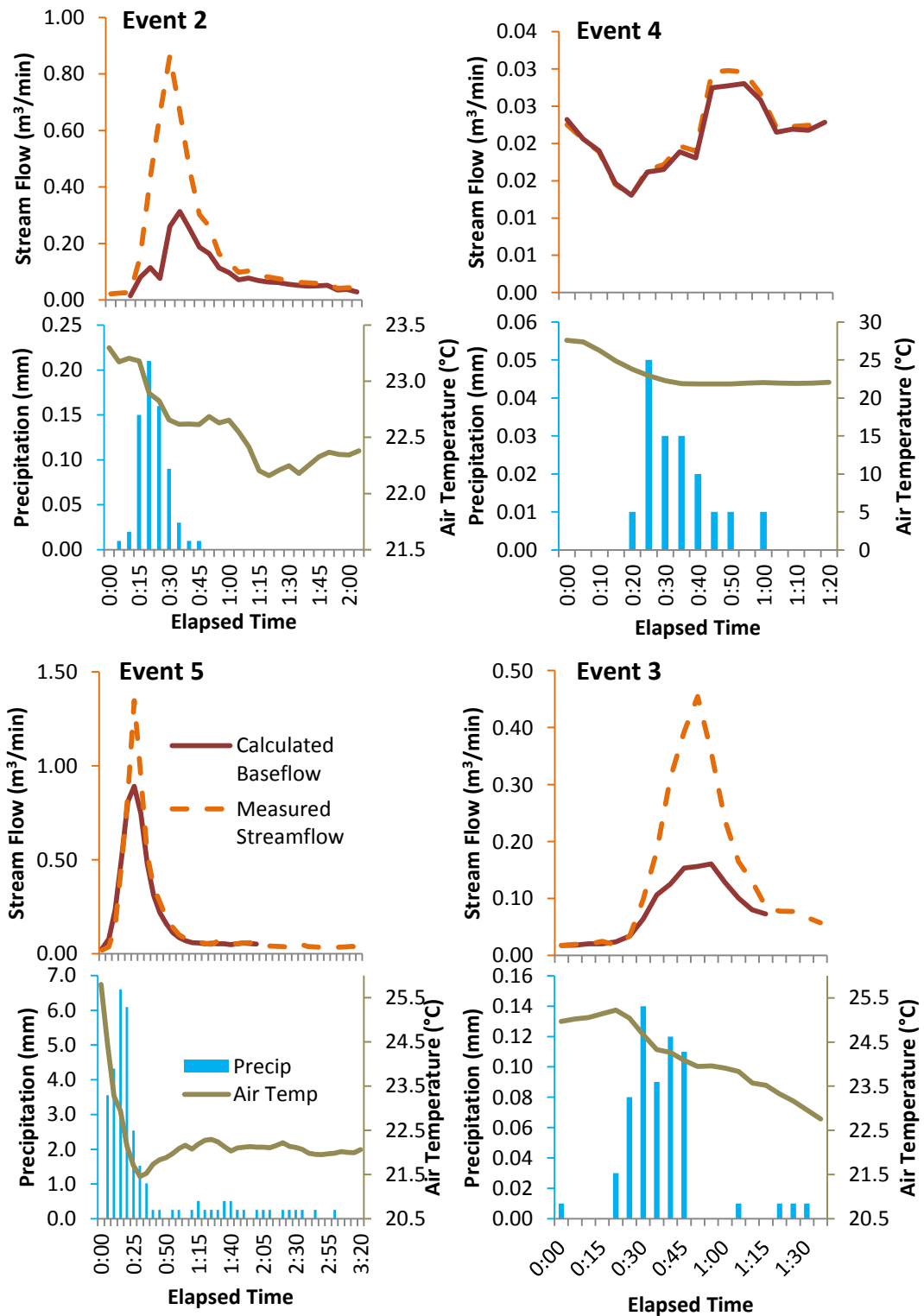


**Figure 7. Baseflow separation using a two component, one tracer mass balance method for events 2-5 where events 3 and 5 were high intensity collections. Averages evaluated over three storms demonstrate a 49.5% baseflow during flows greater than  $0.10 \text{ m}^3/\text{min}$  and 80% during entire event.**

### *Soil Water Contribution*

Interflow appears as a relatively minor component; this leaves the main linkage between precipitation and streamflow to be groundwater contribution even in the wet season. Soil water contributed about 1.1% overall and baseflow contributed 79% to the streamflow averaged over the entirety of both storms with intense collection periods. Total water calculated with the mathematical model was just under 5.5% of measured values. A baseflow comparison between the two different methods shows a 1% difference, which can be attributed to random error in the two methods evaluated (Figure 8). Slightly more soil water contributed to baseflow during event 5, which may be a function of antecedent moisture conditions.



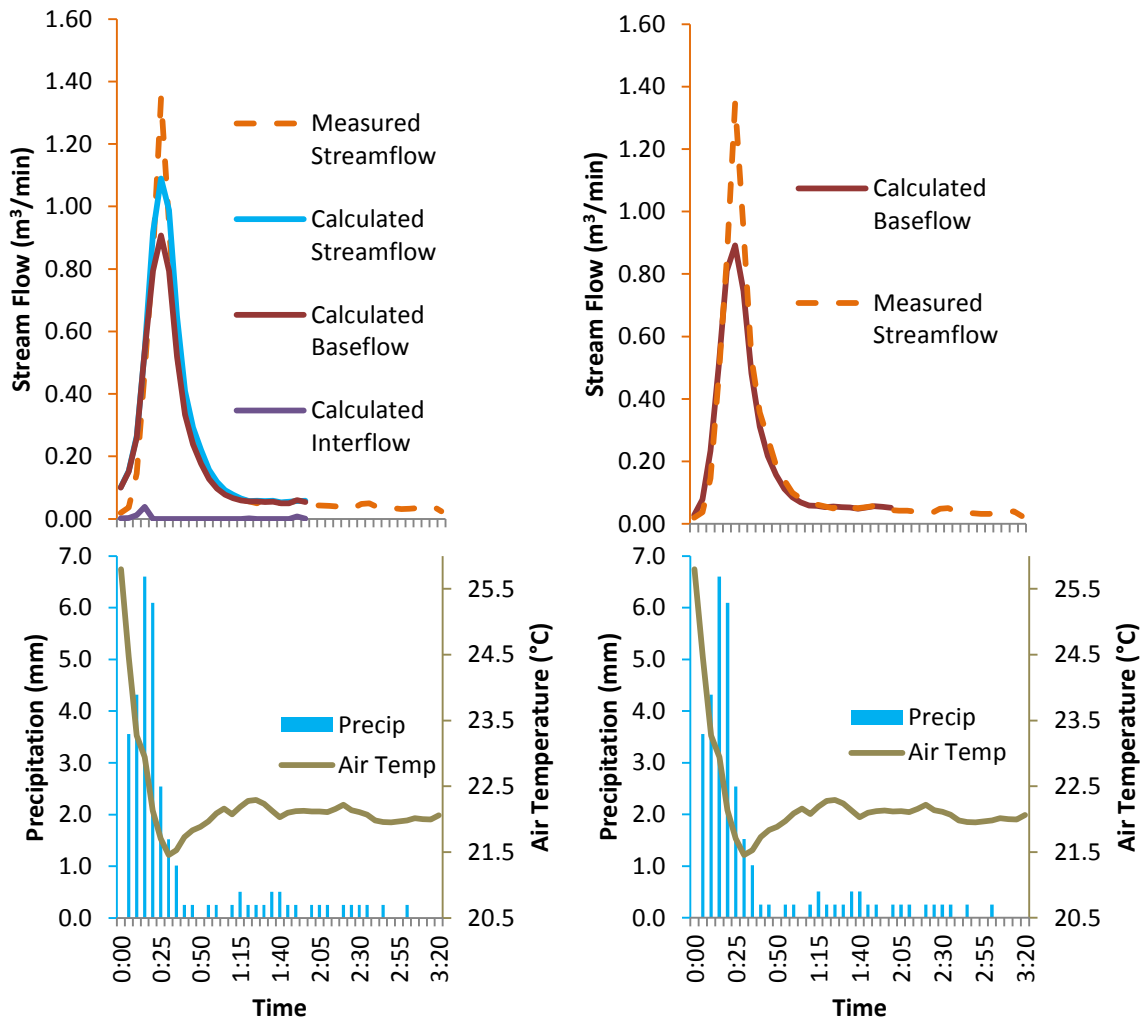


**Figure 8. Soil water contribution is minimal during storm events possibility due to low hydraulic conductivity or vertical aging of water, rather than interflow hydrological processes. Compared with the one tracer, mass balance method, there is a 1.1% difference in the calculated amount of baseflow for events 3 and 5 (shown here).**

### *Seasonal Variation*

The seasonal flux of precipitation was found to be a contributing factor to differences in isotopic changes (Figure 9). For example, in the dry season, water originated as an enriched moisture source ( $0.00 \delta^{18}\text{O}$  which plots on the x-axis on the  $\delta$ -plot and  $10.0 \delta\text{D}$  from the y-axis, written as [ $0.00 \delta^{18}\text{O}$ ,  $10.0 \delta\text{D}$ ]). Wet season precipitation was deeply convective, with some recycling ( $-10.0 \delta^{18}\text{O}$ ,  $-80.0 \delta\text{D}$ ), and originated during the North American Monsoon and positioning of the Intertropical Convergence Zone (ITCZ) over Costa Rica which brings increased rainfall due to a shift in wind patterns. There was some evidence of evaporation during the wet season, as seen by the Local Meteoric Water Line (LMWL, slope of 7.14) having a slightly lower slope than the Global Meteoric Water Line (GMWL, slope of 8.00) which is not statistically significant using a t-test. Stream data varied slightly with variation in precipitation, however because the stream is gaining, streamflow values are representative of groundwater. Due to the muting effect of long groundwater residence times in the watershed, groundwater was mostly unaffected by the seasonal changes ( $-5.0 \delta^{18}\text{O}$ ,  $-25.0 \delta\text{D}$ ). The standard deviation of the d-excess value of groundwater is 0.96, precipitation is 3.40, and streamflow is 1.53. Litter water is extremely variable, and there is little correlation between daily precipitation values and daily litter water collection.

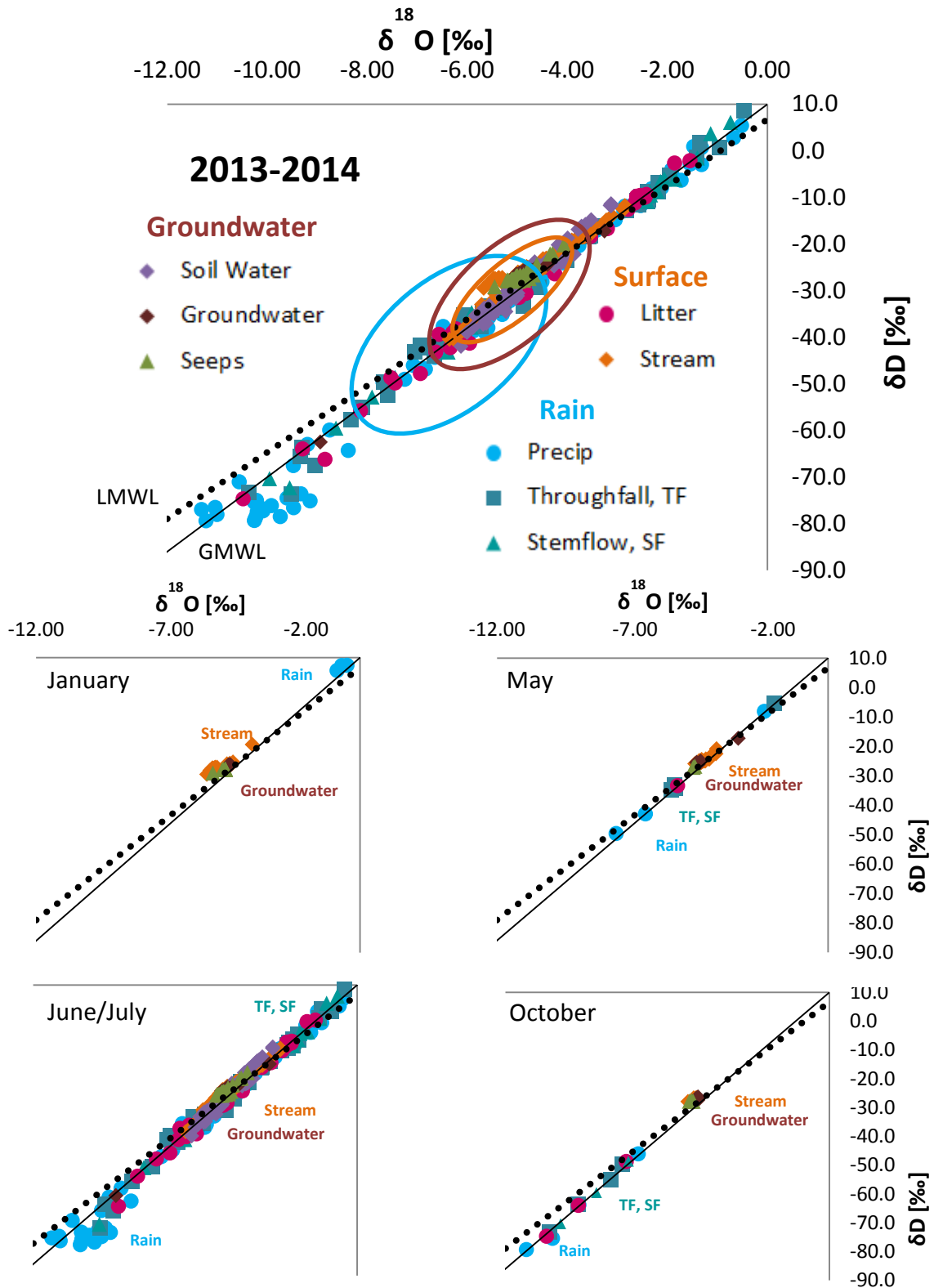


**Figure 9. Seasonal water isotope trends show a distinct seasonal pattern changing from enriched to depleted sources as values move towards the lower quadrant. Evaporation is evident due to the Local Meteoric Water Line (LMWL) exhibiting a slope of less than the slope of the GMWL.**

### Soil Water Behavior

Soil water plotted as a  $\delta$ -plot has a positive enrichment trend with increased depths (Figure 10). Groundwater from June and July 2013 was taken from one well roughly 2 meters for total depth and near the stream; it is also plotted in Figure 10 and has similar isotopic signatures to the 60 cm and 80 cm soil samples. Top soil waters at 20 cm and 35 cm have evaporative signatures (shown with a green arrow and seen by a slope of less than 8 on the delta-plot).

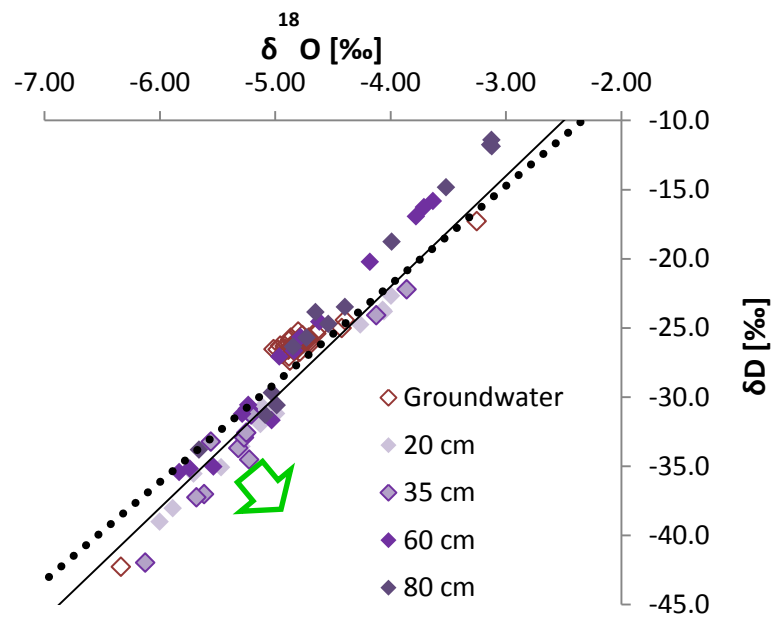


**Figure 10. O-D relationship describes evaporation of surface samples with green arrow.**

Figure 11 describes the enrichment by depth as soil water travels towards the water table; as depth increases values become more enriched due to evaporation of the lighter isotopes near the surface soil layers. Signatures of top soils have a median of around 9‰, relatively similar to precipitation values at a yearly scale. At larger depths within the substrate, isotopic signatures have a median near 12‰ which reflect the average groundwater signatures. Note that groundwater is from one well (P-mid) near the weir with groundwater levels around 2 meters below the ground surface; lysimeters are sampled from three locations throughout the watershed at much higher elevations from the stream. Soil samples by location are plotted on Figure 12.

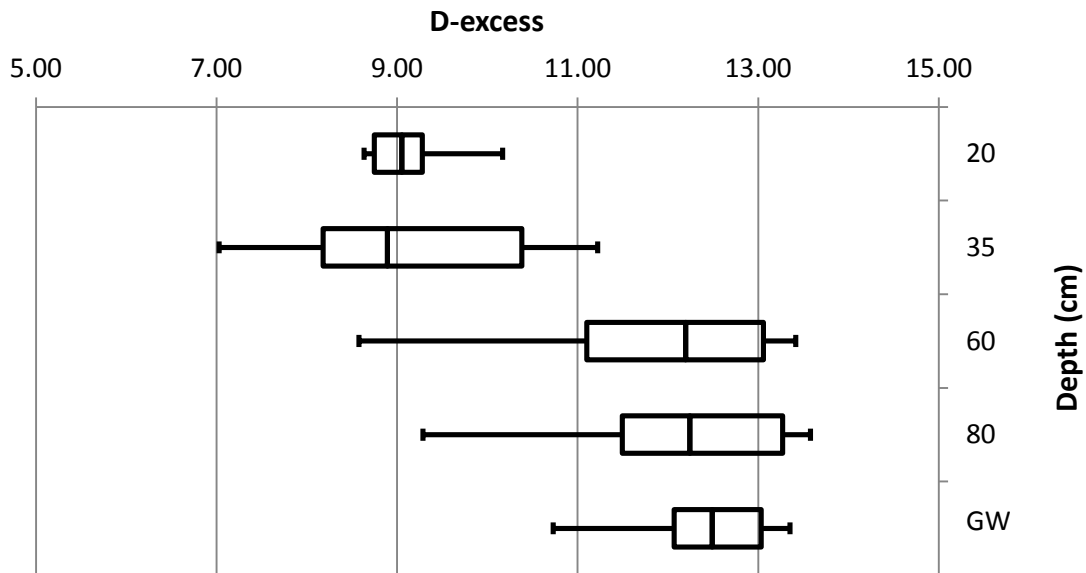


**Figure 11. Box and whisker plot shows median and upper/lower quartiles of sample distribution. With increased depth in the top soil layers (20 and 35 cm), samples from the three lysimeter locations are roughly similar in deuterium-excess; at larger depths into the clay substrate, samples are similar but more enriched than top soils indicating evaporation in the top layers.**

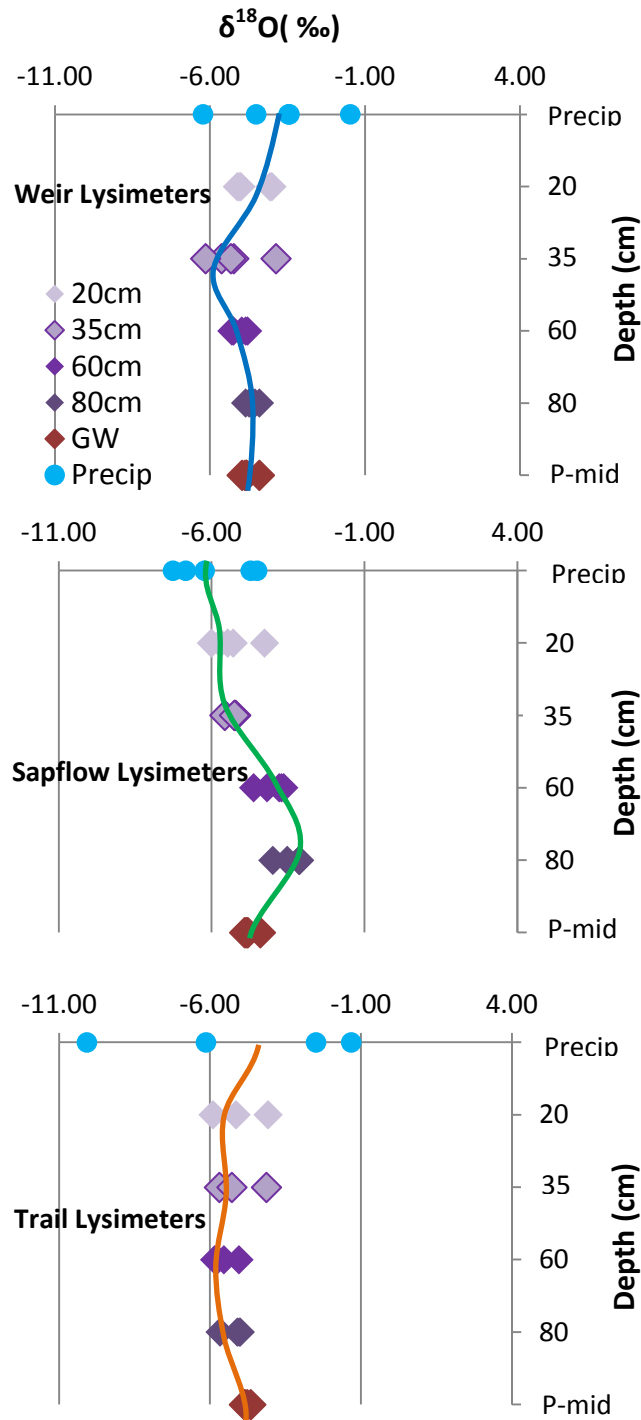


**Figure 12. Lysimeter sample results divided by position in the watershed show similar enrichment across the site and variable precipitation during June and July 2013. The sapflow lysimeter set which is in a location with less tree cover shows the most enrichment of heavy isotopes indicating more evaporation of the lighter isotopes. Weir and trail lysimeter locations have characteristics closer to groundwater and are located at closer elevations to the sampled groundwater well than the lysimeter set located at the sapflow site.**

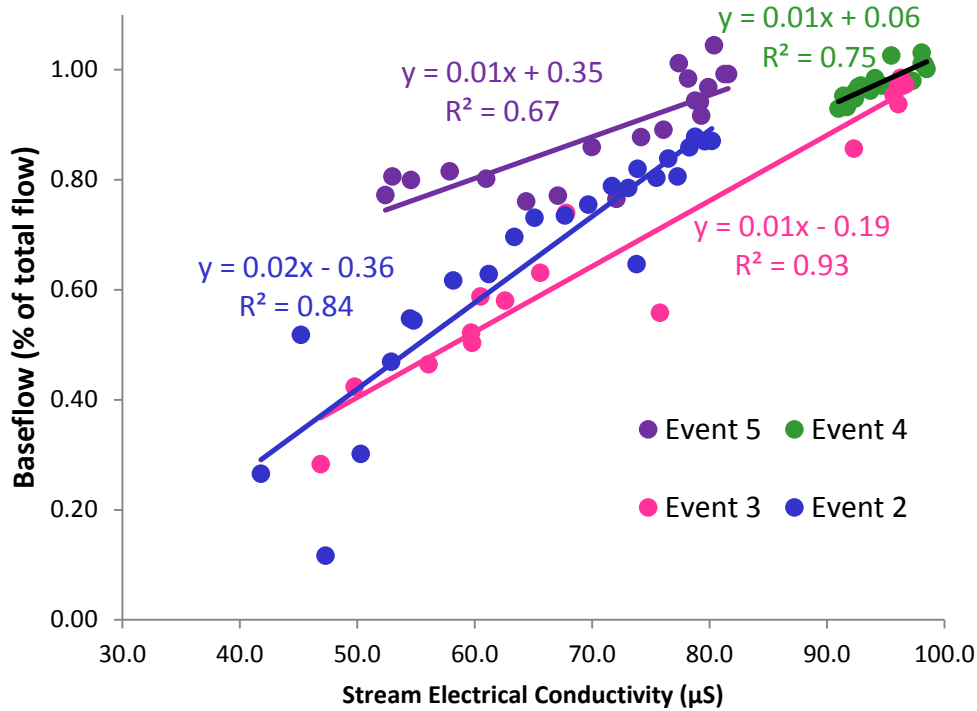


**Figure 13: Scatter plot comparison for electrical conductivity ( $\mu\text{S}$ ) and baseflow percentage of total flow (%) from the one isotopic tracer, two component model.  $R^2$  values ranged from 0.67 to 0.93 with the smallest event which reached peak flow (event 3) being the most statistically similar.**

### *Electrical Conductivity*

Literature has suggested that electrical conductivity (EC) can be used as a conservative tracer instead of isotope concentration (Gonzales et al. 2009, Pellerin et al. 2008). EC has been plotted to show variance between baseflow separation results from the one tracer model previously used (with isotopic concentration to find baseflow separation percentage) in Figure 13.

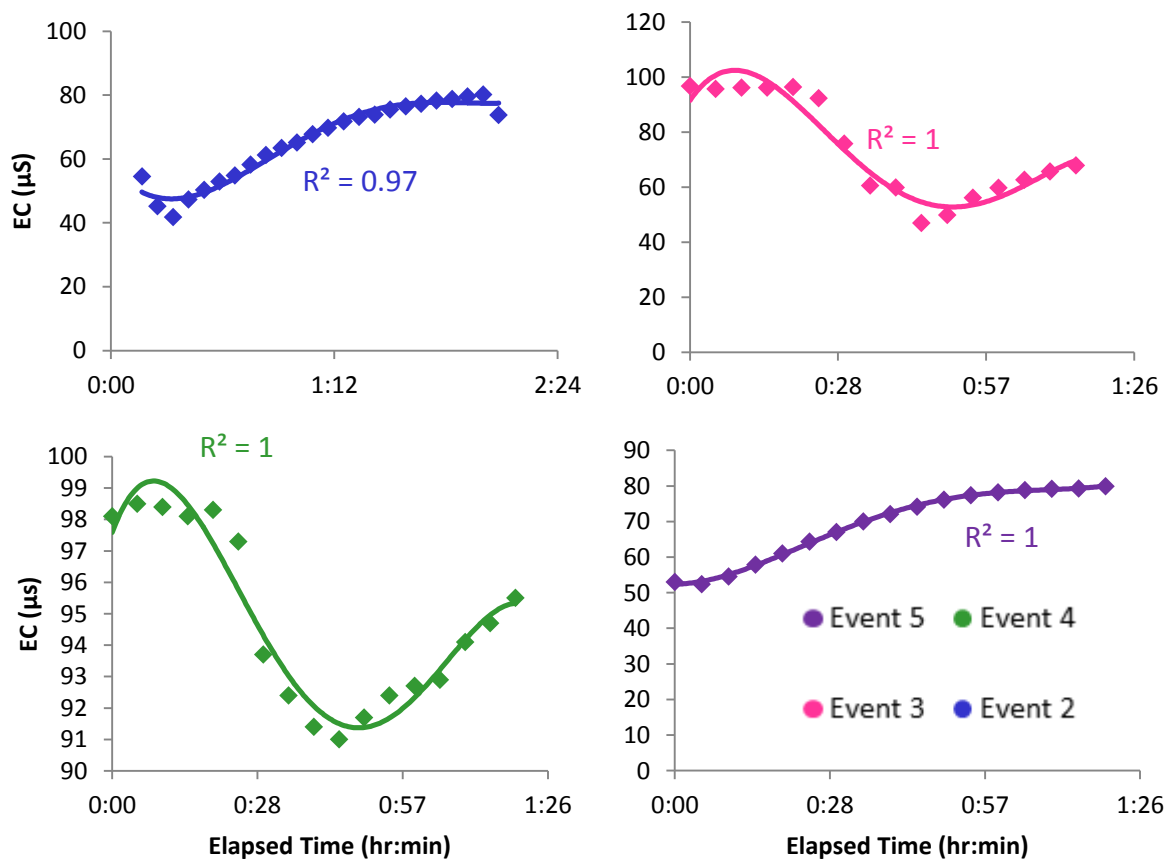


**Figure 14: Elapsed time series-EC ( $\mu\text{S}$ ) plot of events 2-5 with trendlines described by a 4<sup>th</sup> order polynomial. All events have  $R^2$  values of greater than 0.97 with the longest event (event 2) having the most amount of variance from trendline.**

## Discussion

Previous studies describe water flow as lateral flow near the surface through organic layers along hillslopes (Goller et al 2005, Anderson et al. 2009). However, this study finds that surface water measured in the litter layer ( $d = 10\%$  at a yearly scale) is dissimilar to streamflow ( $d = 12\%$ ). Two mechanisms may describe this relationship: differential evaporation happens at the ground surface before reaching litter collectors and/or minimum runoff contributes to streamflow at a yearly time scale. The differences



between litter and precipitation can also be seen at a daily time scale. Because of these differences, it can be inferred that water which flows down the surface as Hortonian overland flow is not the biggest contributing factor to event flow. Furthermore, because interflow is such a small portion of baseflow (1.1%), it can be assumed that interflow contributes more to raising the groundwater table (through vertical flow paths and macropores) rather than reemerging to the surface and contributing to streamflow as event water.

The results of this study, that water moves in a vertical direction to contribute to groundwater (50-80% of baseflow during a storm) rather than shallow subsurface flow (1.1%), agree with conclusions drawn by Muñoz-Villers and McDonnell (2012). The authors found that by determining water aging patterns, a vertical direction was seen that may be caused by macropores or highly porous material in the subsurface. Additionally, during the progression of the wet season, interflow influence during storm events did not increase significantly, as was expected with increasing antecedent moisture conditions. It may be concluded that this is due to the same circumstances of vertical water movement associated with vertical pressure gradients and preferential flow paths in the vertical direction.

Along the hillslope, the watershed has several seeps and weeping walls which were confirmed to be similar to groundwater originating from an upgradient sinkhole (González 2013,  $d = 12\text{‰}$  for seeps compared to  $d = 12\text{‰}$  for groundwater). It can be concluded that there is some mixing in an underground reservoir before exiting the seeps because of the dampening of the isotopic signal similar to the groundwater aquifer.

Soil water was collected only during the rainy season and had a short exposure time to the subsurface; a percolation effect was seen as the water becomes enriched with vertical movement. This may be due more to evaporation of shallow subsurface soils than to mixing with antecedent pore waters.

Hydraulic conductivity was found through several slug tests ( $k = 1.3 \times 10^{-6}$ ) to be smaller than those calculated nearby at the hydroelectric plant (González 2013,  $k = 9.2 \times 10^{-2}$ ); this could be attributed to boulders and cobbles impeding piston flow through the subsurface, the scale at which the slug tests were conducted, or slight differences in geology between the locations.

All water which may have organics (soil water, litter layer water, etc.) should be confirmed with mass spectrometer results for verification, since organics can interfere with infrared spectroscopy analysis like the Picarro (West et al. 2010). It is because of this uncertainty that litter layer and soil water may show signs of dissimilarity due to machine error rather than true differences in the data.

#### *Electrical Conductivity*

In Figure 14, event 1 was not plotted due to data gaps in total flow during event collection. Events 2-5 were plotted as a time series of event with a trendline described by a 4<sup>th</sup> order polynomial for use with discussion of variance comparison. The electrical conductivity results suggest that there is some differentiation between the two tracers (isotopic tracers and EC) but it is unclear whether this is from random error or systematic error. To narrow in on the source of error, the differences in precipitation during the events are examined in further detail below.

### Rain Intensity Positioning

Events 2 and 5 had similar trend changes to EC as time progressed with an increase in EC by  $\sim 20\mu\text{S}$  spread over the entire collection event. Events 3 and 4 also had similar EC progressions however they differed from the other events by exhibiting a sine wave pattern. This could be due to the differences in precipitation amount versus time: events 2 and 5 precipitation with highest intensity at the beginning of the event where as events 3 and 4 experienced the most amount of precipitation towards the middle of the event. There was no visible correlation between positioning of rain intensity and use of EC as a baseflow separation tracer.

### Rain Duration

Statistically, the longest event (event 2) had the highest correlation in electrical conductivity values when plotted as a time series ( $R^2 = 0.97$ ). However, event 2 had the second to highest correlation ( $R^2 = 0.84$ ) when compared with the previous model. Contrarily, the most statistically similar plot when comparing the two methods (event 3,  $R^2 = 0.93$ ) had the shortest duration. Because of these results, there is no visible correlation between duration of rain and use of EC as a baseflow separation tracer. It is assumed that correlation variance between methods is due to random error.

### Rain Amount

Event 4, which never reached peak flow ( $Q_{\text{max}} = 0.035 \text{ m}^3/\text{min}$ ) had a much tighter spread when compared with baseflow ( $R^2 = 0.75$ ). Event 3 was the smallest event which reached peak flow, had the most amount of correlation in the comparison

plot ( $R^2 = 0.93$ ). There is no visible correlation between rain amount and use of EC as a baseflow separation tracer.

### **Conclusion**

In this study, we quantified the contributions of baseflow and interflow to total, wet season stream flows in the watershed; additionally, soil water delineation helped to define critical flow path directions through the subsurface. Baseflow dominates (~50 - 80%) due to macropore flow and the heterogeneous geology. As the wet season progresses, some interflow is evident but baseflow remains the governing source, even during large storms. Soil water resembled groundwater more closely with depth for lysimeter sets near the stream than water collected in the litter layer post-storm or near the higher elevation sapflow site. This coupled with the small influence of interflow indicates that water movement is a consequence of vertical percolation, not overland flow. Electrical conductivity was seen to be correlated to baseflow methods as a one tracer, two component model ( $R^2 = 0.67 - 0.93$ ).

Seasonal trends indicate that groundwater sources are not responsive to changes in precipitation origination. The assumption that seeps at the northwestern edge of the watershed are groundwater fed was verified due to similarities between seep flow and groundwater isotopic signatures and the isotopic muting of signatures by water mixing in an underground reservoir. The little variation seen yearly with seeps and groundwater data can be accounted for with long residence times (unquantified) and mixing with existing groundwater. The LMWL line which was configured by data collected in this

project shows that it is not statistically significant to the GMWL and there is some evaporation happening by precipitation sources either before or after arrival to the watershed.

CHAPTER III  
TROPICAL PRECIPITATION INFLUENCE ON HYDROLOGICAL CONDITIONS  
IN A COSTA RICAN WATERSHED

**Introduction**

The climatic patterns over tropical montane rainforests influence the ecological and hydrological processes that support the diverse ecosystems found in Costa Rica. Fog adds complexity as a type of precipitation; fog acts by depositing water droplets on leaves, called occult precipitation, however its presence is not persistent in lower elevation forests and studies have generally assumed it to contribute negligible amounts in tropical montane cloud forests (Goldsmith et al. 2012, Muñoz-Villers and McDonnell 2012, Holwerda et al. 2010). Additionally, this precipitation is difficult to quantify with standard collection techniques (Bruijnzeel et al. 2011, Scholl et al. 2011). Stemflow accounts for very little in the hydrologic budget, about 0-2% (Bruijnzeel et al. 2010) and is often not collected in rainforest studies (Goller et al. 2005, Muñoz-Villers and McDonnell 2012). Net precipitation, stemflow and throughfall, which reaches the forest floor forms about 83% of the precipitation with less than 30% evaporated back into the atmosphere (Bruijnzeel et al. 2010, Fujieda et al. 1997).

The ocean-atmosphere dynamics influence the Pacific Ocean, which becomes seasonably warm starting in June. Seasonality, coupled with the Intertropical Convergence Zone (ITCZ) movement over Costa Rica and the North American Monsoon, leads to wet/dry seasons in the country. Furthermore, the high elevations can

exacerbate the amount of precipitation which falls during this time of the year (Webster et al. 1998, Trenberth et al. 2000, Mook 2000). Additionally, a biennial oscillation of the ENSO-monsoon system enhances the seasonality (Webster et al. 1998). Because of these phenomena, rainfall is fully monsoonal in August, September, and October with a ramping up and waning of the monsoon (May to August and November to December, respectively, Coen 1983, Jarvis and Mulligan 2010).

### *Isotopic Effects*

Isotopic concentration changes are due to kinetic fractionations associated with changes on a regional and a catchment scale. The isotopic concentration of liquid water has two controlling factors: the concentration of the parent vapor source and the temperature at which the water vapor condenses into precipitation (Ingraham 1998).

### Regional Effects

Regionally, the trajectory of the air mass has an influence on precipitation due to the so-called isotopic effects: continental, elevation, latitude, and amount (Rozanski et al. 1993, Ingraham 1998, Dansgaard 1964, Trenberth et al. 2000, Mook 2000). These effects follow a Rayleigh type distillation where heavier isotopes will rain-out (become distilled) first.

A continental effect is observed when water vapor in air masses becomes more depleted further from the source because lighter isotopes are removed from the vapor first. At higher elevations, rainwater will be more depleted due to orographic uplift which is linked with increased (adiabatic) cooling, called the elevation effect. The last feature related to this study is the amount effect which is due to higher relative humidity

during the wet season forcing less evaporation. In addition to these regional effects, the ITCZ is responsible for isotopically lighter air masses reaching inland in tropical locations (Webster et al. 1998).

#### Local Effects

These effects can also be witnessed at the catchment scale and at a smaller temporal scale, such as during large rainstorm events. During a single event, heavy isotopes are the first to rain-out, but their concentrations can sharply increase during prolonged collections due to an amount effect (Ingraham 1998). This effect is caused by a condensing of vapor within the saturated air during large storms as well as a decrease in evaporation due to air saturation. In smaller events, partial evaporation of the liquid phase during its descent to the ground surface will produce more enriched rainfall. The merging of these processes can be seen in studies which associate temperature changes with isotopic concentration changes; Dansgaard (1964) found that for moist-adiabatic cooling starting at 20°C,  $\delta D$  decreases by 2.6‰ and  $\delta^{18}O$  decreases by 0.33‰ per degree of temperature change.

#### *Rainforest Signatures*

The signatures from different sources of precipitation in the rainforest are known to be diverse. Throughfall is comparatively enriched, but these changes are dependent on temperature, humidity, and residence time of the water in the canopy (Scholl et al. 2011). Isotopic signatures of precipitation show slight seasonal variations. During the dry season, precipitation is generated via orographic uplift, whereas the wet season corresponds to the months when the ITCZ is located over Costa Rica and precipitation is



a consequence of convection (Rhodes 2006, Rhodes 2010, Lachneit and Patterson 2002). This ITCZ-related convective precipitation in the wet season is isotopically lighter than the orographic precipitation (Rhodes 2010) implying that this precipitation is recycled via evaporation and re-precipitation (Lachneit and Patterson 2002). During May, the transition between the seasons, variability of isotopes is at its highest due to the migration of the ITCZ over Costa Rica (Lachneit and Patterson 2002). Furthermore, as the rain events progress, a rain-out effect on a regional scale can be witnessed with the removal of the condensed phase depleting the heavier isotopes (Clark and Fritz 1997, Scholl et al. 2011).

## **Methods**

### *Study Site*

The small watershed used in this research is located in Peñas Blancas, Costa Rica at the Texas A&M Soltis Center for Research and Education. Complex geology due to the igneous nature of the site exists alongside a thick andisol clay substrate and dense vegetation. Predominant biota in the area ranges from primary forest trees to grasses in selectively logged areas. The site has been gauged for streamflow with a V-notch weir, stemflow and throughfall monitoring, and piezometers including one piezometer with a pressure transducer. A meteorological station was installed in an open area near the center building; it has measured humidity and temperature at 10 ft and 30 ft, as well as precipitation, wind speed, and solar radiation since 2010.

The objectives of this part of the study were to collect samples at daily intervals and during storms, labeled high frequency events, to characterize precipitation with

respect to streamflow and other collected samples. Water samples were collected in the 2.2 ha watershed for stemflow and throughfall in the tree stand, precipitation outside of the canopy at the center, and streamflow near the V-notch weir (Figure 15). Samples, if sufficient water was available, were taken daily and data from automated tipping bucket precipitation gauges were reported at five minute intervals. Additionally, during five wet season storm events in 2013, high frequency samples were collected at five-minute intervals. Streamflow collection during storms was completed with an ISCO 6712 autosampler and moved to sample bottles the following morning.

#### *Sample Collection*

Over 300 samples were collected during the course of this study. The conductivity and temperature of the samples were measured on site with a YSI 85, and their O and H stable isotope ratios were later determined in the laboratory. Streamflow, stemflow, throughfall and precipitation were collected in 5 high frequency events during June/July 2013; collection during two of these storms can be described as “intense” as they also included throughfall, stemflow, and litter water sampling. Daily samples were also collected for 15 days in January, 5 days in May, 40 days in June and July, and 5 days in October, 2013. Samples were collected in 30 mL high-density polyethylene bottles sealed with Parafilm. Vials which contained headspace due to not enough source water were flagged as possible sources of error and outliers were discarded.

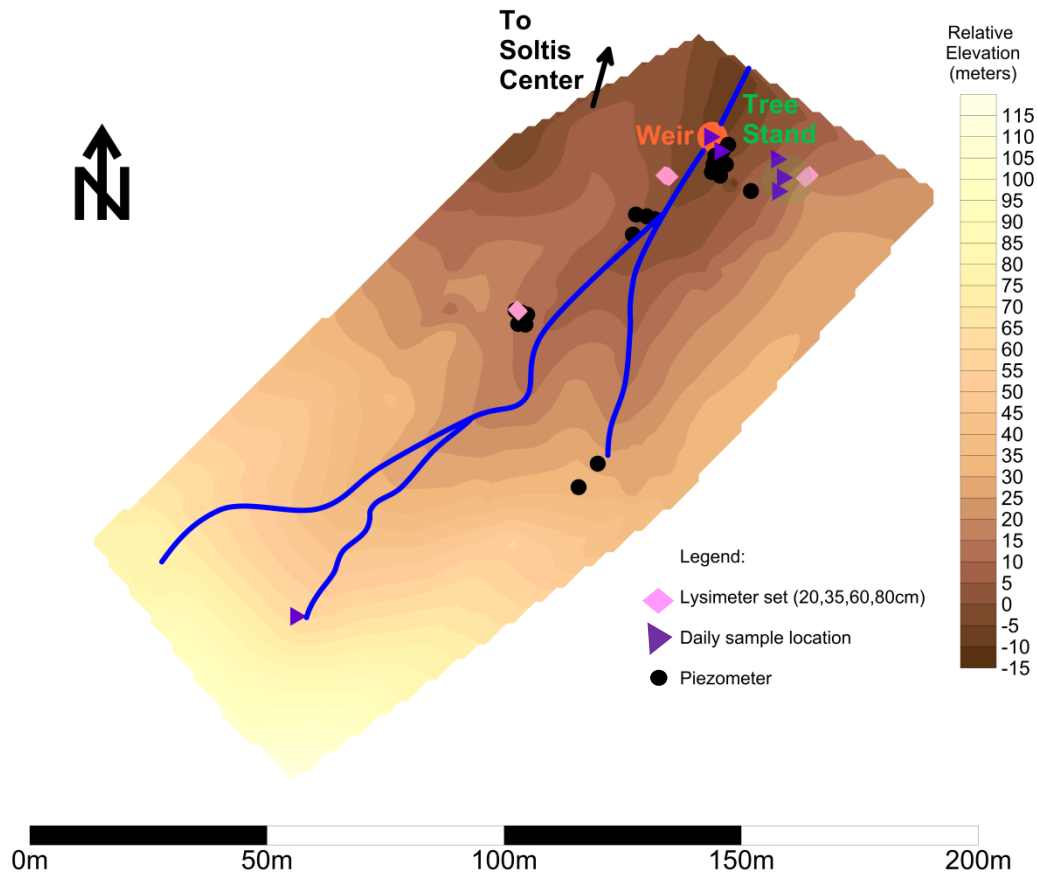


**Figure 15. Gauged locations and daily sampling where elevation gradient is relative to stream outlet at weir. Major elevation changes are located at the S-SW sector and between the weir and tree stand.**

### *Isotope Analysis Techniques*

A Picarro Cavity Ring-Down Spectrometer L2120-i was used to determine  $\delta^{18}\text{O}$  and  $\delta\text{D}$  values in the water samples (Picarro Inc. 2012, Shuss and Seibold 2010). The ring-down spectroscope works by illuminating the cavity and gaseous material ( $\text{H}_2\text{O}$ ) up to 20 km in length using a single-frequency laser diode and three high precision mirrors (Picarro 2012). Once the laser is switched off (in a few tens of microseconds), light decays from the cavity due to optical loss and resonant absorption by the gas (Picarro

2012). The identification of concentrations is evident because the strength of the absorption peak can be recognized with a long effective pathlength (Picarro 2012). Light abundance can then be calculated using the Beer-Lambert Law:  $I(t, \lambda) = I_0 e^{-t/\tau(\lambda)}$  where  $I_0$  is the initial transmitted light intensity and  $\tau(\lambda)$  is the ring down time constant; for a given wavelength, the decay rate,  $R$ , is known for an empty cavity and from that concentration,  $C$ , can be identified using  $R(\lambda, C) = 1/(\lambda) = R(\lambda, O) + c\varepsilon(\lambda)C$  where  $c$  is the speed of light and  $\varepsilon$  is the extinction coefficient (Picarro 2012). The isotope concentration over the abundant isotope concentration gives a ratio that is expressed as a ‰ value and is labeled with a  $\delta$  (delta, Dansgaard 1964, Kendall and McDonnell 1998). Samples were calibrated against an existing international standard VSMOW (NIST RM#8535) and an internal standard SIGF2013 (working lab standard). External precision of the analyzed were  $\pm 0.3\text{‰}$  for  $\delta D$  and  $\pm 0.12$  for  $\delta^{18}O$ .

### *Results Processing*

In this study, data are plotted along with the Global Meteoric Water Line (GMWL) at  $\delta D = 8\delta^{18}O + 10$  and a Local Meteoric Water Line (LMWL) developed on site using established methods (Dansgaard 1964, Craig and Gordon 1965). Evaporation is evident when the trendline of local values depart from the trendline of equilibrium conditions, generally from a slope of 8 to a slope of  $\sim 5$  (Craig and Gordon 1965).

For high frequency samples collected in June and July, air parcels were backward tracked using the HYbrid Single-Particle Lagrangian Integrated Trajectory (HYSPLIT) model (Draxler and Rolph 2014, Draxler and Hess 1999, Draxler and Hess 1998, Draxler and Hess 1997, Rolph 2014).

## **Results and Discussion**

### *Seasonal Variation*

Isotopic ratios in precipitation at the site had a very distinct seasonal trend (Figure 16). Rain sources are enriched in January ( $0.00 \delta^{18}\text{O}$ ,  $10.0 \delta\text{D}$ ) and become more depleted through the transition into the wet season due to the regional rain-out effect ( $-11.0 \delta^{18}\text{O}$ ,  $-80.0 \delta\text{D}$ ). Throughfall and stemflow closely resemble rainfall with slight enrichment at this scale which was expected due to rain-out and amount effects. There is some evidence of evaporation during the wet season as seen by the Local Meteoric Water Line (slope of 7.14) having a slightly lower slope than the Global Meteoric Water Line (slope of 8.00).

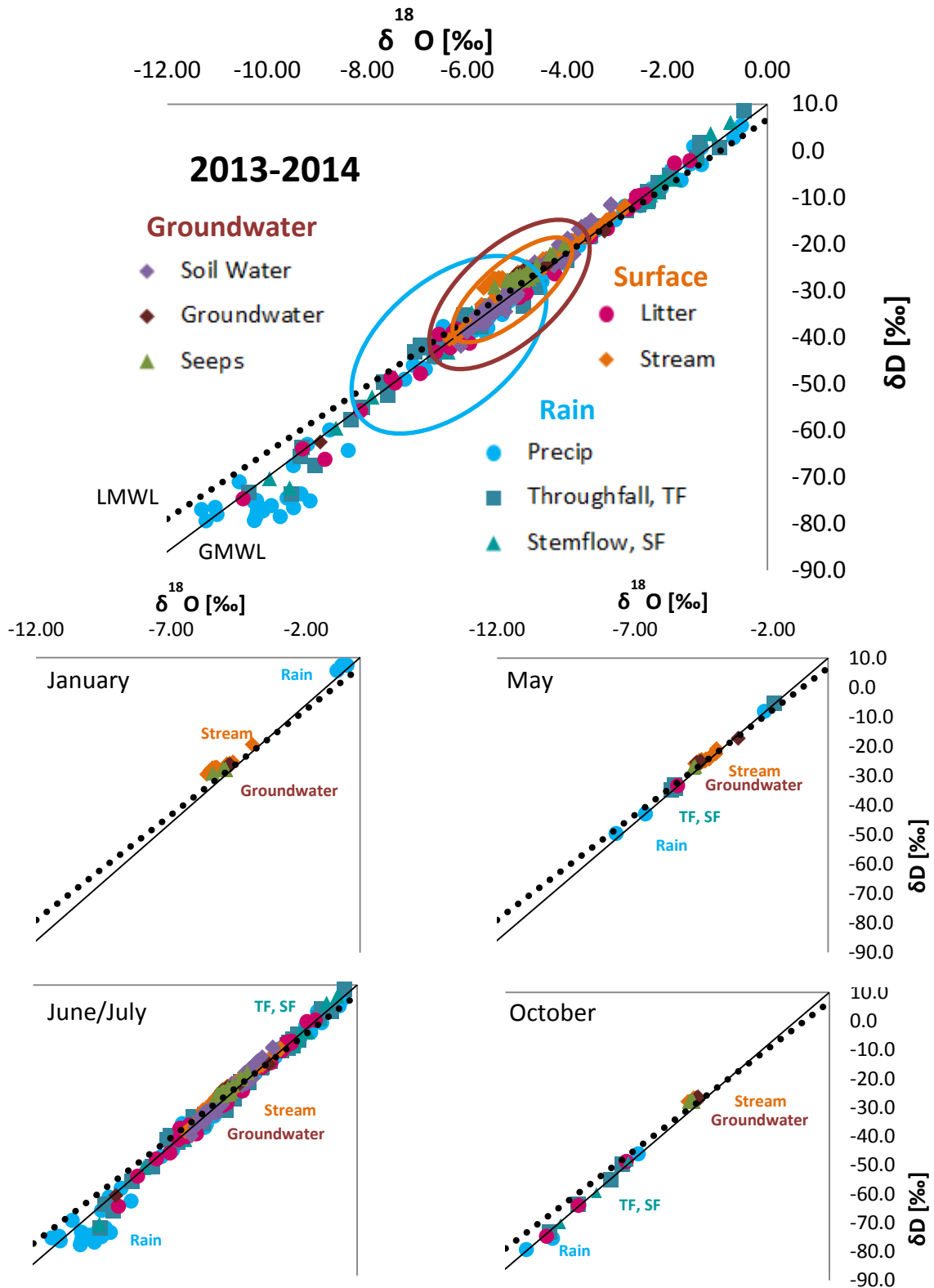


**Figure 16. Annual water isotope trends including precipitation which varies seasonally and streamflow which has less variation. Trends indicate a rain-out and amount effect depletion corresponding to their trajectory over the continent and across the mountain range.**

### *Individual Events*

Storm tracking results from the NOAA HYSPLIT model can display a backward trajectory of air masses which reside at the Soltis Center during each individual event. The HYSPLIT results show that air during the start of the wet season (June-July 2013) can be traced to a range of origins: both the Pacific Ocean (Event 1) and Caribbean Sea (Events 2-5) with some fast, deep convective events (Event 3) and some evapotranspiration recycling (Event 4) as discussed below.

#### Event 1

Event 1 was collected on June 30, 2013 and is the only event without corresponding streamflow discharge amount data from the V-notch weir. In Figure 17, the stream isotopic concentration values and precipitation concentration values are denoted with a delta-plot. Stream values are included because it is a non-fractionating process (Inghrahn 1998) and therefore represents groundwater plus event water. The trendline of precipitation during this event is  $m = 3.72$  which is much less than the trendline of the LMWL ( $m = 6.68$ ). The plot designates that precipitation during the event was evaporated before collection, either during the storm event when the water is traveling to the ground or before reaching the Soltis Center at a more regional scale.

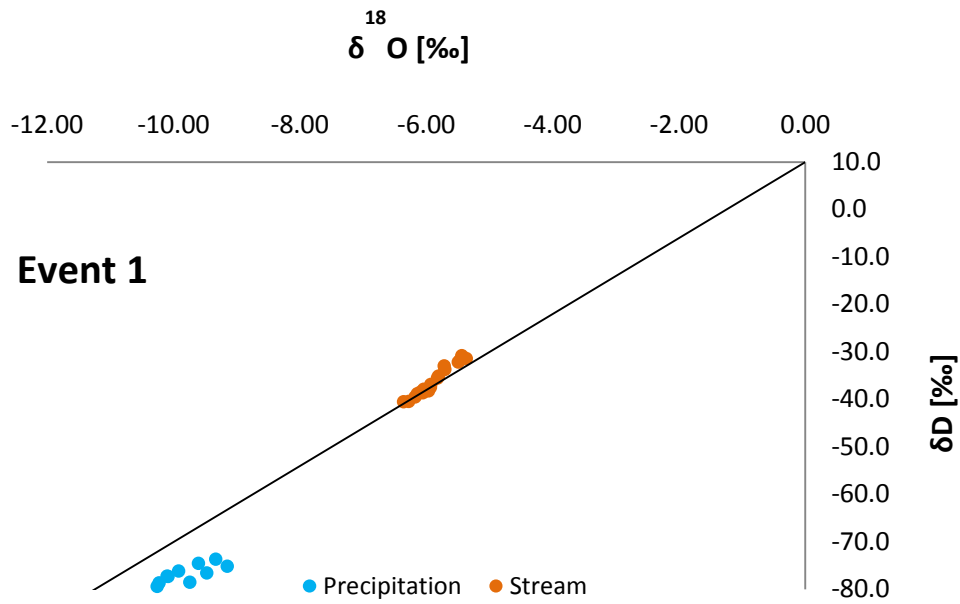


**Figure 17. Event 1 plotted as a  $\delta$ -plot shows stream values (groundwater + event flow) are consistent with the GMWL while the precipitation has an evaporated signature. Baseflow (groundwater) is likely to be a major component of the stream during this storm because the stream values still remain along the GMWL.**

#### Event 2

The second event occurred on July 8, 2013 and lasted for over 2:00 hours. Rain signatures are more depleted which indicates that the rain-out effect was present before and during this storm event (Figure 18).



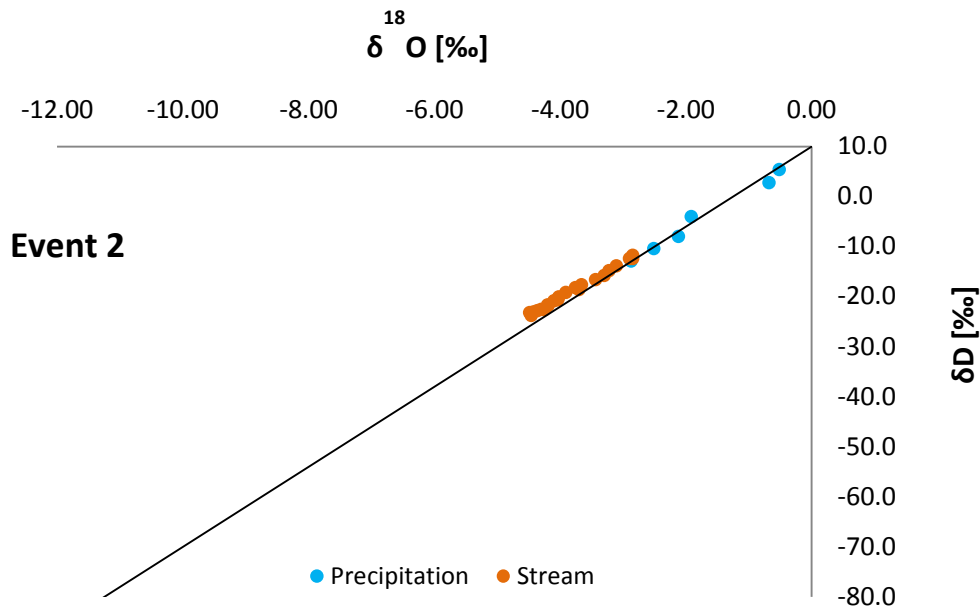


**Figure 18. Event 2 shows an isotopic rain signature which is depleted in heavy isotopes due to rain-out. Stream values are similar to event water but still have an influence from groundwater.**

### Event 3

Event 3 was the first high intensity collection event during this study. Collection of litter water, seeps, throughfall, and stemflow supplemented stream and precipitation samples. The seeps, which are groundwater fed, are mid-range in isotopic composition just like groundwater seen at a daily scale (Figure 19). Compared with the groundwater, precipitation is depleted, possibly from rain-out at a regional scale. However, the stream falls midway between groundwater and precipitation as is expected because it has contributions from both sources. The different types of precipitation are difficult to distinguish showing that at a local scale, evaporation is minimal.

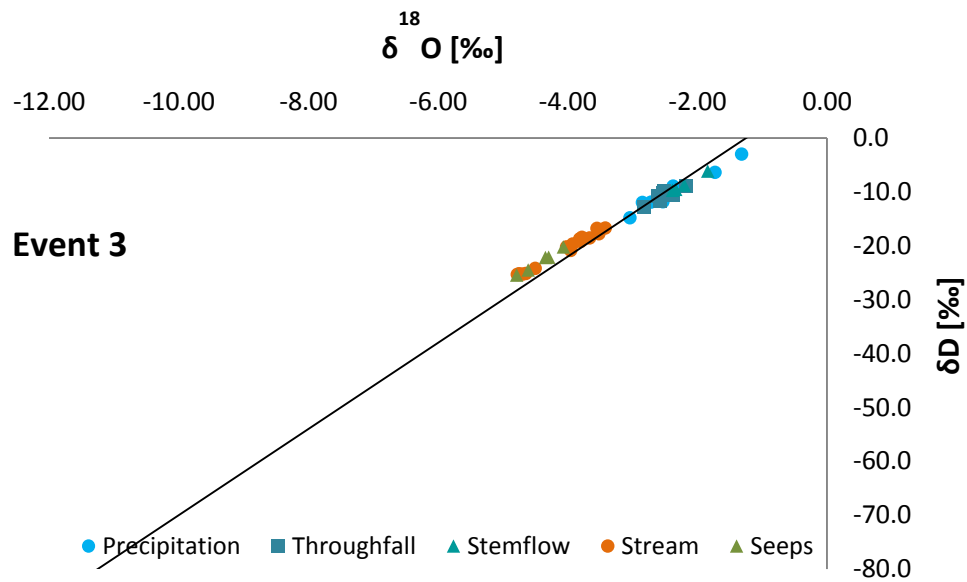


**Figure 19. Event 3 was a deep, fast convection event with heavy isotopic values and a short intensity and duration; precipitation types are similar proving little to no canopy evaporation on site.**

#### Event 4

The HYSPLIT model for event 4 shows a trajectory which crosses over itself in a circular pattern. It also shows that the air mass circulates for about 18:00 hours (3 triangles on the model print-out, Figure 20). This means that the air mass may experience evapotranspiration of water which has previously been rained out; recycled water can then be distributed again further along in the path of the air mass. When comparing to the delta-plot for event 4 (Figure 21), the precipitation has a trendline with a slope of 4.26. This slope is less than the LMWL ( $m = 6.68$ ) indicating evaporation. There may be some evaporation locally, but it is obvious from the slow path of the air mass, that evaporation is also happening on a regional scale.

NOAA HYSPLIT MODEL  
 Backward trajectory ending at 0000 UTC 13 Jul 13  
 GDAS Meteorological Data

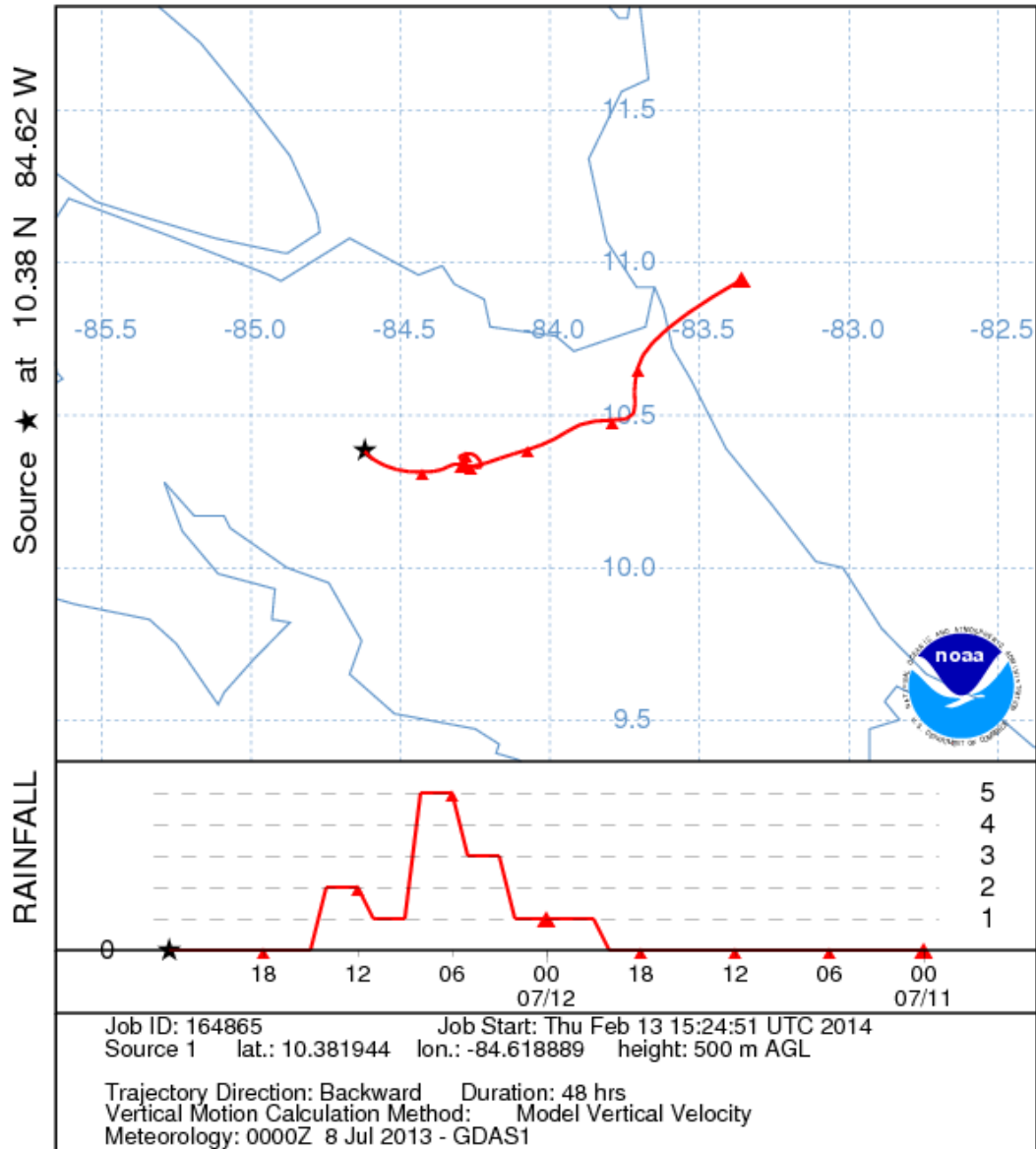
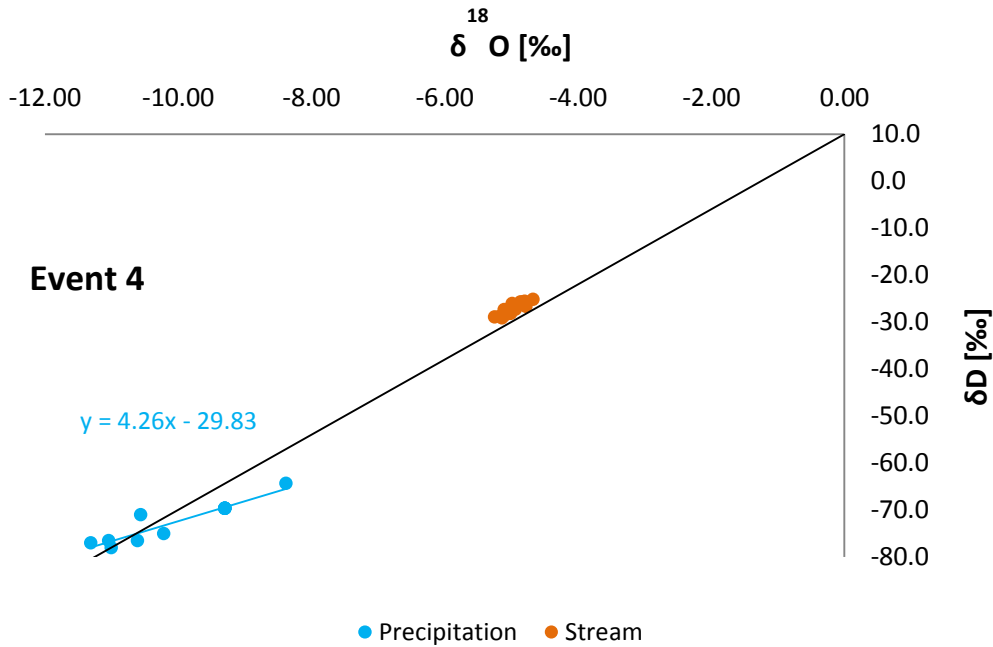


Figure 20. Event 4, which occurred on July 12, 2013, is shown with the HYSPLIT model to see the trajectory backcasted to the Caribbean Ocean. There is recycling of precipitation before the air parcel reaches the Soltis Center as seen by the circular trajectory path.



**Figure 21. Relationship between O-D for event 4 shows that precipitation has an evaporated trend which may occur at a regional scale.**

#### Event 5

There is a similarity between precipitation and streamflow data which is illustrated in Figure 22 showing the last high intensity collection event. Streamflow mimics the isotopic concentration of precipitation until the rain dies off and it is presumed that streamflow becomes mostly baseflow (groundwater) again. Additionally, there is a local rain-out effect seen at 0:30 when values become depleted (-7.00 ‰), and an amount effect at 1:30 (-5.50 ‰) and 2:45 (-5.75 ‰). Because there is a drop in temperature, there is some isotopic enrichment (about 0.33‰ with every 1°C). At -4°C, over 1‰ of change is due to temperature fluctuations. The other change in isotopic signatures can be attributed to an overall rain-out depletion which follows a Rayleigh type distillation. Throughfall mimics precipitation trends with no enrichment due to

evaporation. Figure 23 shows the consistency of throughfall and stemflow to precipitation on a delta-plot.

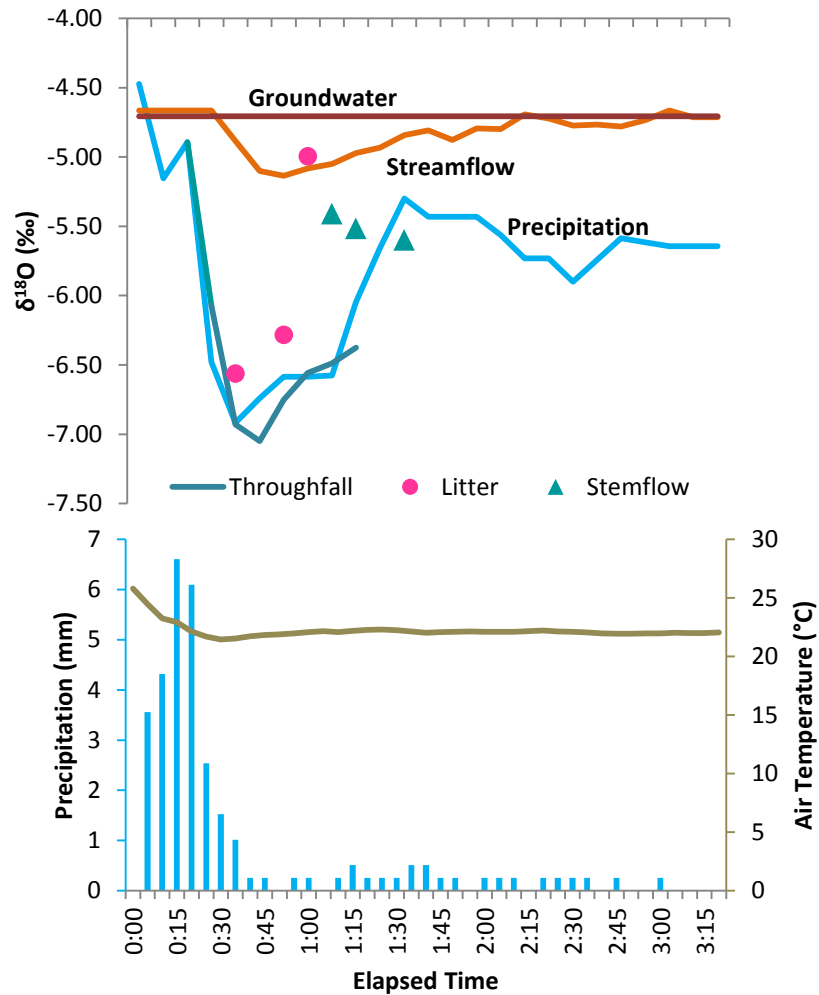


**Figure 22. The rain-out and amount effect is seen at a local scale during event 5. Streamflow follows precipitation patterns until precipitation slows to a minimum. There is some isotopic enrichment with a drop in temperature but an overall rain-out depletion. Precipitation sources (throughfall, stemflow, and litter water) mimic precipitation trends.**

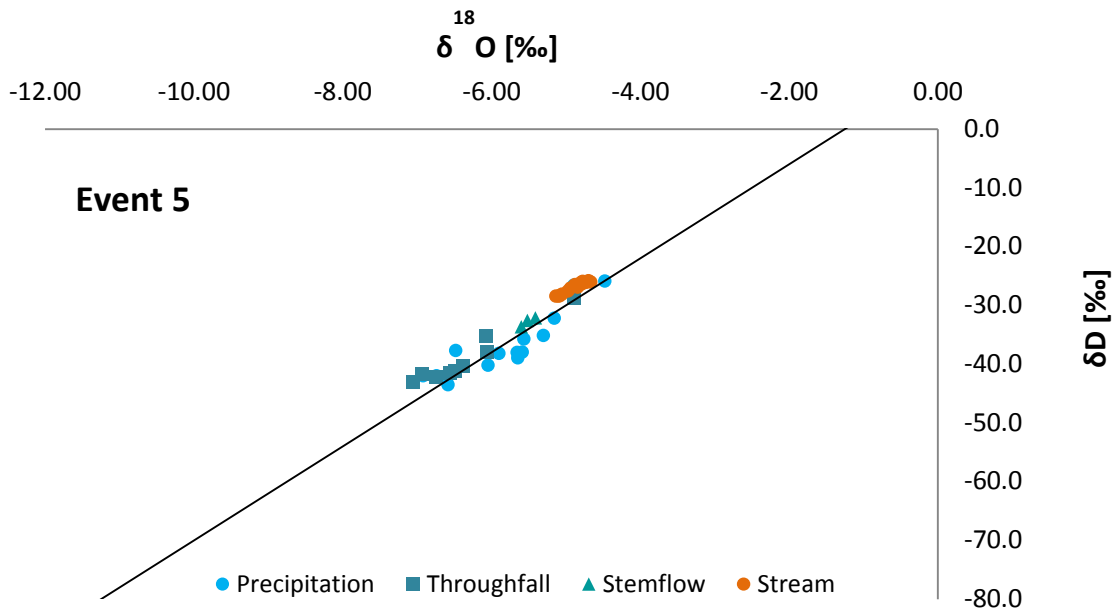


**Figure 23. Event 5 was a slightly slower event where rain-out and a lengthened collection period contributed to the light isotopic values. Throughfall is enriched to precipitation due to its collection at the beginning of the rain event.**

#### All Events

Figure 24 can be referenced as an elapsed time-series comparison for all events and the effect precipitation has on streamflow. Events 2-5 are plotted along with daily collection data for groundwater. Precipitation signatures for  $\delta^{18}\text{O}$  are variable by storm; some storms are more depleted in heavy isotopes than others which indicates that more rain-out occurred at a regional scale during those storms (events 4 and 5). Streamflow shows slight variations in concentration due to event water concentrations, however, all stream data is still influenced by baseflow. Because isotopic concentrations are mass dependent, amount of rainfall is also plotted on the secondary axis.

At the start of event 2, there is a significant fluctuation in streamflow concentration which then attenuates as the rainfall lessens. Event 3 has a small rain-out effect (-1‰) during the storm event. Event 4 has not been plotted with amount data due to the minimal rainfall during the storm. However, as it rains during event 4, there is an amount effect: the air is less saturated during the smaller storm which increases the possibility of evaporation. Evaporation during a storm can create a localized amount effect, so this pattern is not unusual. The largest storm, event 5, has the most variability of rainfall signatures which is to be expected due to a localized amount effect during prolonged storms.

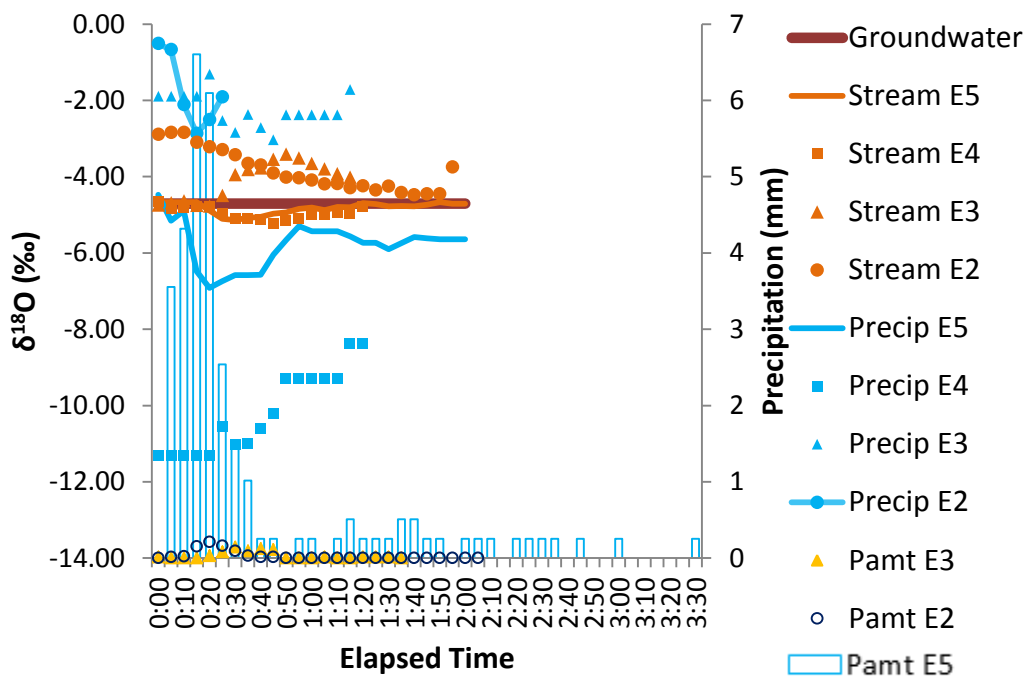


**Figure 24. Comparison of events with a time-series plot shows the localized amount effects during storms 4 and 5 and a rain-out effect during storm 2.**

## Conclusion

Rain sources during the wet season indicated deep convection associated with the ITCZ and the North American Monsoon. This is seen in the HYSPLIT models with acceleration of air masses as it travels across Costa Rica. These air masses originate in both the Pacific Ocean and the Caribbean Sea. As the air masses rise up the mountain in elevation, thermal convection occurs; there is also dynamically forced convection which occurs during the ITCZ in Costa Rica.

The majority of the data was collected during the monsoonal ramping up in May, June, and July with some sampling occurring in October during the wettest month when ocean temperatures are at their warmest. As the wet season progresses, depletion in heavy isotopes occurs that is associated with the raining out of heavy isotopes. Precipitation data collected at this field station are consistent with prior studies conducted in the tropics.

A sharp seasonal trend is visible as well as temporal trends associated with air mass trajectories originating in the Pacific Ocean and the Caribbean Sea. Streamflow shows fluctuations based on precipitation values; however, general streamflow is not completely influenced by precipitation signifying that groundwater plays an important role in this catchment. It was demonstrated that sampling of storm events shows classic rain-out and amount effects. Additionally, some dry season data collection shows the overall seasonality in the rainforest and representation of different precipitation sources.



## CHAPTER IV

### CONCLUSION

#### **Further Studies**

Further research at this small watershed site may include three objectives using data previously collected:

1. DIC tracing as an indicator of geochemical and petrologic reactions in the subsurface including residence times and tracing through litter layer and soil layers;
2. Xylem water analysis as markers for water origin delineated from several sources in the watershed using cryogenic distillation (West et al. 2006); and
3. Mass spectroscopy of water which contains organics (soil, xylem, litter layer) to verify results in accordance with West et al. (2010).

It is important to know the transport mechanisms of water to further identify processes in the watershed and, more importantly, for its fit with larger impact issues. For example, this watershed represents the headwaters which eventually form electricity downstream at the hydroelectric plant in Peñas Blancas; water is also used for consumption by locals (OCIC 2002). The influence of these headwaters could have detrimental effects if pollutants were to travel to the source water and transport processes were not completely understood. Likewise, further study could include the analysis of groundwater at a geochemical level to completely understand advection and dispersion processes occurring at this site. Even with the confidence we put into isotope tracing, there is still a high degree of uncertainty due to different sources and their non-conservative effect as tracers; it can sometimes be difficult to differentiate noise and different signals (Ogunkoya and Jenkins 1993, Kendall and Caldwell 1998).

Data collected during this research was infrequent and only lasted a single year which leads to speculation on groundwater data. Any conclusions drawn about transit times were not reliable due to non-continuous and infrequent data collection which may have left out major groundwater signals. Research which would be instrumental to clarifying the role of groundwater within the system could include using isotope tracers and other non-conservative tracers to fully determine residence, cycling, and transport times with minimal uncertainties. However, this is a lofty goal because it would require deeper wells, perhaps using a portable drill rig described by Gabrielli and McDonnell (2011). Wells would have to be constructed with the utmost care that they are completely sealed to prevent water from bypassing the vadose zone. Data would need to be collected for a much longer time periods including several years with consistent data and with sampling collection refined to less than 1 day between samples. Installation of wells should be placed around the watershed to characterize the entire catchment, and not just close to the stream. For groundwater to stream determination, water would need to be analyzed within a well and the stream at extremely close intervals to determine transit times. Soil water should also be collected to trace water moving through the vadose zone based on its isotopic signature.

### **Closing Remarks**

Precipitation which originates in both the Pacific Ocean and Caribbean Sea moves inland and undergoes the continental, amount, and latitude effects as it is precipitated and re-evaporated along its course. Vapor condenses and precipitates

locally because of orographic uplift associated with adiabatic cooling of the air masses; depending on temperature, relative humidity, intensity, and duration of the storm, a rain-out and amount effect variance can be seen in precipitation concentrations.

Within the canopy, some evaporation may occur but the liquid phase will mostly contribute to stemflow and throughfall as slightly enriched values. These travel in preferential flow directions, down root structures, fractures and fissures in rocks, macropores and animal burrows, down hillslopes (as runoff) and eventually interact with streamflow or groundwater. Soil water has minute contributions to individual stream events; however, it plays an important role in groundwater chemistry and residence/transit time as all subsurface water passes through the soil matrix.

In each event, there is a rapid response between rainfall and streamwater flux which can happen within 10 minutes. Groundwater responds at a slower rate of around 30 minutes. During the entirety of these storms, groundwater is the dominating source of streamflow (80% during the entire storm and at 49% during peak times when flows are above  $0.10 \text{ m}^3/\text{min}$ ).

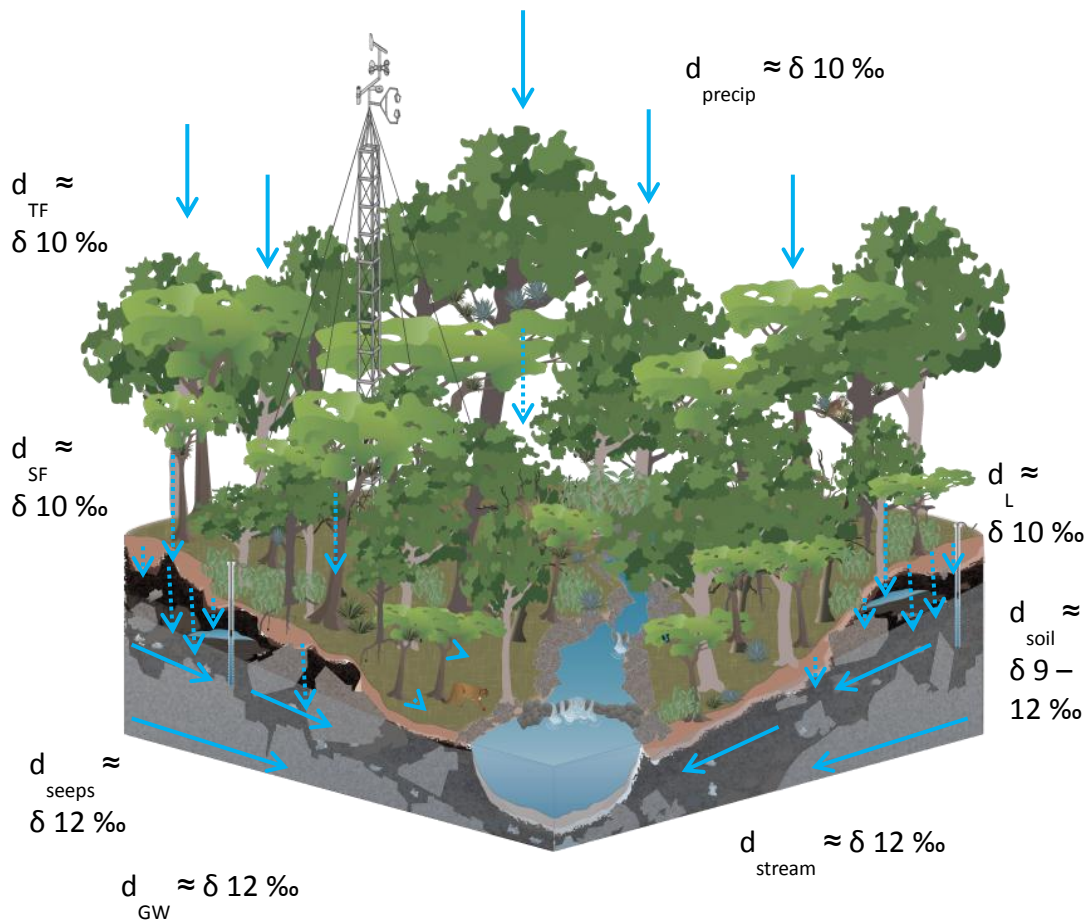


**Figure 25: Model shows a yearly time scale for d-excess values of different sources of water within the watershed as well as the finalized conceptual model. Changes from the initial model include vertical flow pathways and decreased overland flows.**

A conceptual model is shown below to chronicle processes concluded by this thesis (Figure 25). Overall, the isotope transfer function (ITF, which shows how the isotopic signature of water changes as the water moves throughout the watershed) is described at a yearly scale using d-excess values. Precipitation types were found to be very similar ( $d_{\text{precip}} = 10\text{‰}$ ). Throughfall (TF,  $d_{\text{TF}} = 10\text{‰}$ ) and stemflow (SF,  $d_{\text{SF}} = 10\text{‰}$ ) are non-discriminating processes with respect to isotope abundances so they see little change from precipitation values. At a yearly scale, differences in precipitation are

averaged out as well as minor differences in TF and SF due to local evaporation. The watershed was found to infiltrate water in a vertical pathway, unlike what was suspected due to the steep natural topography ( $d_{\text{soil}} = 9 - 12\text{‰}$ ). Additionally, the litter layer water (runoff,  $d_L = 10\text{‰}$ ) is representative of precipitation. The litter layer is minimal during event flows as represented by smaller runoff arrows. Seeps ( $d_{\text{seeps}} = 12\text{‰}$ ) were found to be similar to groundwater values ( $d_{\text{GW}} = 12\text{‰}$ ) which indicate that seeps are fed by an underground reservoir. Lastly, at the yearly scale, stream flow is comprised mostly of baseflow ( $d_{\text{stream}} = 12\text{‰}$ ) with a flow volume of  $0.06 \text{ m}^3/\text{min}$ .

## REFERENCES

- Anderson, A.E., M. Weiler, Y. Alila, and R.O. Hudson. 2009. "Subsurface Flow Velocities in a Hillslope with Lateral Preferential Flow." *Water Resources Research* 45 (11).
- Bachmair, S. and M. Weiler. 2011. "New Dimensions of Hillslope Hydrology." *Ecological Studies: Analysis and Synthesis*. 216: 455-482.
- Bonell, M. and L.A. Bruijnzeel. 2005. "Runoff Generation in Tropical Forests." In *Forests, Water and People in the Humid Tropics: Past, Present and Future Hydrological Research for Integrated Land and Water Management*, 314-406. Cambridge: Cambridge University Press.
- Bruijnzeel L.A., M. Mulligan, and F.N. Scatena. 2011. "Hydrometeorology of Tropical Montane Cloud Forests: Emerging Patterns." *Hydrol. Processes* 25 (3): 465-498.
- Bruijnzeel, L.A., F.N. Scatena, and L.S. Hamilton. 2010. *Tropical Montane Cloud Forests: Science for Conservation and Management*. Cambridge; New York: Cambridge University Press.
- Brutsaert, W. 2005. *Hydrology: An Introduction*. Cambridge; New York: Cambridge University Press.
- Buckwalter, E., N. Tourtellotte, K. Brumbelow, T. Cahill, and G.R. Miller. 2012. Hydrological Processes in a Pre-montane Tropical Forest, 51C-1360, poster presentation at AGU Fall Meeting. San Francisco, California.
- Burns, J.N., R.P. Oien, J. Ackerson, and C. Morgan. 2012. Water Retention Properties of Soil in a Tropical Pre-Montane Transitional Forest, H51-1357, poster presentation at AGU Fall Meeting. San Francisco, California.
- Butler, J.J. 1998. *The Design, Performance and Analysis of Slug Tests*. Lewis publishers; Boca Raton.
- Buttle, J.M. 2006. "Isotope Hydrograph Separation of Runoff Sources." In *Encyclopedia of Hydrological Sciences*: John Wiley & Sons, Ltd. doi:10.1002/0470848944.hsa120.
- Clark, I.D. and P. Fritz. 1997. *Environmental Isotopes in Hydrogeology*. Boca Raton, FL: CRC Press/Lewis Publishers.

- Coen, E. 1983. "Climate." In *Costa Rican Natural History*, edited by Daniel H. Janzen, 35. Chicago: The University of Chicago Press.
- Cohen, L., G.R. Miller, A. DuMont. 2013. Hydrogeologic Processes in a Transitional Tropical Forest, poster presentation at the AGU Fall Meeting. San Francisco, California.
- Craig, H. and L. Gordon. Irwin Conference on Stable Isotopes in Oceanographic Studies and Paleotemperatures. 1965. "Deuterium and Oxygen 18 Variations in the Ocean and the Marine Atmosphere." Consiglio nazionale delle ricerche, Laboratorio de geologia nucleare.
- Dansgaard, W. 1964. "Stable Isotopes in Precipitation." *Tellus (Sweden)* Vol: 16: 436-68.
- Draxler, R.R. and G.D. Hess. 1997. *Description of the HYSPLIT\_4 Modeling System*. Silver Spring, MD: NOAA Air Resources Laboratory.
- Draxler, R.R. and G.D. Hess. 1998. "An Overview of the HYSPLIT\_4 Modeling System of Trajectories, Dispersion, and Deposition." *Aust. Meteor. Mag.* 47: 295-308.
- Draxler, R.R. and G.D. Hess. 1999. *HYSPLIT4 User's Guide*. Silver Spring, MD: NOAA Air Resources Laboratory.
- Draxler, R.R. and G.D. Rolph. 2014. *HYSPLIT (HYbrid Single-Particle Lagrangian Integrated Trajectory) Model Access Via NOAA ARL READY Website (Http://ready.Arl.Noaa.gov/HYSPLIT.Php)*. Silver Spring, MD: NOAA Air Resources Laboratory.
- ESRI. "World Topographic Map.", accessed 01/10, 2014, <http://www.arcgis.com/home/item.html?id=30e5fe3149c34df1ba922e6f5bbf808f>.
- Freeze, R.A. and J.A. Cherry. 1979. *Groundwater*. Englewood Cliffs, N.J.: Prentice-Hall.
- Fujieda, M., T. Kudoh, V. de Cicco, and J.L. de Calvarcho. 1997. "Hydrological Processes at Two Subtropical Forest Catchments: The Serra do Mar, São Paulo, Brazil." *Journal of Hydrology* 196 (1-4): 26-46. doi:10.1016/S0022-1694(97)00015-2.
- Gabrielli, C.P. and J.J. McDonnell. 2012. "An Inexpensive and Portable Drill Rig for Bedrock Groundwater Studies in Headwater Catchments." *HYP Hydrological Processes* 26 (4): 622-632.

- Gabrielli, C.P., J.J. McDonnell, and W.T. Jarvis. 2012. "The Role of Bedrock Groundwater in Rainfall-Runoff Response at Hillslope and Catchment Scales." *Journal of Hydrology* 450-451: 117-133.
- Gat, J. "Isotope Hydrology a Study of the Water Cycle." Imperial College Press.
- Goldsmith, G.R., L.E. Muñoz-Villers, F. Holwerda, J.J. McDonnell, H. Asbjornsen, and T.E. Dawson. 2012. "Stable Isotopes Reveal Linkages among Ecohydrological Processes in a Seasonally Dry Tropical Montane Cloud Forest." *Ecohydrology* 5 (6): 779-790.
- Goller, R., W. Wilcke, M.J. Leng, H.J. Tobschall, K. Wagner, C. Valarezo, and W. Zech. 2005. "Tracing Water Paths through Small Catchments Under a Tropical Montane Rain Forest in South Ecuador by an Oxygen Isotope Approach." *Journal of Hydrology*. 308 (1): 67.
- Gonfiantini, R., K. Fröhlich, L. Araguás-Araguás, and K. Rozanski. 1998. "Isotopes in Groundwater Hydrology." In *Isotope Tracers in Catchment Hydrology*, edited by Carol Kendall and J. J. McDonnell, 87. New York: Elsevier.
- Gonzales, A.L., J. Nonner, J. Heijkers, S. Uhlenbrook. 2009. "Comparison of Different Base Flow Separation Methods in a Lowland Catchment." *Hydrology and Earth System Sciences* 13: 2055-2068.
- González, J.O. 2013. *Proyecto: Geología Del Soltis Center for Research and Education y Alrededores*. Costa Rica: Escuela Centroamericana de Geología.
- Hinton, M.J., S.L. Schiff, and M.C. English. 1994. "Examining the Contributions of Glacial Till Water to Storm Runoff using Two- and Three-Component Hydrograph Separations." *Water Resources Research* 30 (4): 983-993.  
doi:10.1029/93WR03246.
- Holwerda F., L.A. Bruijnzeel, H. Asbjornsen, L.E. Munoz-Villers, and M. Equihua. 2010. "Rainfall and Cloud Water Interception in Mature and Secondary Lower Montane Cloud Forests of Central Veracruz, Mexico." *J. Hydrol. Journal of Hydrology* 384 (1-2): 84-96.
- Hooper, R.P. and C.A. Shoemaker. 1986. "A Comparison of Chemical and Isotopic Hydrograph Separation." *Water Resources Research* 22 (10): 1444-1454.
- Ingraham, N.L. 1998. "Isotopic Variations in Precipitation." In *Isotope Tracers in Catchment Hydrology*, edited by Carol Kendall and J. J. McDonnell, 87. New York: Elsevier.



- Jarvis A. and M. Mulligan. 2011. "The Climate of Cloud Forests." *Hydrol. Processes Hydrological Processes* 25 (3): 327-343.
- Kendall, C. and E.A. Caldwell. 1998. "Fundamentals of Isotope Geochemistry." In *Isotope Tracers in Catchment Hydrology*, edited by Carol Kendall and J. J. McDonnell, 87. New York: Elsevier.
- Kendall, C. and J.J. McDonnell. 1998. *Isotope Tracers in Catchment Hydrology*. Amsterdam; New York: Elsevier.
- Lachniet, M.S. and W.P. Patterson. 2002. "Stable Isotope Values of Costa Rican Surface Waters." *Journal of Hydrology*. 260 (1): 135.
- McDonnell, J.J., M. Sivapalan, K. Vaché, S. Dunn, G. Grant, R. Haggerty, C. Hinz, et al. 2007. "Moving Beyond Heterogeneity and Process Complexity: A New Vision for Watershed Hydrology." *Water Resources Research* 43 (7).
- McGuire, K.J. and J.J. McDonnell. 2010. "W10543 Hydrological Connectivity of Hillslopes and Streams: Characteristic Time Scales and Nonlinearities (Doi 10.1029/2010WR009341)." *Water Resources Research*. 46 (10): n.p.
- Miller, G., G. Moore, G. Orozco, and A. DuMont. 2013. "Transpiration Rates and Responses in a Tropical Pre-Montane Forest." [http://costaricareu.tamu.edu/files/2013\\_atbc.pdf](http://costaricareu.tamu.edu/files/2013_atbc.pdf).
- Mook, W.G. 2000. *Environmental Isotopes in the Hydrological Cycle: Principles and Applications*. Paris: International Atomic Energy Agency and United Nations Education, Scientific and Cultural Organization.
- Munoz-Villers, L.E. and J.J. McDonnell. 2012. "Runoff Generation in a Steep, Tropical Montane Cloud Forest Catchment on Permeable Volcanic Substrate." *Water Resources Research* 48 (9): W09528.
- OCIC. 2002. *Baseline Report Penas Blancas Hydroelectric Project*. Costa Rica: SENTER International.
- Ogunkoya, O.O. and A. Jenkins. 1993. "Analysis of Storm Hydrograph and Flow Pathways using a Three-Component Hydrograph Separation Model." *Journal of Hydrology Journal of Hydrology* 142 (1-4): 71-88.
- Pellerin, B.A., W.M. Wollheim, X. Feng, and C.J. Vorosmarty. 2008. "The Application of Electrical Conductivity as a Tracer for Hydrograph Separation in Urban Catchments." *Hydrological Processes* 22 (12): 1810-1818.

- Picarro. 2013. "Isotope Analyzers", accessed January/11, 2013, [http://www.picarro.com/isotope\\_analyzers](http://www.picarro.com/isotope_analyzers).
- Pinder, G.F. and J.F. Jones. 1969. "Determination of the Ground-Water Component of Peak Discharge from the Chemistry of Total Runoff." *WRCR Water Resources Research* 5 (2): 438-445.
- Rhodes, A.L., A.J. Guswa, and S.E. Newell. 2010. "Using Stable Isotopes to Identify Orographic Precipitation Events at Monteverde, Costa Rica." In *Tropical Montane Cloud Forests: Science for Conservation and Management*, edited by L. A. Bruijnzeel, F. N. Scatena and L. S. Hamilton, 242. Cambridge, U.K.: Cambridge University Press.
- Rhodes, A.L., A.J. Guswa, and S.E. Newell. 2006. "Seasonal Variation in the Stable Isotopic Composition of Precipitation in the Tropical Montane Forests of Monteverde, Costa Rica (DOI 10.1029/2005WR004535)." *Water Resources Research* 42 (11): W11402.
- Ridolfi, L., P. D'Odorico, A. Porporato, and I. Rodriguez-Iturbe. 2003. "Stochastic Soil Moisture Dynamics Along a Hillslope." *Journal of Hydrology -Amsterdam-* 272 (1-4): 264-275.
- Rodriguez-Iturbe, I. 2000. "Ecohydrology: A Hydrologic Perspective of Climate-Soil-Vegetation Dynamics (Paper 1999WR900210)." *Water Resources Research* 36: 3-12.
- Rolph, G.D. 2014. *Real-Time Environmental Applications and Display System (READY) Website (<Http://ready.Arl.Noaa.Gov>)*. Silver Spring, MD: NOAA Air Resources Laboratory.
- Rozanski, K., L. Araguás, and R. Gonfiantini. 2013. "Isotopic Patterns in Modern Global Precipitation." 1-36.
- Schaap, M.G., F.J. Leij, and M.T. van Genuchten. 2001. "Rosetta: A Computer Program for Estimating Soil Hydraulic Parameters with Hierarchical Pedotransfer Functions." *Journal of Hydrology*. 251 (3): 163.
- Scholl M., W. Eugster, and R. Burkard. 2011. "Understanding the Role of Fog in Forest Hydrology: Stable Isotopes as Tools for Determining Input and Partitioning of Cloud Water in Montane Forests." *Hydrological Processes* 25 (3): 353-366.
- Shuss, H. and C. Seibold. "Picarro L1102-i Isotopic Liquid Water Analyzer." accessed 02/12, 2014, [http://snobear.colorado.edu/cgi-bin/Kiowa/Kiowa.com.pl?PicarroL1102\\_i.doc.html](http://snobear.colorado.edu/cgi-bin/Kiowa/Kiowa.com.pl?PicarroL1102_i.doc.html).

- Sivapalan, M. 2003. "Prediction in Ungauged Basins: A Grand Challenge for Theoretical Hydrology." *Hydrological Processes* 17 (15): 3163-3170.
- Sklash, M.G. and R.N. Farvolden. 1979. "The Role of Groundwater in Storm Runoff." *Journal of Hydrology* 43 (1-4): 45-65.
- Soltis Center. "Environmental Education." accessed March/13, 2014, <http://soltiscentercostarica.tamu.edu/content/environmental-education>.
- Texas A&M University. 2013. *The Soltis Center for Research and Education*. <http://soltiscentercostarica.tamu.edu/>.
- Tobon, C., L.A. Bruijnzeel, F.K.A. Frumau, J.C. Calvo-Alvarado. 2010. "Changes in Soil Physical Properties After Conversion of Tropical Montane Cloud Forest to Pasture in Northern Costa Rica." In *Tropical Montane Cloud Forests: Science for Conservation and Management*, edited by L. A. Bruijnzeel, 502-515. Cambridge, U.K.: Cambridge University Press.
- Toledo-Aceves, T., J.A. Meave, M. Gonzalez-Espinosa, and N. Ramirez-Marcial. 2011. "Tropical Montane Cloud Forests: Current Threats and Opportunities for their Conservation and Sustainable Management in Mexico." *Journal of Environmental Management* 92 (3): 974-981.
- Trenberth, K.E., D.P. Stepaniak, and J.M. Caron. 2000. "The Global Monsoon as seen through the Divergent Atmospheric Circulation." *Journal of Climate* 13 (22): 3969-3993.
- Turner, J.V. and C.J. Barnes. 1998. "Modeling of Isotope and Hydrogeochemical Responses in Catchment Hydrology-Chapter 21."
- UMS. "UMS", accessed 02/13, 2014, <http://www.ums-muc.de/>.
- Webster, P.J., V.O. Magaña, T.N. Palmer, and J. Shukla. 1998. "Monsoons: Processes, Predictability, and the Prospects for Prediction." *Journal of Geophysical Research*. 103 (C7): 14.
- Weiler, M. and J.J. McDonnell. 2004. "Virtual Experiments: A New Approach for Improving Process Conceptualization in Hillslope Hydrology." *Journal of Hydrology -Amsterdam* 285 (1-4): 3-18.
- West A.G., G.R. Goldsmith, P.D. Brooks, and T.E. Dawson. 2010. "Discrepancies between Isotope Ratio Infrared Spectroscopy and Isotope Ratio Mass Spectrometry for the Stable Isotope Analysis of Plant and Soil Waters." *Rapid Communications in Mass Spectrometry: RCM* 24 (14): 1948-54.

West A.G., S.J. Patrickson, and J.R. Ehleringer. 2006. "Water Extraction Times for Plant and Soil Materials used in Stable Isotope Analysis." *Rapid Communications in Mass Spectrometry: RCM* 20 (8): 1317-21.

APPENDIX A

TABLES

Month	Year	Air_T(10ft) avg	RH%_10ft avg	SlW/m2_Avg avg	AirTC_30_A RH%_30ft avg	VPD_10 avg	Precip (mm) extrap for month	Q Har mea in dfs	Q Har mea in m3/min	StandT (mm) _sum
Jun	2010	23.93	86.67	180.73	24.13	86.22	0.45	312.17		
Jul	2010	23.72	87.60	163.54	23.96	86.69	0.40	387.86		
Aug	2010	23.65	88.13	168.59	23.83	87.12	0.38	471.42		
Sept	2010	23.61	85.00	173.81	23.91	82.71	0.48	476.25		
Oct	2010	23.21	84.81	146.22	23.46	82.62	0.47	389.13		
Nov	2010	22	87.49	119.65	22.23	85.67	0.40	479.04		
Dec	2010	20.14	88.79	89.45	20.33	87.35	0.28	600.46		
Jan	2011	21.75	87.4	109.24	21.90	86.54	0.36	370.84		
Feb	2011	22.26	85.76	137.15	22.33	85.08	0.42	222.76		
Mar	2011	22.7	80.8	171.53	22.79	79.91	0.58	95.25		
Apr	2011	23.68	78.33	178.79	23.89	77.17	0.70	87.88		
May	2011	24.15	82.56	179.39	24.44	80.95	0.58	490.73		
Jun	2011	24.29	84.68	167.45	24.46	83.20	0.51	342.39		
Jul	2011	23.46	88.02	154.48	23.58	86.42	0.70	599.19		
Aug	2011	23.93	85.20	173.49	24.11	82.94	0.88	313.94		
Sept	2011	23.96	85.52	179.83	24.14	83.38	0.88	511.56		
Oct	2011	23.16	85.62	137.38	23.41	83.11	0.81	496.82		
Nov	2011	21.95	90.35	94.37	22.12	88.38	0.50	410.21		
Dec	2011	21.64	89.29	96.88	21.79	87.57	0.55	440.18		
Jan	2012	22.39	81.62	156.23	22.42	80.45	0.53	37.59	76.02	
Feb	2012	22.68	81.88	164.17	22.71	80.71	0.54	131.32	54.31	
Mar	2012	22.59	82.43	146.29	22.65	80.99	0.52	147.83	45.21	
Apr	2012	23.71	82.39	171.94	23.78	80.95	0.57	199.14	48.67	
May	2012	24.16	85.49	164.04	24.29	83.73	0.48	325.63	46.89	
Jun	2012	24.13	85.41	168.93	24.30	83.38	0.49	351.54	45.35	
Jul	2012	23.20	85.41	115.36	23.27	88.14	0.32	281.94	51.05	
Aug	2012	23.69	86.46	163.44	23.87	84.42	0.44	487.43	53.17	
Sept	2012	23.33	88.90	137.59	23.49	87.20	0.35	546.61	43.06	
Oct	2012	23.24	86.47	138.24	23.50	83.99	0.41	398.78	46.50	
Nov	2012	23.24	86.47	138.24	23.50	83.99	0.41	398.78	32.10	
Dec	2012	22.07	90.35	87.33	22.16	89.19	0.27	429.51		
Jan	2013	23.05	80.98	138.40	23.05	79.95	0.57	37.34		
Feb	2013	22.77	80.47	130.08	22.82	79.25	0.58	54.36	0.166	0.282
Mar	2013	22.44	85.21	107.86	22.48	84.39	0.45	320.55	44.30	
Apr	2013	24.01	81.68	144.98	24.05	80.60	0.59	64.52	0.117	0.199
May	2013	23.92	83.19	146.31	23.99	82.23	0.55	417.83	0.061	0.104
Jun	2013	24.07	85.39	85.01	24.14	84.21	0.47	176.02		
Jul	2013	23.71	87.37	125.68	23.38	82.03	0.40	224.79	0.010	0.017
Aug	2013	25.87	79.09		25.53	79.13	0.70	226.60	0.02	0.034
Sept	2013	26.45	76.45		26.18	76.13	0.81	11.85	0.019	0.032
Oct	2013	25.70	81.18		25.46	81.21	0.62	0.00	0.026	0.044
Nov	2013								0.029	0.049
Dec	2013									

- Notes:
- 1) Gray spots represent no data or a calculated data point
  - 2) Gray and NA values for Precip indicate that the second tipping bucket was taken offline
  - 3) Values which do not include a full month are highlighted in green
  - 4) Graphed values have been extrapolated to represent an entire month, where applicable

Daily Sample Collection January									
Date	I.D.	Weather	Type	Time	Comments	Conductivity (µS)	Temp (°C)	d18O vsmow	dD vsmow
1/7/2013	J1	S	Clear, sunny	Frogs	10:10	NA	NA	-5.67	-29.6
1/8/2013	J2	S	Clear, sunny	Snakes	10:17	NA	NA	-5.56	-28.3
1/9/2013	J3	S	Partly cloudy	Snakes	14:50	NA	NA	-5.38	-27.4
1/9/2013	J3	S	Partly cloudy	US weir, DS piezos	14:00	NA	NA	-5.30	-27.2
1/9/2013	J3	NA	Clear, sunny	Bridge	10:24	NA	NA	-5.61	-28.6
1/9/2013	J3	NA	Partly cloudy	Bridge	15:00	NA	NA	-5.44	-27.3
1/9/2013	J3	NA	Partly cloudy	S. Stream	14:05	NA	NA	-5.65	-28.3
1/9/2013	J3	NA	Partly cloudy	Confluence	14:10	NA	NA	-5.32	-27.3
1/9/2013	J3	E	Clear, sunny	Seeps	12:45	NA	NA	-5.45	-29.2
1/10/2013	J4	S	Clear, sunny	Stream	10:40	NA	NA	-5.47	-27.4
1/10/2013	J4	NA	Partly cloudy	Lab 2 Faucet	16:00	NA	NA	-5.67	-29.1
1/11/2013	J5	S	Clear, sunny	Stream	10:45	NA	NA	-5.44	-27.5
1/12/2013	J6	NA	Clear, sunny	S. Stream	10:50	NA	NA	-5.67	-28.4
1/13/2013	J7	S	Clear, sunny	Weir at V-notch	13:15	NA	NA	-5.36	-27.2
1/14/2013	J8	NA	Clear, sunny	Confluence	13:20	NA	NA	-5.48	-27.4
1/15/2013	J9	NA	Clear, sunny	Frog pond inlet hose	15:15	NA	NA	-5.62	-28.0
1/6/2014	J1.14	E	Partly Cloudy		14:34	77.5	22.1	-4.99	-27.9
1/6/2014	J1.14	S	Partly Cloudy		16:50	104.1	22.0	-4.75	-26.1
1/6/2014	J1.14	G	Partly Cloudy		16:55	79.96	NA	-4.80	-26.5
1/7/2014	J2.14	E	Partly Cloudy		16:15	74.5	21.9	-4.99	-27.7
1/7/2014	J2.14	S	Light rain		16:40	89.2	21.1	-3.99	-19.5
1/7/2014	J2.14	G	Light rain		16:45	78.5	NA	-4.80	-26.4
1/7/2014	J2.14	P			20:00	28.9	23	-0.68	7.3
1/8/2014	J3.14	E	Clear and sunny		11:20	78.6	22	-5.09	-27.9
1/8/2014	J3.14	S	Cloudy		4:15	97.5	21.9	-4.82	-25.8
1/9/2014	J4.14	E	Partly cloudy		11:00	72.7	21.9	-4.97	-28.0
1/9/2014	J4.14	S			15:25	97.8	22	-4.93	-26.0
1/9/2014	J4.14	G			15:19	78.4	NA	-4.84	-26.4
1/9/2014	J4.14	P	Not enough for EC/T		21:45	NA	NA	-0.85	5.6
1/10/2014	J5.14	E			12:10	74.3	21.9	-5.05	-27.9
1/10/2014	J5.14	S			13:45	96.8	22	-4.70	-25.4
1/10/2014	J5.14	G			13:40	79.1	NA	-4.87	-26.3
1/10/2014	J5.14	P			21:30	NA	NA	-0.48	7.3

Notes:

- 1) Blue values are from Picarro
- 2) Green values are flagged for head

Daily Sample Collection May										
Date	I.D.	Weather	Type	Time	Comments	Conductivity (µS)	Temp (°C)	d18O vsmow	dD vsmow	
8-May M1	S	Cloudy 81F	Bridge	1025		50.5	23.4	-4.75	-26.6	
	S		Snakes	1035		97.8	22.2	-4.60	-25.6	
	G		P-mid	1115	WL 1.854 m TD 1.918 m	NA	NA	-4.76	-25.5	
	S		Weir	1120		46.9	23.4	-4.83	-25.9	
	S		Btw W&P	1425		99.8	22.4	-4.51	-25.0	
	S		US W&P	1415		100.6	23.1	-4.49	-25.1	
	NA		Confluence	1143		97.7	23.0	-4.71	-25.2	
	NA		S.Stream	1420		61.0	22.9	-4.71	-26.5	
	E		Seeps	1340		38.5	23.4	-4.82	-26.8	
	NA		Frog Pond	1152	inlet hose	58.1	23	-4.83	-26.5	
	NA		Soltis Center Lab 2	1215	from faucet	45.0	27.9	-4.80	-27.1	
	10-May M2		S	Raining	Bridge	947		81.7	22.8	-4.04
S		Snakes	950			105.1	22.1	-4.06	-22.6	
S		Weir	925			101.1	22.1	11.02	12.6	
S		Btw W&P	912			101.0	22.5	-4.19	-22.9	
S		US W&P	915			102.4	22.3	-4.20	-22.9	
NA		Confluence	920			98.2	22.2	-1.88	-5.9	
T		Throughfall	955		bulk sample	NA	NA	-1.95	-5.3	
P		Rain	1020		without mineral oil	NA	NA	-2.31	-8.2	
NA		Bungalow Stream	1025		in front of dorm 1	69.8	23.1	-4.42	-23.5	
11-May M3	E	Cloudy	Seeps	750		79.6	23.4	-4.88	-27.2	
	G		P-mid	825	1.848 depth, recharged	NA	NA	-3.25	-17.3	
	NA		S. Stream	830		70.8	22.8	-4.44	-25.5	
12-May M4	P	Cloudy, rain during night	Rain	915	no oil, no sun out	20.0	24.3	-7.68	-49.7	
	P		Rain	915	with oil, no sun out	6.1	24.6	-6.62	-43.0	
	NA		Dorm stream	930		77.2	23.3	-4.76	-27.1	
	NA		Soltis Center Lab 2	920	very turbid faucet ~25.0	86.6	26	-4.82	-27.0	
13-May M5	S	Cloudy, rain during night	V-notch weir	829		98.4	22.2	-4.43	-24.3	
	S		Snakes	820		100.3	22.0	-4.67	-24.9	
	NA		Frog Pond	805		73.7	22.7	-4.69	-25.1	
	G		P-mid	845	bailed dry, after sample, WL 1.	NA	NA	-4.62	-25.1	
	S		Ups All	837		97.2	22.1	-4.58	-24.5	
	NA		S. Stream	835		65.4	22.4	-4.64	-25.0	
	T		TF Bottom	1010	mineral oil	29.9	22.8	-5.69	-34.7	
	T		TF top	1300	mineral oil	26.8	23.5	-5.57	-33.3	
	S		DS Weir	832		93.3	22.2	-4.30	-24.5	
	S		Bridge	815		65.4	22.0	-4.55	-25.2	
	L		Litter	925		NA	NA	-5.46	-33.4	
	T		TF Mid	930	mineral oil	37.4	22.8	-5.52	-34.3	
	S		Btw weir and P	840		97.5	22.1	-4.44	-25.0	
	G		P-trans	850		NA	NA	-4.70	-26.2	

Notes:

- 1) Blue values are from Picarro
- 2) Green values are flagged for head



**Daily Sample Collection June-July**

Date	I.D.	Weather	Type	Time	Comments	Conductivity (µS)	Temp (°C)	D180 vsmow	dD vsmow
Monday, June 10	D1	P Cloudy/drizzle and two storms (am and pm)	Precip	1215	w/min oil; morning storm	NA	NA	-4.28	-22.8
			Litter	1330	3 wk old water	NA	NA	-6.34	-42.3
			P-Mid	1332	1.935m TD	NA	NA	-4.64	-25.8
			Stream	1340	US piezos	100.7	23.9	-4.58	-25.7
			TF	1355	mid and top	NA	NA	-4.31	-23.5
			E Seeps	1405		75.5	23.2	-4.80	-26.8
Tuesday, June 11	D2	S Partly cloudy, no rain	Stream	1250		101.9	22.7	-4.67	-25.8
			Litter	1310	by dataloggers	NA	NA	-5.95	-41.3
			TF	1315	bot and mid	NA	NA	-4.87	-33.3
			E Seeps	1335		75.3	22.4	-4.78	-27.0
Wednesday, June 12	D3	S	Stream	950		58.9	22.6	-4.55	-25.9
			Litter	955		NA	NA	-4.25	-26.5
			G P-mid	1000	dry well	NA	NA	-4.74	-26.0
			TF	1015	mid&bot, param on top/bot	13.4	22.5	-4.02	-23.5
			E Seeps	1025		70.5	22.1	-4.68	-26.7
			P Precip	1245		5.7	24.3	-4.06	-24.1
Thursday, June 13	D4	S Rain in pm	Stream	1350	E&G sandbagged at 1015	103.6	23.3	-4.63	-25.6
			Litter	1400		NA	NA	-4.96	-31.5
			TF	1405		NA	NA	-5.27	-33.2
			E Seeps	1415		79.0	22.4	-4.91	-27.3
			P Precip	1500		6.3	23.4	-8.75	-59.9
Friday, June 14	D5	S	Stream	815		96.2	22.3	-4.74	-26.2
			G P-mid	820	1.860m WL, 1.922m TD	NA	NA	-8.94	-62.5
			Litter	825	top collector	NA	NA	-4.62	-25.9
			TF	845	middle	13.0	22.7	-9.33	-65.5
			E Seeps	900		76.0	22.2	-4.76	-27.5
			P Precip	915		NA	NA	-9.47	-67.6
Saturday, June 15	D6	S Nice day out	Stream	830		83.4	23	-4.88	-26.2
			Litter	840	near stream	14.1	23	-7.44	-49.9
			TF	857	middle	10.8	23.4	-6.66	-44.1
			E Seeps	910		75.2	22.3	-5.17	-27.9
			P Precip	1055		11.5	29.6	-6.65	-44.4
Sunday, June 16	D7	S Misty in the morning	Stream	805		89.8	22.7	-5.00	-26.7
			TF	807	bottom	10.8	22.7	-4.57	-29.3
			Litter	825	top collector	6.3	22.5	-6.19	-41.1
			E Seeps	845		76.8	22.1	-5.20	-27.8
			P Precip	915		5.9	25.1	-4.67	-29.1
Monday, May 17	D8	S No rain	Stream	1300		98.1	23.8	-5.02	-26.5
			G P-mid	1305		NA	NA	-5.01	-26.5
			E Seeps	1325		77.6	23.2	-5.11	-27.9
Tuesday, May 18	D9	S T-storms in afternoon Rain night before	Stream	1310		99.4	23.3	-4.93	-26.2
			Litter	1320		NA	NA	-6.63	-43.3
			TF	1322	to pand mid	NA	NA	-5.73	-37.7
			E Seeps	1340		78.4	22.8	-5.18	-27.9
			P Precip	1510	not enough	NA	NA	-5.88	-38.7
Wednesday, June 19	D10	S 2" at night	Stream	0800		92.3	22.6	-4.95	-26.2
			G P-mid	0807		NA	NA	-4.82	-26.3
			Litter	0825	by sapflow	NA	NA	-4.42	-25.0
			TF	0827	middle	17.0	23.1	-4.35	-24.2
			E Seeps	0842		76.0	22.5	-4.95	-27.3
			P Precip	1015		14.5	26	-4.27	-24.1
Thursday, June 20	D11	S Rain in am	Stream	0819		94.5	22.6	-4.76	-25.3
			TF	0835	top collector	16.8	22.9	-3.53	-18.3
			E Seeps	0847		76.4	22.2	-5.03	-27.2
			P Precip	905		9.7	23	-3.46	-16.4
			35 Weir	1430	bulk params	124.1	25.3	-5.62	-37.0
			60	1430		NA	NA	-4.78	-25.7
			80	1430		NA	NA	-4.54	-24.7
			20	1430		NA	NA	-4.99	-31.2

Friday, June 21	D12	S	Some rain in late afternoon	Stream	835	102.5	22.7	-4.82	-26.2		
		G		GW	840	p-mid	NA	NA	-4.84	-26.6	
		20		Sapflow	Lysimeter	1505	sapflow	NA	NA	-6.00	-39.0
		35			Lysimeter	1505		NA	NA	-5.23	-30.9
		60			Lysimeter	1505		30.0	25	-3.71	-16.3
		80			Lysimeter	1505		NA	NA	-3.12	-11.4
		L			Litter	902	by sapflow	16.9	23.6	-4.13	-23.4
		T			TF	905	top collector	NA	NA	-3.56	-18.5
		E			Seeps	920		77.7	22.5	-5.08	-27.6
		P			Precip	1610		NA	NA	-7.25	-49.1
Saturday, June 22	D13	S		Stream	945	106.3	22.5	-4.72	-25.5		
		G		GW	950	p-mid (til dry) and p-ds	NA	NA	-4.71	-25.7	
		L		Litter	1020	litter	16.9	23.7	-6.93	-47.8	
		T		TF	1025	TF-mid + TF-Top	16.0	23.5	-7.58	-52.5	
		E		Seeps	1035		79.9	22.6	-4.87	-27.8	
		P		Precip	1110		NA	NA	-6.89	-46.7	
Sunday, June 23	D14	S	No rain	Stream	608	102.8	22.3	-4.73	-26.2		
		E		Seeps	627		81.2	22.2	-4.92	-27.5	
Monday, June 24	D15	S	Light Drizzle night before	Stream	947	106.4	22.6	-4.78	-26.0		
		G		GW	957	S1	NA	NA	-4.64	-25.4	
		L		Litter	1001	near stream	NA	NA	-4.82	-30.6	
		E		Seeps	1019		82.4	22.3	-4.87	-27.5	
		P		Precip	1146		NA	NA	-6.13	-41.1	
		20		Trail	Lysimeter	1538	trail; sample from ea.	59.4	24.1	-5.89	-38.0
		35			Lysimeter	1538	3/4	NA	NA	-5.68	-37.3
		60			Lysimeter	1538	1/2	NA	NA	-5.83	-35.4
80	Lysimeter	1538	3/4		NA	NA	-5.03	-29.7			
Tuesday, June 25	D16	S	1mm rain	Stream	824	103.3	22.3	-4.79	-25.6		
		G		GW	830	S2B	NA	NA	-4.81	-26.0	
		P		Precip	804		NA	NA	-4.50	-28.1	
		L		Litter	842	sapflow	NA	NA	-3.19	-16.7	
		E		Seeps	856	3/4	81.5	22.3	-5.01	-27.2	
		20W		Lysimeter	1120	Weir; sample from ea.	45.6	24.5	-5.05	-31.2	
		35W		Lysimeter	1120	20 and 35, 1/2	NA	NA	-5.22	-34.5	
		60W		Lysimeter	1120		NA	NA	-4.84	-26.7	
		80W		Lysimeter	1120		NA	NA	-4.39	-23.5	
		20SF		Lysimeter	1625	SF; sample from ea.	36.1	22.2	-5.47	-35.1	
		35SF		Lysimeter	1625	all 7/8	NA	NA	-5.22	-31.1	
		60SF		Lysimeter	1625		NA	NA	-3.63	-15.8	
		80SF		Lysimeter	1625		NA	NA	-3.14	-11.7	
Wednesday, June 26	D17	P	30mm rain	Precip	834	7.4	23.9	-6.22	-38.2		
		S		Stream	934	103.2	22.2	-4.87	-26.0		
		G		GW	916	S2B	NA	NA	-4.39	-24.4	
		L		Litter	1019	sapflow	15.6	22.8	-6.22	-38.3	
		T		TF	1022		14.8	22.8	-5.98	-36.7	
		F		SF	1025	Murky, poss. Contaminated	132.2	22.6	-5.91	-34.8	
		E		Seeps	1041		80.4	22.4	-4.93	-27.4	
		20W		Lysimeter	1255	by weir; sample from ea.	49.3	24.7	-5.11	-30.7	
		35W		Lysimeter	1255		NA	NA	-5.32	-33.7	
		60W		Lysimeter	1255		NA	NA	-4.96	-27.1	
		80W		Lysimeter	1255		NA	NA	-4.65	-23.9	
		20SF		Lysimeter	1255		NA	NA	-5.29	-33.6	
		35SF		Lysimeter	1255		NA	NA	-5.21	-31.3	
60SF	Lysimeter	1255		NA	NA	-3.78	-16.9				
80SF	Lysimeter	1530	by sf; sample from ea.	34.0	23.8	-3.12	-11.9				
Thursday, June 27	D18	S		Stream	825	96.2	22.3	-4.68	-24.7		
		L		Litter	835		14.8	22.7	-2.42	-9.4	
		F		Stemflow	840	top, was completely filled	55.6	22.3	-2.13	-6.7	
		T		TF	845	top	21.3	22.5	-2.18	-6.9	
		E		Seeps	850		76.5	22.2	-4.87	-26.7	
		P		Precip	1020		8.0	22.9	-1.87	-5.8	
Friday, June 28	D19	S	No rain all day/night	Stream	1515	103.2	23.6	-4.67	-25.3		
		E		Seeps	1530		79.5	22.4	-4.96	-27.1	
Saturday, June 29	D20	S	No rain	Stream	1340	98.7	22.9	-4.79	-25.7		
		G		GW	1345	p-mid	NA	NA	-4.82	-26.2	
		E		Seeps	1400		74.9	22.5	-5.00	-27.0	

Sunday, June 30	D21	S	Light drizzle in pm	Stream	1100	99.6	23	-4.91	-26.6
		G		GW	1104 p-mid	NA	NA	-4.85	-26.3
		L		Litter	1107 by weir, bulk from last time sampled	19.0	23.3	-4.85	-28.9
		F		Stemflow	1145 top	162.3	25	-6.38	-43.2
		T		TF	1150 mid, param bulk	26.3	24	-9.04	-67.6
		20		Lysimeter	1130 trail	31.7	23.9	-5.13	-32.0
		35		Lysimeter	1130	NA	NA	-5.27	-32.9
		60		Lysimeter	1130 3/4	NA	NA	-5.74	-35.2
		80		Lysimeter	1130	NA	NA	-5.66	-33.8
		P		Precip	1413	6.9	28.6	-10.07	-76.9
		E		Seeps	1615	73.2	22.6	-5.12	-27.7
Monday, July 1	D22	S	(EVENT 1 YESTERDAY)	Stream	837	96.7	22.8	-4.89	-27.0
		G		GW	840	NA	NA	-4.88	-27.1
		L		Litter	853 by sf; sample from ea.	10.7	23.2	-8.84	-66.2
		E		Seeps	915	73.6	22.3	-5.07	-27.7
		P		Precip	1157	NA	NA	-10.20	-77.5
		T		TF	858	10.6	23.2	-9.52	-73.6
		F		SF	855	NA	NA	-9.55	-72.3
Tuesday, July 2	D23	S	Sprinkled x2	Stream	1440	97.7	22.8	-5.00	-26.7
		G		GW	1515 p-mid	NA	NA	-4.98	-26.6
		E		Seeps	1525	73.2	22.2	-5.03	-28.0
Wednesday, July 3	D24	E	1 mm rain	Seeps	842	74.4	22.4	-5.04	-27.5
		S		Stream	935	101.5	22.8	-4.85	-26.2
		G		GW	940 p-mid	NA	NA	-4.92	-26.3
		60		Lysimeter	1350 SF; sample from ea.	24.0	26.3	-4.18	-20.2
		20		Lysimeter	1350	NA	NA	-5.71	-35.5
		80		Lysimeter	1350	NA	NA	-3.52	-14.8
	35		Lysimeter	1350	NA	NA	-5.56	-33.2	
Thursday, July 4	D25	S	Rain during night	Stream	600	96.8	22.5	-4.87	-26.4
		G		GW	602 p-mid	NA	NA	-4.89	-26.6
		L		Litter	615 by sf	12.6	22	-5.99	-38.3
		F		SF	619 mid; yellow tinge	121.6	21.6	-5.92	-37.9
		T		TF	625 top	14.5	21.6	-6.15	-39.8
		E		Seeps	637	73.8	22.1	-5.06	-27.6
		P		Precip	720	8.2	22.8	-6.83	-46.9
Sunday, July 7	D26	P		Precip	1500	13.0	27.1	-1.47	0.9
Monday, July 8	D27	S		Stream	825	91.6	22.6	-4.78	-25.0
		G		GW	835 p-mid	NA	NA	-4.86	-25.7
		L		Litter	845 by SF	17.0	22.8	-1.85	-2.7
		F		SF	850 top	53.9	22.5	-1.13	3.6
		T		TF	852 top	16.6	22.5	-1.34	1.7
		E		Seeps	905	72.1	22.3	-4.94	-26.7
		20		Lysimeter	1340 by stream	34.6	25.2	-4.06	-23.8
		60		Lysimeter	1340	NA	NA	-5.23	-30.6
		35		Lysimeter	1340	NA	NA	-6.13	-42.0
		80		Lysimeter	1340	NA	NA	-4.84	-26.4
Tuesday, July 9	D28	S	Storm in afternoon (EVENT 2)	Stream	845	91.2	22.1	-4.78	-25.3
		G		GW	850 p-mid	NA	NA	-4.81	-26.1
		L		Litter	900 by sf	12.2	23.1	-1.54	-2.1
		T		TF	905 bottom	13.9	23	-1.41	-1.5
		F		SF	907 top	52.3	22.7	-1.40	-1.6
		E		Seeps	920	73.6	22.2	-5.02	-26.9
		P		Precip	1140	14.3	27	-1.54	-2.9
Wednesday, July 10	D29	S		Stream	1005	95.5	23.2	-4.67	-25.0
		G		GW	1010 p-mid	NA	NA	-4.83	-26.0
		L		Litter	1020 by SF	15.1	24.3	-2.61	-9.8
		T		TF	1025 mid	15.8	24.2	-2.38	-8.8
		F		SF	1030 top	91.0	23.5	-2.34	-8.9
		E		Seeps	1040	74.8	22.8	-4.92	-27.0
		P		Precip	1100	9.4	29.7	-2.48	-9.7
		20	Trail	Lysimeter	1620 params on 20cm	38.6	29.3	-4.07	-23.7
		35		Lysimeter	1620 params on 35cm	32.7	25.5	-4.12	-24.1
		60		Lysimeter	1620 1/2 full	NA	NA	-5.53	-35.0
	80		Lysimeter	1620	NA	NA	-4.98	-30.6	
Thursday, July 11	D30	S		Stream	1020	95.3	22.1	-4.66	-25.3
		G		GW	1022 p-mid	NA	NA	-4.75	-26.0
		L		Litter	1032 by SF	12.8	22.2	-2.78	-12.6
		T		TF	1035 bottom; yellow	15.1	22.1	-2.39	-11.0
		F		SF	1039 top	132.1	21.8	-2.40	-10.9
		E		Seeps	1050	77.1	22	-4.85	-27.3
		P		Precip	1225	9.7	23.9	-3.08	-14.9

Friday, July 12	D31	S		Stream	830	98.6	22.5	-4.72	-25.6
		G		GW	832	NA	NA	-4.87	-25.9
		L		Litter	845 by SF; 1/2 full	NA	NA	-3.53	-18.4
		T		TF	849 all; yellow	NA	NA	-3.24	-16.3
		F		SF	850 mid, caulk in bottom; brown	292.9	23.4	-4.16	-23.3
		E		Seeps	905	81.0	22.4	-4.91	-27.3
		20	SF	Lysimeter	1405	NA	NA	-4.26	-24.8
		35		Lysimeter	1405	NA	NA	-5.25	-32.6
		60		Lysimeter	1410	NA	NA	-4.62	-24.6
		80		Lysimeter	1410	NA	NA	-3.99	-18.8
		P		Precip	920	NA	NA	-4.71	-25.6
Saturday, July 13	D32	S	EVENT 4 night before	Stream	820	99.4	22.1	-4.82	-25.8
		G		GW	825 p-mid	NA	NA	-4.79	-26.7
		L		Litter	845 by SF; 3/4	NA	NA	-8.13	-55.8
		T		TF	850 bulk sample	NA	NA	-8.33	-57.7
		F		SF	852 top; 1/4	NA	NA	-7.90	-52.9
		E		Seeps	900	76.4	22.3	-5.01	-27.8
		P		Precip	930	NA	NA	-9.19	-63.0
Sunday, July 14	D33	S	No rain	Stream	958	101.8	22.5	-4.84	-26.0
		G		GW	1015 p-mid	NA	NA	-4.91	-26.5
		E		Seeps	1041	76.7	22.1	-5.09	-27.7
Monday, July 15	D34	S	Light sprinkles	Stream	1330	107.3	23.0	-4.86	-26.0
		L		Litter	1335 by SF; 3/4	NA	NA	-4.35	-23.6
		T		TF	1340 top/mid; 1/4	NA	NA	-0.94	0.7
		F		SF	1342 top/mid; 1/7	NA	NA	-2.05	-6.1
		E		Seeps	1350	78	22.7	-5.03	-27.5
		P		Precip	1425	NA	NA	-3.42	-17.1
		35		Lysimeter	1745 3/4	NA	NA	-4.84	-31.6
		20		Lysimeter	NA not enough, 20; 1/8	NA	NA	-2.01	-11.7
		G		GW	1730	NA	NA	-4.95	-26.3
		80		Lysimeter	1745	NA	NA	-4.73	-25.7
	60		Lysimeter	1745 by weir, param on 80/60; 1/2	34.8	24.7	-5.28	-31.2	
Tuesday, July 16	D35	S	Light sprinkles	Stream	800	101.4	22.6	-4.81	-24.9
		G		GW	805 p-mid	NA	NA	-4.76	-26.1
		L		Litter	806 by stream, since last sample	22.1	22	-2.54	-9.6
		T		TF	815 mid/top	NA	NA	-0.47	8.6
		F		SF	816 top	NA	NA	-0.73	6.0
		E		Seeps	827	76.7	22.1	-4.99	-26.8
		P		Precip	910	NA	NA	-1.31	0.7
		80		Lysimeter	1555 80	NA	NA	-5.09	-31.3
		60		Lysimeter	1553 by trail, 60	NA	NA	-5.03	-31.7
		20		Lysimeter	1550 params on 20cm	46.1	25.5	-4.00	-22.7
	35		Lysimeter	1552 params on 35cm	35.5	25.4	-3.86	-22.2	
Wednesday, July 17	D36	S	Light sprinkles, EVENT 5	Stream	740	99.8	22.4	-4.66	-25.2
		G		GW	745 p-mid	NA	NA	-4.71	-25.8
		E		Seeps	800	77	22.1	-4.88	-26.9
Thursday, July 18	D37	S		Stream	1055	100.4	22.6	-4.67	-25.3
		G		GW	1100 p-mid	NA	NA	-4.70	-26.0
		L		Litter	1110 by SF	14.9	24	-4.89	-28.2
		T		TF	1115 mid	11.9	23.6	-5.65	-34.4
		F		SF	1117 top	164.3	23.6	-5.43	-33.8
		E		Seeps	1130	81.6	22.5	-4.84	-26.9
		P		Precip	1150	10.3	32.8	-5.39	-32.3
Friday, July 19	D38	S		Stream	610	100.7	22.6	-4.56	-25.2
		G		GW	612	NA	NA	-4.73	-25.9
		P		Precip	620	NA	NA	-4.25	-24.6
Saturday, July 20	D39	S		Stream	1640	105.3	23.2	-4.75	-25.9
		G		GW	1625	NA	NA	-4.80	-25.3
		P		Precip	1710	NA	NA	-3.77	-20.4

Notes:

- 1) Blue values are from Picarro
- 2) Green values are flagged for head

October Sampling Event											
Date	I.D.	Weather	Type	Time	Comments	Conductivity (µS)	Temp (°C)	d18O vsmow	dD vsmow		
25-Oct	O1	snakes G weir S	Sunny, P. cloudy, Afternoon storm	Snakes	920		98.9	22.4	-4.93	-26.6	
				p-mid	910	2.173 m btoc	NA	NA	-4.94	-26.9	
				Weir	900		94.0	22.6	-5.03	-26.7	
				Stream	905		91.6	22.3	-4.94	-26.8	
26-Oct	O2	Afternoon storm	TF top	850		11.1	22.8	-7.67	-49.6		
			p-mid	830		NA	NA	-4.87	-26.4		
			Stream	825		93.9	22.5	-4.90	-27.5		
			Precip	955		19.1	25.0	-7.08	-46.1		
			Litter by stand	840		13.4	23.0	-7.52	-48.7		
			SF top	845		26.4	23.5	-7.44	-48.7		
			Seeps	915		74.5	22.3	-5.10	-27.9		
27-Oct	O3	Sunny, evening storm	Stream	825		93.1	22.4	-4.92	-26.6		
			Precip	800		10.2	25.0	-10.25	-75.4		
			TF	840	mid/bot	NA	NA	-8.10	-55.1		
			Seeps	855		75.7	22.5	-5.05	-27.9		
28-Oct	O4		TF	830	top	8.9	23.2	-10.37	-73.3		
			Stream	805		93.1	22.5	-4.94	-26.9		
			Seeps	910		75.5	22.5	-5.10	-27.6		
			P-mid	815	0.323 m in well	NA	NA	-4.86	-26.5		
			Litter	825	by stand	12.2	23.2	-10.48	-74.7		
			Stemflow	835	top	22.5	23.4	-9.95	-70.4		
			Precip	650		5.4	24.1	-11.22	-79.4		
29-Oct	O5	Large evening Storm	Precip	1500		NA	NA	-9.28	-63.8		
			Stream	805		84.2	22.6	-5.24	-28.0		
			TF	840	top	6.9	23.0	-9.31	-63.7		
			Seeps	910		73.3	22.6	-5.18	-27.9		
			Litter	835	by stand	9.3	23.1	-9.29	-64.0		
			SF	845	top	12.0	22.9	-8.63	-59.6		
			p-mid	810		NA	NA	-4.87	-27.4		

Notes:

- 1) Blue values are from Picarro
- 2) Green values are flagged for head

Day	Depth (cm)	Location	d180 vsmow	dD vsmow	d-excess	Whisker Plot Values
D11	20	W	-4.99	-31.2	8.74	Min 8.63572
D16	20	W	-5.05	-31.2	8.99	Max 10.1702
D17	20	W	-5.11	-30.7	9.05	Q1 8.74939
D27	20	W	-4.06	-23.8	8.67	Q3 9.27975
D35	20	W	-4.00	-22.7	9.19	Median 9.05387
D12	20	SF	-6.00	-39.0	8.75	Mean 9.13979
D16	20	SF	-5.47	-35.1	10.17	Std Error 0.49984
D17	20	SF	-5.29	-33.6	9.06	Q1-min 0.11367
D24	20	SF	-5.71	-35.5	10.12	Q1 8.74939
D31	20	SF	-4.26	-24.8	8.64	median-Q1 0.30448
D15	20	T	-5.89	-38.0	8.84	Q3-median 0.22588
D21	20	T	-5.13	-32.0	9.34	max-q3 0.8904
D29	20	T	-4.07	-23.7	9.28	
D11	35	W	-5.62	-37.0	7.89	Min 7.02719
D16	35	W	-5.22	-34.5	11.01	Max 11.2207
D17	35	W	-5.32	-33.7	8.18	Q1 8.18243
D27	35	W	-6.13	-42.0	10.63	Q3 10.3808
D35	35	W	-3.86	-22.2	7.27	Median 8.89285
D12	35	SF	-5.23	-30.9	10.38	Mean 9.12609
D16	35	SF	-5.22	-31.1	8.84	Std Error 1.36933
D17	35	SF	-5.21	-31.3	9.22	Q1-min 1.15524
D24	35	SF	-5.56	-33.2	11.22	Q1 8.18243
D31	35	SF	-5.25	-32.6	7.03	median-Q1 0.71042
D15	35	T	-5.68	-37.3	8.89	Q3-median 1.488
D21	35	T	-5.27	-32.9	9.42	max-q3 0.83982
D29	35	T	-4.12	-24.1	8.65	
D11	60	W	-4.78	-25.7	12.57	Min 8.57697
D16	60	W	-4.84	-26.7	13.42	Max 13.4165
D17	60	W	-4.96	-27.1	11.24	Q1 11.1012
D27	60	W	-5.23	-30.6	13.22	Q3 13.0585
D34	60	W	-5.28	-31.2	12.03	Median 12.1966
D17	60	SF	-3.78	-16.9	13.31	Mean 11.7771
D12	60	SF	-3.71	-16.3	12.63	Std Error 1.51118
D16	60	SF	-3.63	-15.8	10.75	Q1-min 2.52422
D24	60	SF	-4.18	-20.2	13.20	Q1 11.1012
D31	60	SF	-4.62	-24.6	11.28	median-Q1 1.09546
D15	60	T	-5.83	-35.4	9.24	Q3-median 0.86188
D21	60	T	-5.74	-35.2	12.37	max-q3 0.35796
D29	60	T	-5.53	-35.0	11.06	
D35	60	T	-5.03	-31.7	8.58	
D11	80	W	-4.54	-24.7	11.60	Min 9.28633
D16	80	W	-4.39	-23.5	13.58	Max 13.5796
D17	80	W	-4.65	-23.9	10.52	Q1 11.4942
D27	80	W	-4.84	-26.4	13.34	Q3 13.2706
D34	80	W	-4.73	-25.7	11.68	Median 12.2422
D12	80	SF	-3.12	-11.4	13.10	Mean 12.0165
D16	80	SF	-3.14	-11.7	13.34	Std Error 1.45151
D17	80	SF	-3.12	-11.9	11.46	Q1-min 2.20789
D24	80	SF	-3.52	-14.8	13.31	Q1 11.4942
D31	80	SF	-3.99	-18.8	12.38	median-Q1 0.74802
D15	80	T	-5.03	-29.7	9.29	Q3-median 1.02835
D21	80	T	-5.66	-33.8	13.15	max-q3 0.309
D29	80	T	-4.98	-30.6	12.10	
D35	80	T	-5.09	-31.3	9.40	
D1	GW		-4.64	-25.8	11.31	Min 8.98076
D10	GW		-4.82	-26.3	12.28	Max 13.5776
D12	GW		-4.84	-26.6	12.11	Q1 11.935
D13	GW		-4.71	-25.7	11.95	Q3 12.8131
D15	GW		-4.64	-25.4	11.71	Median 12.2778
D16	GW		-4.81	-26.0	12.51	Mean 12.2103
D17	GW		-4.39	-24.4	10.73	Std Error 0.91234
D20	GW		-4.82	-26.2	12.33	Q1-min 2.95422
D21	GW		-4.85	-26.3	12.48	Q1 11.935
D22	GW		-4.88	-27.1	11.97	median-Q1 0.34281
D23	GW		-4.98	-26.6	13.26	Q3-median 0.53531
D24	GW		-4.92	-26.3	13.01	max-q3 0.76448
D25	GW		-4.89	-26.6	12.48	
D27	GW		-4.86	-25.7	13.19	
D28	GW		-4.81	-26.1	12.39	
D29	GW		-4.83	-26.0	12.57	
D3	GW		-4.74	-26.0	11.93	
D30	GW		-4.75	-26.0	12.05	
D31	GW		-4.87	-25.9	13.09	
D32	GW		-4.79	-26.7	11.56	
D33	GW		-4.91	-26.5	12.81	
D34	GW		-4.95	-26.3	13.35	
D35	GW		-4.76	-26.1	11.94	
D36	GW		-4.71	-25.8	11.80	
D37	GW		-4.70	-26.0	11.58	
D38	GW		-4.73	-25.9	12.00	
D39	GW		-4.80	-25.3	13.13	
D5	GW		-8.94	-62.5	8.98	
D8	GW		-5.01	-26.5	13.58	

Notes:

- 1) Blue values are from Picarro
- 2) Green values are flagged for head

### Conductivity ( $\mu$ S) Time Series

Date	Notation	Precip	Stream	Seeps	Litter	TF	SF	Lys	Precip (mm)
8-May	M1		79.1	38.5					0
10-May	M2		98.3						25.27
11-May	M3			79.6					49.53
12-May	M4	13.1							10.29
13-May	M5		92.0			31.4			15.11
10-Jun	D1		100.7	75.5					22.61
11-Jun	D2		101.9	75.3					55.45
12-Jun	D3	5.7	58.9	70.5		13.4			7.36
13-Jun	D4	6.3	103.6	79.0					44.83
14-Jun	D5		96.2	76.0		13.0			101.17
15-Jun	D6	11.5	83.4	75.2	14.1	10.8			30.53
16-Jun	D7	5.9	89.8	76.8	6.3	10.8			1.72
17-Jun	D8		98.1	77.6					4.14
18-Jun	D9		99.4	78.4					55.97
19-Jun	D10	14.5	92.3	76.0		17.0			20.77
20-Jun	D11	9.7	94.5	76.4		16.8			2.26
21-Jun	D12		102.5	77.7	16.9				15.34
22-Jun	D13		106.3	79.9	16.9	16			0.00
23-Jun	D14		102.8	81.2					1.21
24-Jun	D15		106.4	82.4				59.4	0.86
25-Jun	D16		103.3	81.5				45.6	30.00
26-Jun	D17	7.4	103.2	80.4	15.6	14.8	132.2	49.3	33.95
27-Jun	D18	8.0	96.2	76.5	14.8	21.3	55.6		2.77
28-Jun	D19		103.2	79.5					0.00
29-Jun	D20		98.7	74.9					28.13
30-Jun	D21		99.6	73.2	19.0	26.3	162.3	31.7	15.99
1-Jul	D22		96.7	73.6	10.7	10.6			0.00
2-Jul	D23		97.7	73.2					1.35
3-Jul	D24		101.5	74.4				24.0	24.38
4-Jul	D25	8.2	96.8	73.8	12.6	14.5	121.6		1.52
5-Jul	NA								6.86
6-Jul	NA								16.76
7-Jul	D26	13.0							56.90
8-Jul	D27		91.6	72.1	17.0	16.6	53.9	34.6	24.67
9-Jul	D28	14.3	91.2	73.6	12.2	13.9	52.3		18.09
10-Jul	D29	9.4	95.5	74.8	15.1	15.8	91.0	35.7	18.86
11-Jul	D30	9.7	95.3	77.1	12.8	15.1	132.1	21.8	4.04
12-Jul	D31		98.6	81.0			292.9		5.46
13-Jul	D32		99.4	76.4					0.00
14-Jul	D33		101.8	76.7					6.89
15-Jul	D34		107.3	78.0				34.8	5.41
16-Jul	D35		101.4	76.7	22.1			40.8	3.05
17-Jul	D36		99.8	77.0					32.26
18-Jul	D37	10.3	100.4	81.6	14.9	11.9	164.3		5.59
19-Jul	D38		100.7						3.05
20-Jul	D39		105.3						2.79
25-Oct	O1		94.8						NA
26-Oct	O2	19.1	93.9	74.5	13.4	11.1	26.4		NA
27-Oct	O3	10.2	93.1	75.7					NA
28-Oct	O4	5.4	93.1	75.5	12.2	8.9	22.5		NA
29-Oct	O5		84.2	73.3	9.3	6.9	12.0		NA
AVERAGE		10.1	96.8	75.7	14.2	15.1	101.5	37.8	17.68

EVENT 1		Air Temp		Event		Event		Event		Event		Event	
Time	Precip (mm)	(C)	Type	id	Comment	d180 vsnow	dD vsnow	Conductivity (µS)	id	Type	id	d180 vsnow	dD vsnow
6/30/13 12:00	12.00 0	28.056905											
6/30/13 12:05	12.05 0	27.944275											
6/30/13 12:10	12.10 0	28.349285											
6/30/13 12:15	12.15 0	28.43223											
6/30/13 12:20	12.20 0	28.045535											
6/30/13 12:25	12.25 0	27.827105											
6/30/13 12:30	12.30 0	27.71106											
6/30/13 12:35	12.35 0	27.547235											
6/30/13 12:40	12.40 0	27.52107											
6/30/13 12:45	12.45 0	27.55179											
6/30/13 12:50	12.50 0.254	27.43605											
6/30/13 12:55	12.55 0.254	26.34827											
6/30/13 13:00	13.00 0.254	25.456325											
6/30/13 13:05	13.05 0.762	24.826295											
6/30/13 13:10	13.10 0.508	24.65314											
6/30/13 13:15	13.15 0.254	24.63117											
6/30/13 13:20	13.20 0	24.571405											
6/30/13 13:25	13.25 0	24.57882											
6/30/13 13:30	13.30 0	24.542055											
6/30/13 13:35	13.35 0	24.371655											
6/30/13 13:40	13.40 0.254	24.352945											
6/30/13 13:45	13.45 0	24.271495											
6/30/13 13:50	13.50 0	24.08315											
6/30/13 13:55	13.55 0	24.085825											
6/30/13 14:00	14.00 0.254	23.887715											
6/30/13 14:05	14.05 1.27	23.642025											
6/30/13 14:10	14.10 0.508	23.468977											
6/30/13 14:15	14.15 1.27	23.194745											
6/30/13 14:20	14.20 0.508	23.29275											
6/30/13 14:25	14.25 0.508	23.20884											
6/30/13 14:30	14.30 0.508	23.269425											
6/30/13 14:35	14.35 1.016	23.19471											
6/30/13 14:40	14.40 1.016	23.005505											
6/30/13 14:45	14.45 0.762	22.80188											
6/30/13 14:50	14.50 0.254	22.73253											
6/30/13 14:55	14.55 0	22.67171											
6/30/13 15:00	15.00 0.254	22.64085											
6/30/13 15:05	15.05 0.762	22.71161											
6/30/13 15:10	15.10 0.762	22.723785											
6/30/13 15:15	15.15 0.508	22.73108											
6/30/13 15:20	15.20 0.254	22.64479											
6/30/13 15:25	15.25 0.254	22.54522											
6/30/13 15:30	15.30 0	22.58935											
6/30/13 15:35	15.35 0.254	22.647065											
6/30/13 15:40	15.40 0	22.49658											
6/30/13 15:45	15.45 0.254	22.397175											
6/30/13 15:50	15.50 0	22.362315											
6/30/13 15:55	15.55 0	22.26325											
6/30/13 16:00	16.00 0	22.220675											
6/30/13 16:05	16.05 0	21.96818											
D21	P	D21P				-10.07	-76.9						
		E1P1				-9.60	-74.5						
		E1P2				-9.91	-76.1						
		E1P3				-10.10	-77.2						
		E1P4				-10.08	-77.3						
		E1P5				-9.33	-73.7						
		E1P6				-10.23	-78.7						
		E1P7				-10.26	-79.4						
		E1P8				-9.74	-78.5						
		E1P9				-9.47	-76.6						
		E1P10				-9.14	-75.2						
D22	P	D22P				-10.20	-77.5						
D22	S	D22.S				96.7	-4.89						-27.0

- Notes:
- 1) No discharge data for this event
  - 2) Blue values are from Picarro
  - 3) Flagged values for head are in green
  - 4) Orange values are not during event 1



EVENT 2 Day 27		Precip (mm)	Air Temp (°C)	Event	Type	id	Conductivity (µS)	Sample Temp (°C)	Comment	d18O vsmow	dD vsmow
7/8/13 15:55	0:00	0	23.29847								
7/8/13 16:00	0:05	0.01	23.17189								
7/8/13 16:05	0:10	0.02	23.20481				28	26.6		-0.51	5.3
7/8/13 16:10	0:15	0.15	23.18112			E2.P1				-0.67	2.7
7/8/13 16:15	0:20	0.21	22.89336			E2.P2	14.2	24.3		-2.11	-8.0
7/8/13 16:20	0:25	0.16	22.82486			E2.P3	4.6	23.1		-2.87	-13.0
7/8/13 16:25	0:30	0.09	22.65571			E2.P4	4	23.1		-2.51	-10.4
7/8/13 16:30	0:35	0.03	22.61683			E2.P5	10.5	23.2		-1.91	-4.1
7/8/13 16:35	0:40	0.01	22.61891			E2.P6	NA	NA	3/4	-1.72	-3.48
7/8/13 16:40	0:45	0.01	22.6132	D28	P	D28.P	14.3	27.0		-1.54	-2.9
7/8/13 16:45	0:50	0	22.6858								
7/8/13 16:50	0:55	0	22.62896	D27	G	D27.G				-4.86	-25.7
7/8/13 16:55	1:00	0	22.6525	D27	E	D27.E				-4.94	-26.7
7/8/13 17:00	1:05	0	22.54585	D28	G	D28.G				-4.81	-26.1
7/8/13 17:05	1:10	0	22.41397	D28	E	D28.E				-5.02	-26.9
7/8/13 17:10	1:15	0	22.20448								
7/8/13 17:15	1:20	0	22.15902								
7/8/13 17:20	1:25	0	22.20807								
7/8/13 17:25	1:30	0	22.24686								
7/8/13 17:30	1:35	0	22.17851								
7/8/13 17:35	1:40	0	22.25259								
7/8/13 17:40	1:45	0	22.32552								
7/8/13 17:45	1:50	0	22.36768								
7/8/13 17:50	1:55	0	22.34831								
7/8/13 17:55	2:00	0	22.34261								
7/8/13 18:00	2:05	0	22.38047								

Notes:

- 1) Blue values are from Picarro
- 2) Flagged values for head are in green
- 3) Orange values are not during event 2
- 4) Blue text used in baseflow separation calculations
- 5) Gray spots represent no data or a calculated data point, not a sample
- 6) Red values represent peak streamflow during storm (>0.1 cmm)

EVENT 2		Event		Type		id		Qt (cmm)		Qgw		Qb (cmm)		using O		Conductivity (µS)		Comment		GWO		d18O		dD	
Day 27																						vsmow		vsmow	
								Cp=								D27		S		D27.S		Cp=		-25.0	
								0.021														-4.78		-12.5	
								0.024														Ct=		-11.8	
7/8/13 15:55																									
7/8/13 16:00																									
7/8/13 16:05	2	S	E2.S1	0.015	0.548	0.016	0.548	0.016	0.548	0.016	0.548	0.016	0.548	0.016	0.548	0.016	0.548	0.016	0.548	0.016	0.548	-4.86	-2.89	-12.5	
7/8/13 16:10	2	S	E2.S2	0.080	0.518	0.098	0.518	0.098	0.518	0.098	0.518	0.098	0.518	0.098	0.518	0.098	0.518	0.098	0.518	0.098	0.518	-4.86	-2.84	-11.8	
7/8/13 16:15	2	S	E2.S3	0.431	0.265	0.274	0.265	0.274	0.265	0.274	0.265	0.274	0.265	0.274	0.265	0.274	0.265	0.274	0.265	0.274	0.265	-4.86	-2.84	-12.4	
7/8/13 16:20	2	S	E2.S4	0.659	0.116	0.456	0.116	0.456	0.116	0.456	0.116	0.456	0.116	0.456	0.116	0.456	0.116	0.456	0.116	0.456	0.116	-4.86	-3.10	-13.9	
7/8/13 16:25	2	S	E2.S5	0.864	0.301	0.633	0.301	0.633	0.301	0.633	0.301	0.633	0.301	0.633	0.301	0.633	0.301	0.633	0.301	0.633	0.301	-4.86	-3.22	-14.9	
7/8/13 16:30	2	S	E2.S6	0.668	0.469	0.499	0.469	0.499	0.469	0.499	0.469	0.499	0.469	0.499	0.469	0.499	0.469	0.499	0.469	0.499	0.469	-4.86	-3.29	-15.9	
7/8/13 16:35	2	S	E2.S7	0.464	0.544	0.353	0.544	0.353	0.544	0.353	0.544	0.353	0.544	0.353	0.544	0.353	0.544	0.353	0.544	0.353	0.544	-4.86	-3.43	-16.7	
7/8/13 16:40	2	S	E2.S8	0.303	0.616	0.239	0.616	0.239	0.616	0.239	0.616	0.239	0.616	0.239	0.616	0.239	0.616	0.239	0.616	0.239	0.616	-4.86	-3.66	-17.7	
7/8/13 16:45	2	S	E2.S9	0.261	0.628	0.208	0.628	0.208	0.628	0.208	0.628	0.208	0.628	0.208	0.628	0.208	0.628	0.208	0.628	0.208	0.628	-4.86	-3.70	-18.6	
7/8/13 16:50	2	S	E2.S10	0.163	0.696	0.135	0.696	0.135	0.696	0.135	0.696	0.135	0.696	0.135	0.696	0.135	0.696	0.135	0.696	0.135	0.696	-4.86	-3.91	-19.2	
7/8/13 16:55	2	S	E2.S11	0.132	0.731	0.112	0.731	0.112	0.731	0.112	0.731	0.112	0.731	0.112	0.731	0.112	0.731	0.112	0.731	0.112	0.731	-4.86	-4.02	-20.1	
7/8/13 17:00	2	S	E2.S12	0.098	0.735	0.083	0.735	0.083	0.735	0.083	0.735	0.083	0.735	0.083	0.735	0.083	0.735	0.083	0.735	0.083	0.735	-4.86	-4.03	-20.7	
7/8/13 17:05	2	S	E2.S13	0.102	0.755	0.088	0.755	0.088	0.755	0.088	0.755	0.088	0.755	0.088	0.755	0.088	0.755	0.088	0.755	0.088	0.755	-4.86	-4.09	-20.9	
7/8/13 17:10	2	S	E2.S14	0.087	0.788	0.077	0.788	0.077	0.788	0.077	0.788	0.077	0.788	0.077	0.788	0.077	0.788	0.077	0.788	0.077	0.788	-4.86	-4.20	-21.7	
7/8/13 17:15	2	S	E2.S15	0.081	0.806	0.069	0.806	0.069	0.806	0.069	0.806	0.069	0.806	0.069	0.806	0.069	0.806	0.069	0.806	0.069	0.806	-4.86	-4.19	-21.8	
7/8/13 17:20	2	S	E2.S16	0.076	0.819	0.068	0.819	0.068	0.819	0.068	0.819	0.068	0.819	0.068	0.819	0.068	0.819	0.068	0.819	0.068	0.819	-4.86	-4.30	-22.6	
7/8/13 17:25	2	S	E2.S17	0.069	0.804	0.061	0.804	0.061	0.804	0.061	0.804	0.061	0.804	0.061	0.804	0.061	0.804	0.061	0.804	0.061	0.804	-4.86	-4.25	-22.6	
7/8/13 17:30	2	S	E2.S18	0.062	0.838	0.057	0.838	0.057	0.838	0.057	0.838	0.057	0.838	0.057	0.838	0.057	0.838	0.057	0.838	0.057	0.838	-4.86	-4.36	-22.8	
7/8/13 17:35	2	S	E2.S19	0.060	0.806	0.054	0.806	0.054	0.806	0.054	0.806	0.054	0.806	0.054	0.806	0.054	0.806	0.054	0.806	0.054	0.806	-4.86	-4.25	-22.6	
7/8/13 17:40	2	S	E2.S20	0.059	0.859	0.054	0.859	0.054	0.859	0.054	0.859	0.054	0.859	0.054	0.859	0.054	0.859	0.054	0.859	0.054	0.859	-4.86	-4.42	-23.1	
7/8/13 17:45	2	S	E2.S21	0.059	0.878	0.055	0.878	0.055	0.878	0.055	0.878	0.055	0.878	0.055	0.878	0.055	0.878	0.055	0.878	0.055	0.878	-4.86	-4.48	-23.2	
7/8/13 17:50	2	S	E2.S22	0.041	0.869	0.038	0.869	0.038	0.869	0.038	0.869	0.038	0.869	0.038	0.869	0.038	0.869	0.038	0.869	0.038	0.869	-4.86	-4.45	-23.4	
7/8/13 17:55	2	S	E2.S23	0.043	0.870	0.040	0.870	0.040	0.870	0.040	0.870	0.040	0.870	0.040	0.870	0.040	0.870	0.040	0.870	0.040	0.870	-4.86	-4.46	-23.8	
7/8/13 18:00	2	S	E2.S24	0.044	0.646	0.034	0.646	0.034	0.646	0.034	0.646	0.034	0.646	0.034	0.646	0.034	0.646	0.034	0.646	0.034	0.646	-4.86	-3.75	-18.2	
		D28		S		D28.S		91.2														-4.86		-25.3	

EVENT 3		Time	Precip (mm)	Air Temp (°C)	Event		d180 vsnow	dD vsnow
Day 29	Type				id			
	D29				P	D29.P	-2.48	-9.7
7/10/13 16:30		0:00	0.01	24.96428			-1.89	-6.3
7/10/13 16:35		0:05	0	25.02147			-1.89	-6.3
7/10/13 16:40		0:10	0	25.05693			-1.89	-6.3
7/10/13 16:45		0:15	0	25.14286			-1.89	-6.3
7/10/13 16:50		0:20	0.03	25.22213	3 P	E3.P1	-1.31	-3.0
7/10/13 16:55		0:25	0.08	25.03871	3 P	E3.P2	-2.53	-11.8
7/10/13 17:00		0:30	0.14	24.66594	3 P	E3.P3	-2.84	-11.9
7/10/13 17:05		0:35	0.09	24.32877	3 P	E3.P4	-2.37	-8.9
7/10/13 17:10		0:40	0.12	24.26614	3 P	E3.P5	-2.71	-11.9
7/10/13 17:15		0:45	0.11	24.08409	3 P	E3.P6	-3.04	-14.8
7/10/13 17:20		0:50	0	23.94774			-2.38	-10.6
7/10/13 17:25		0:55	0	23.9601			-2.38044	-10.5972
7/10/13 17:30		1:00	0	23.90952			-2.38044	-10.5972
7/10/13 17:35		1:05	0.01	23.83294			-2.38044	-10.5972
7/10/13 17:40		1:10	0	23.57074			-2.38044	-10.5972
7/10/13 17:45		1:15	0	23.52152	3 P	E3.P7	-1.72	-6.4
7/10/13 17:50		1:20	0.01	23.32572				
7/10/13 17:55		1:25	0.01	23.16242	D30	D30.P	-3.08	-14.9
7/10/13 18:00		1:30	0.01	22.96351				
7/10/13 18:05		1:35	0	22.75646				

Notes:

- 1) Blue values are from Picarro
- 2) Flagged values for head are in green
- 3) Orange values are not during event 3
- 4) Blue text used in baseflow separation calculations
- 5) Gray spots represent no data or a calculated data point, not a sample
- 6) Red values represent peak streamflow during storm (>0.1 cmm)



EVENT 3		Throughfall		d180		dD		Event		Event		Stemflow		d180		dD		Event		Event		d180		dD	
Day 29		Comment		vsmow		vsmow		Type		id		(mm)		vsmow		vsmow		Type		id		vsmow		vsmow	
7/10/13 16:30																									
7/10/13 16:35																									
7/10/13 16:40																									
7/10/13 16:45																									
7/10/13 16:50																									
7/10/13 16:55																									
7/10/13 17:00																									
7/10/13 17:05																									
7/10/13 17:10																									
7/10/13 17:15																									
7/10/13 17:20																									
7/10/13 17:25																									
7/10/13 17:30																									
7/10/13 17:35																									
7/10/13 17:40																									
7/10/13 17:45																									
7/10/13 17:50																									
7/10/13 17:55																									
7/10/13 18:00																									
7/10/13 18:05																									

EVENT 4 Day 31	Time	Precip (mm)	Air Temp (°C)	Event		d180 vsmow	dD vsmow	Event		Qt (cmm)	Qb (cmm) using O		Conductivity (µS)	GWO	d180 vsmow	dD vsmow
				Type	id			Type	id		D31	S				
				D31	P	D31.P	-4.71	-25.6						D31.S	-4.72	-25.6
	7/12/13 15:30	0.00	0 27.59479				-11.31	-77.0		0.023	0.023	98.1	1.03062381	-4.87	-4.67	-25.2
	7/12/13 15:35	0.05	0 27.38307				-11.31	-77.0		0.021	0.021	98.5	1.00127425	-4.87	-4.86	-25.7
	7/12/13 15:40	0.10	0 26.26161				-11.31	-77.0		0.019	0.019	98.4	1.00647398	-4.87	-4.83	-25.8
	7/12/13 15:45	0.15	0 24.84955				-11.31	-77.0		0.014	0.015	98.1	1.01105744	-4.87	-4.80	-25.6
	7/12/13 15:50	0.20	0.01 23.77795	4 P	E4.P1		-11.31	-77.0		0.013	0.013	98.3	1.01067227	-4.87	-4.80	-25.8
	7/12/13 15:55	0.25	0.05 22.94692	4 P	E4.P2		-10.56	-71.1		0.017	0.016	97.3	0.97969412	-4.87	-4.98	-26.1
	7/12/13 16:00	0.30	0.03 22.30154	4 P	E4.P3		-11.04	-76.5		0.017	0.019	93.7	0.96170552	-4.87	-5.10	-27.4
	7/12/13 16:05	0.35	0.03 21.8809	4 P	E4.P4		-11.00	-78.1		0.020	0.019	92.4	0.95908127	-4.87	-5.12	-28.6
	7/12/13 16:10	0.40	0.02 21.86637				-10.61	-76.6		0.019	0.018	91.4	0.95246772	-4.87	-5.14	-29.1
	7/12/13 16:15	0.45	0.01 21.83752	4 P	E4.P5		-10.21	-75.0		0.030	0.027	91.0	0.92900921	-4.87	-5.25	-29.0
	7/12/13 16:20	0.50	0.01 21.85399				-9.30	-69.7		0.030	0.028	91.7	0.93206059	-4.87	-5.17	-28.8
	7/12/13 16:25	0.55	0 21.94764				-9.30	-69.7		0.030	0.028	92.4	0.94707214	-4.87	-5.10	-28.6
	7/12/13 16:30	1.00	0.01 22.01757				-9.30	-69.7		0.027	0.026	92.7	0.96852522	-4.87	-5.01	-28.2
	7/12/13 16:35	1.05	0 21.95605				-9.30	-69.7		0.022	0.021	92.9	0.97087777	-4.87	-5.00	-27.8
	7/12/13 16:40	1.10	0 21.92446				-9.30	-69.7		0.022	0.023	94.1	0.9840969	-4.87	-4.94	-27.3
	7/12/13 16:45	1.15	0 21.9602	4 P	E4.P6		-8.38	-64.3		0.022	0.022	94.7	0.97097004	-4.87	-4.97	-27.2
	7/12/13 16:50	1.20	0 22.07995				-8.38	-64.3		0.022	0.023	95.5	1.02579198	-4.87	-4.78	-26.7
				D32	P	D32.P	-9.19	-63.0				99.4		-4.82	-25.8	
				D31	G	D31.G	-4.87	-25.9								
				D31	E	D31.E	-4.91	-27.3								
				D32	G	D31.G	-4.79	-26.7								
				D32	E	D31.E	-5.01	-27.8								

- Notes:
- 1) Blue values are from Picarro
  - 2) Flagged values for head are in green
  - 3) Orange values are not during event 4
  - 4) Blue text used in baseflow separation calculations
  - 5) Gray spots represent no data or a calculated data point, not a sample
  - 6) Event 4 does not represent a storm with weir values which exceed 0.1 cmm

EVENT 5 Day 36		Time	Rain (mm)	Air Temp (°C)	Event	Type	id	Conductivity (µS)	Sample Temp (°C)	Comment	d-excess	d18O vsnow	δD vsnow
7/17/13 15:55	0:00	0	25.79649			S P	E5.P1				9.86	-4.47	-25.9
7/17/13 16:00	0:05	3.556	8.99322E-09	24.46698		S P	E5.P2				8.97	-5.15	-32.3
7/17/13 16:05	0:10	4.318	1.61019E-08	23.26855		S P	E5.P3				12.55	-4.89	-26.6
7/17/13 16:10	0:15	6.604	5.76038E-08	22.94466		S P	E5.P4	15.5	26.4		14.11	-6.48	-37.7
7/17/13 16:15	0:20	6.096	4.5307E-08	22.13514		S P	E5.P5	5.9	24.9		13.32	-6.92	-42.0
7/17/13 16:20	0:25	2.54	3.27741E-09	21.70518		S P	E5.P6	4.9	24.7		11.86	-6.74	-42.1
7/17/13 16:25	0:30	1.524	7.07921E-10	21.45633		S P	E5.P7				9.87	-6.6	-42.8
7/17/13 16:30	0:35	1.016	2.09754E-10	21.52821		S P	E5.P8	6.7	23.6		9.11	-6.58	-43.6
7/17/13 16:35	0:40	0.254	3.27741E-12	21.72963		S P	E5.P9				10.59	-6.58	-42.0
7/17/13 16:40	0:45	0.254	3.27741E-12	21.83297		S P	E5.P10			1/8	8.13	-6.05	-40.2
7/17/13 16:45	0:50	0	0	21.88271		S P	E5.P11			<1/8	7.16	-5.66	-38.1
7/17/13 16:50	0:55	0.254	3.27741E-12	21.9699		S P	E5.P11			1/8	7.22	-5.30	-35.2
7/17/13 16:55	1:00	0.254	3.27741E-12	22.08867		S P				1/8	7.97	-5.43	-35.5
7/17/13 17:00	1:05	0	0	22.16099						1/8	7.97	-5.43	-35.5
7/17/13 17:05	1:10	0.254	3.27741E-12	22.07667						1/8	7.97	-5.43	-35.5
7/17/13 17:10	1:15	0.508	2.62193E-11	22.18863		S P	E5.P12				8.72	-5.56	-35.8
7/17/13 17:15	1:20	0.254	3.27741E-12	22.2763							8.85	-5.73	-37.0
7/17/13 17:20	1:25	0.254	3.27741E-12	22.29372							8.85	-5.73	-37.0
7/17/13 17:25	1:30	0.254	3.27741E-12	22.23646		S P	E5.P13				8.98	-5.90	-38.2
7/17/13 17:30	1:35	0.508	2.62193E-11	22.13217							7.83	-5.74	-38.1
7/17/13 17:35	1:40	0.508	2.62193E-11	22.02879		S P	E5.P14				6.67	-5.59	-38.0
7/17/13 17:40	1:45	0.254	3.27741E-12	22.09735							6.42	-5.62	-38.5
7/17/13 17:45	1:50	0.254	3.27741E-12	22.12139		S P	E5.P15				6.16	-5.64	-39.0
7/17/13 17:50	1:55	0	0	22.12945							6.16	-5.64	-39.0
7/17/13 17:55	2:00	0.254	3.27741E-12	22.11809									
7/17/13 18:00	2:05	0.254	3.27741E-12	22.11926									
7/17/13 18:05	2:10	0.254	3.27741E-12	22.10902									
7/17/13 18:10	2:15	0	0	22.15689									
7/17/13 18:15	2:20	0.254	3.27741E-12	22.22207									
7/17/13 18:20	2:25	0.254	3.27741E-12	22.13545									
7/17/13 18:25	2:30	0.254	3.27741E-12	22.11024									
7/17/13 18:30	2:35	0.254	3.27741E-12	22.06821									
7/17/13 18:35	2:40	0	0	21.98159									
7/17/13 18:40	2:45	0.254	3.27741E-12	21.95606									
7/17/13 18:45	2:50	0	0	21.95135									
7/17/13 18:50	2:55	0	0	21.9676									
7/17/13 18:55	3:00	0.254	3.27741E-12	21.98079									
7/17/13 19:00	3:05	0	0	22.01616									
7/17/13 19:05	3:10	0	0	21.99988									
7/17/13 19:10	3:15	0	0	21.9958									
7/17/13 19:15	3:20	0	0	22.0622									
7/17/13 19:20	3:25	0	0	22.04187									
7/17/13 19:25	3:30	0.254	3.27741E-12	21.99869	D57	P	7-18-P	10.3	32.8		-5.39	-32.3	

Notes:

- 1) Blue values are from Picarro
- 2) Flagged values for head are in green
- 3) Orange values are not during event 5
- 4) Purple text used in interflow-baseflow separation calculations
- 5) Gray spots represent no data or a calculated data point, not a sample
- 6) Red values represent peak streamflow during storm (>0.1 cmm)



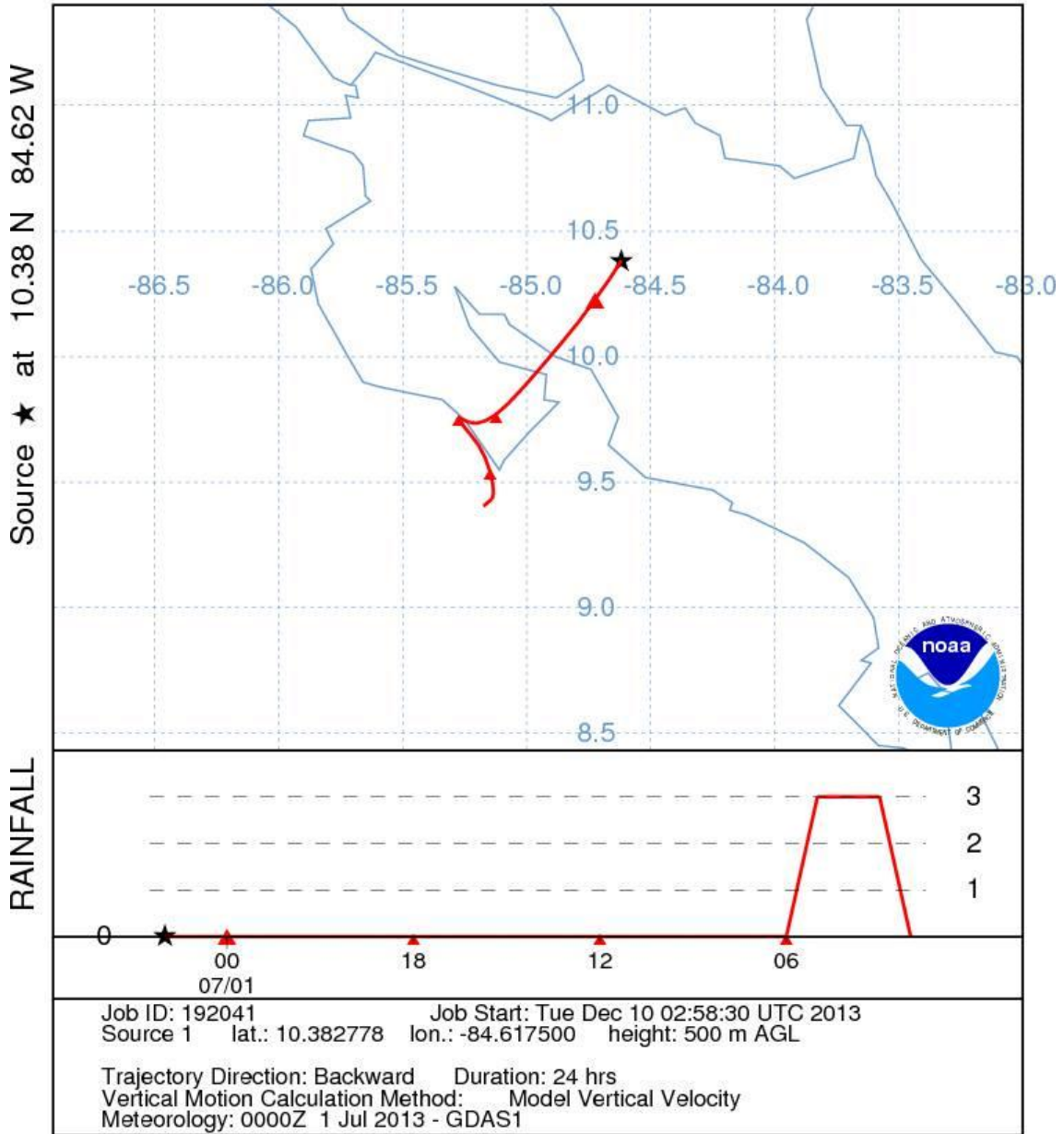




APPENDIX B

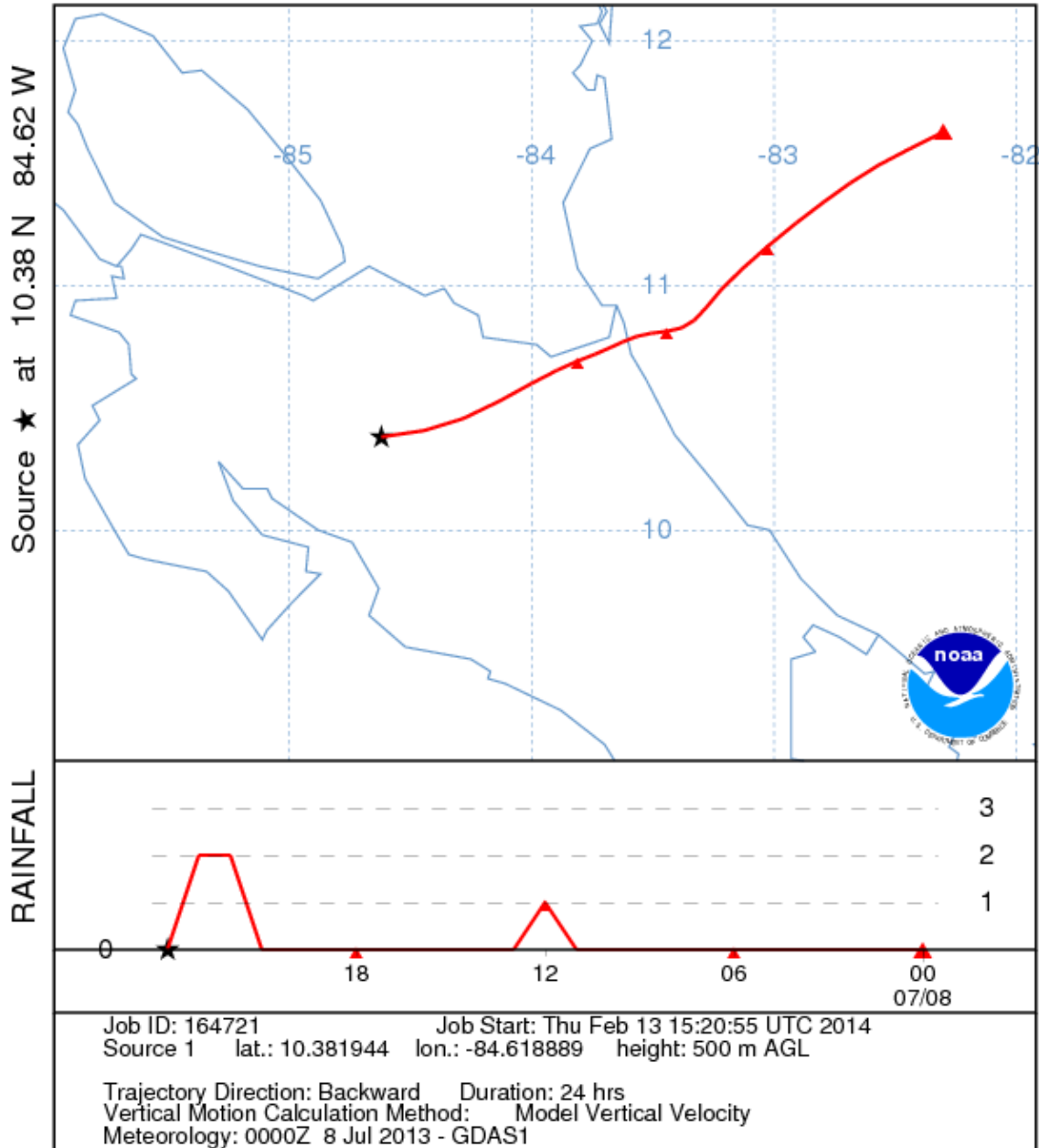
FIGURES

NOAA HYSPLIT MODEL  
 Backward trajectory ending at 0200 UTC 01 Jul 13  
 GDAS Meteorological Data



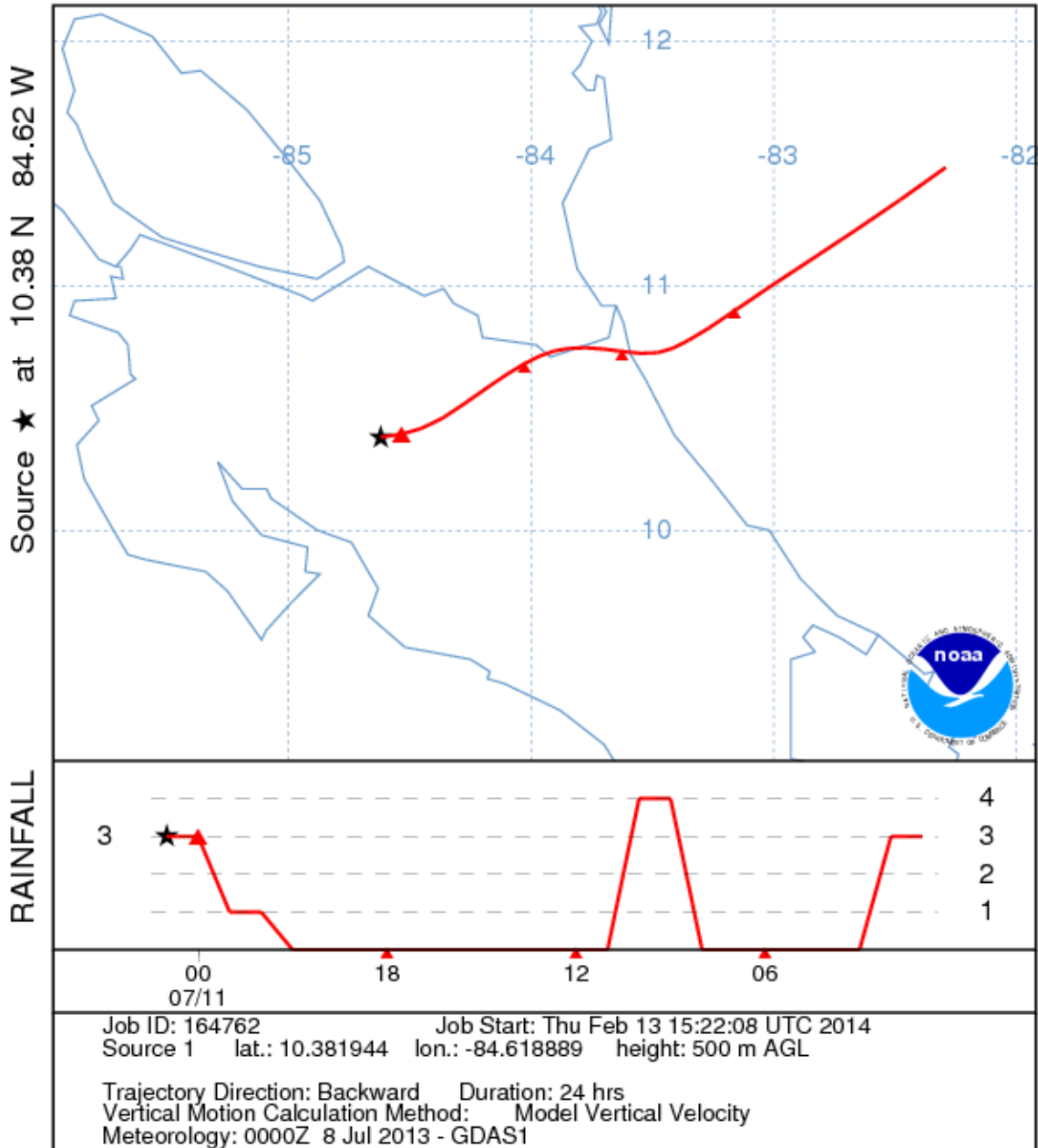
**Event 1 6/30/2013**

NOAA HYSPLIT MODEL  
 Backward trajectory ending at 0000 UTC 09 Jul 13  
 GDAS Meteorological Data



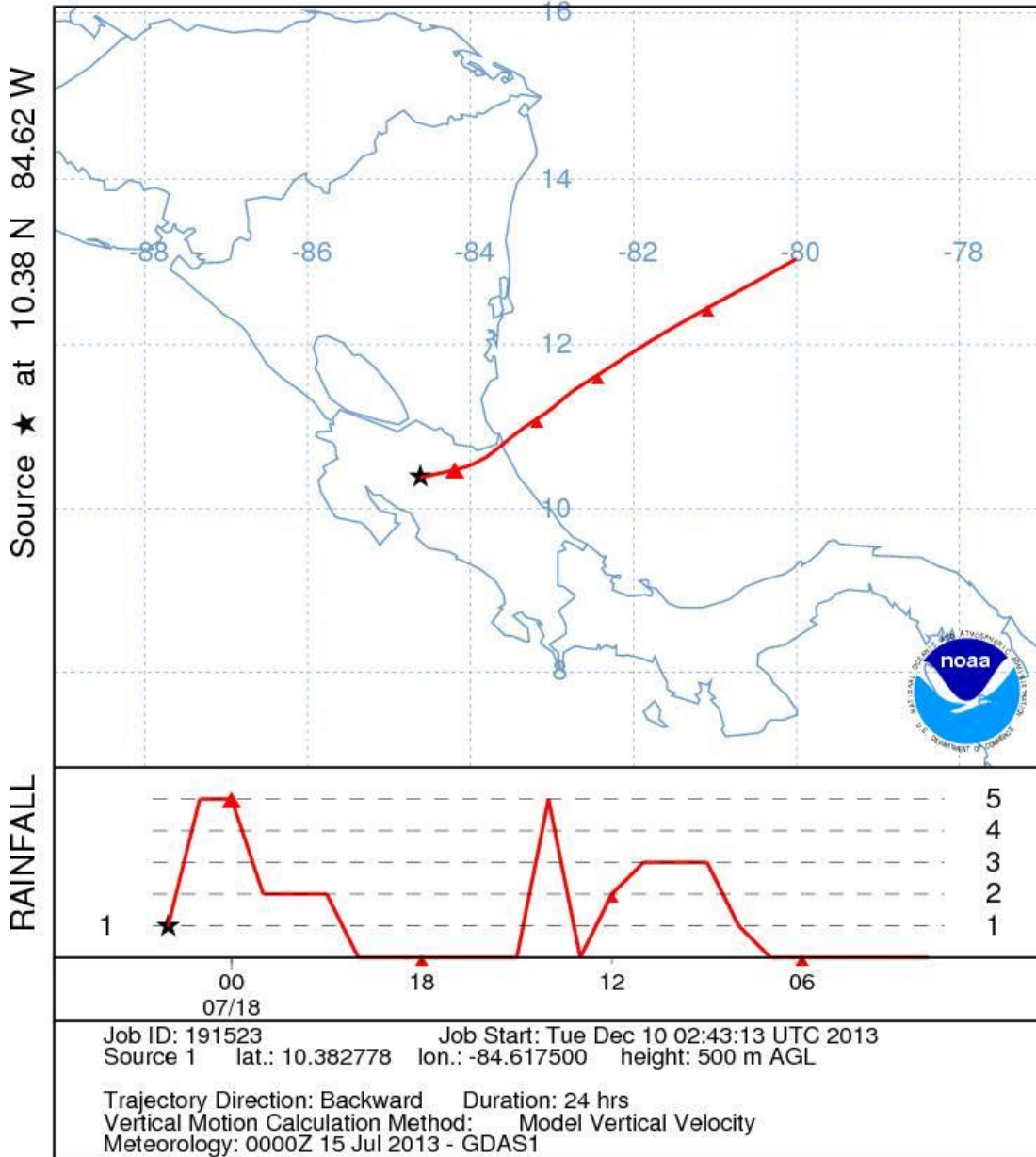
Event 2 7/8/2013

NOAA HYSPLIT MODEL  
 Backward trajectory ending at 0100 UTC 11 Jul 13  
 GDAS Meteorological Data

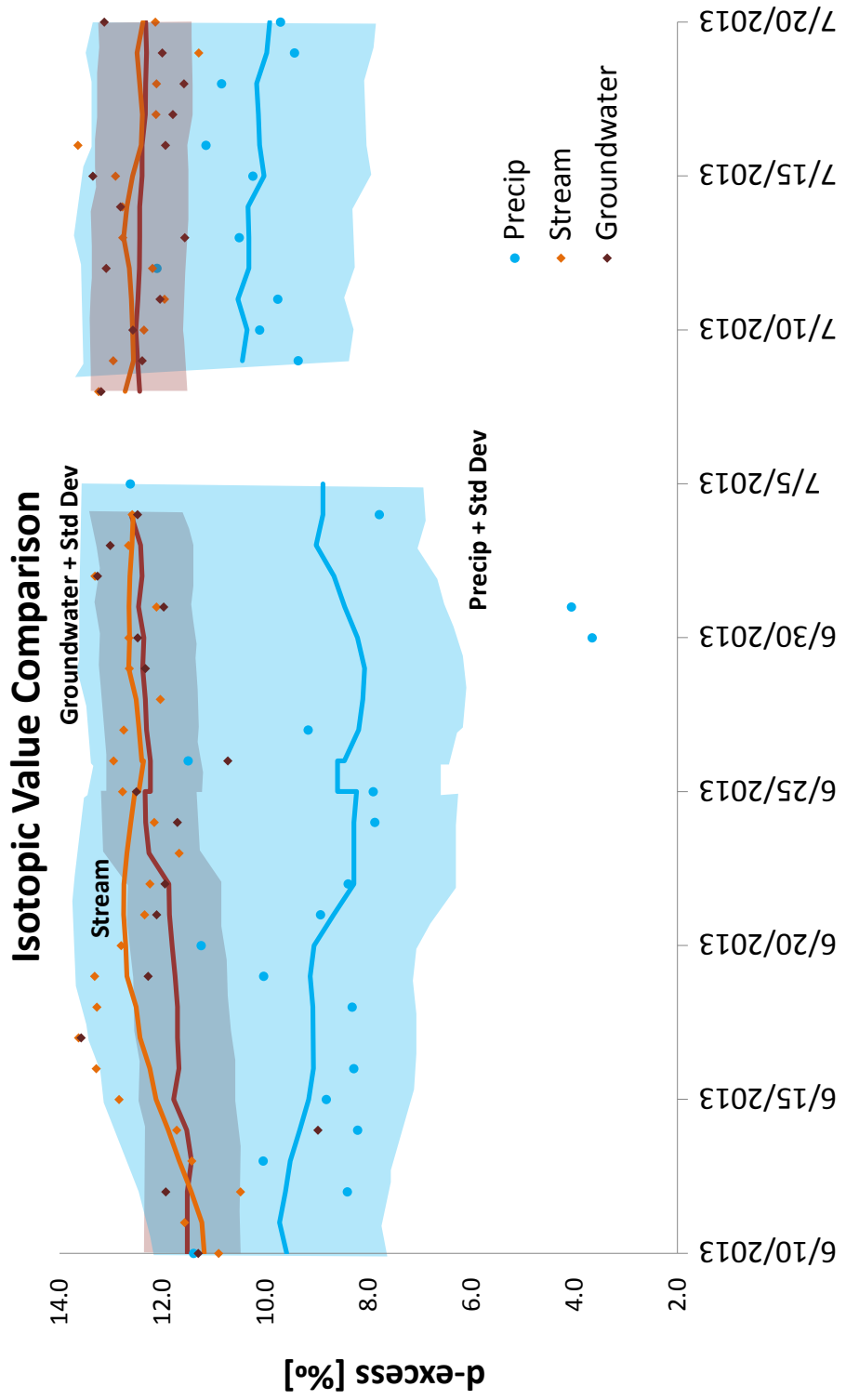


**Event 3 7/10/2013**

NOAA HYSPLIT MODEL  
 Backward trajectory ending at 0200 UTC 18 Jul 13  
 GDAS Meteorological Data



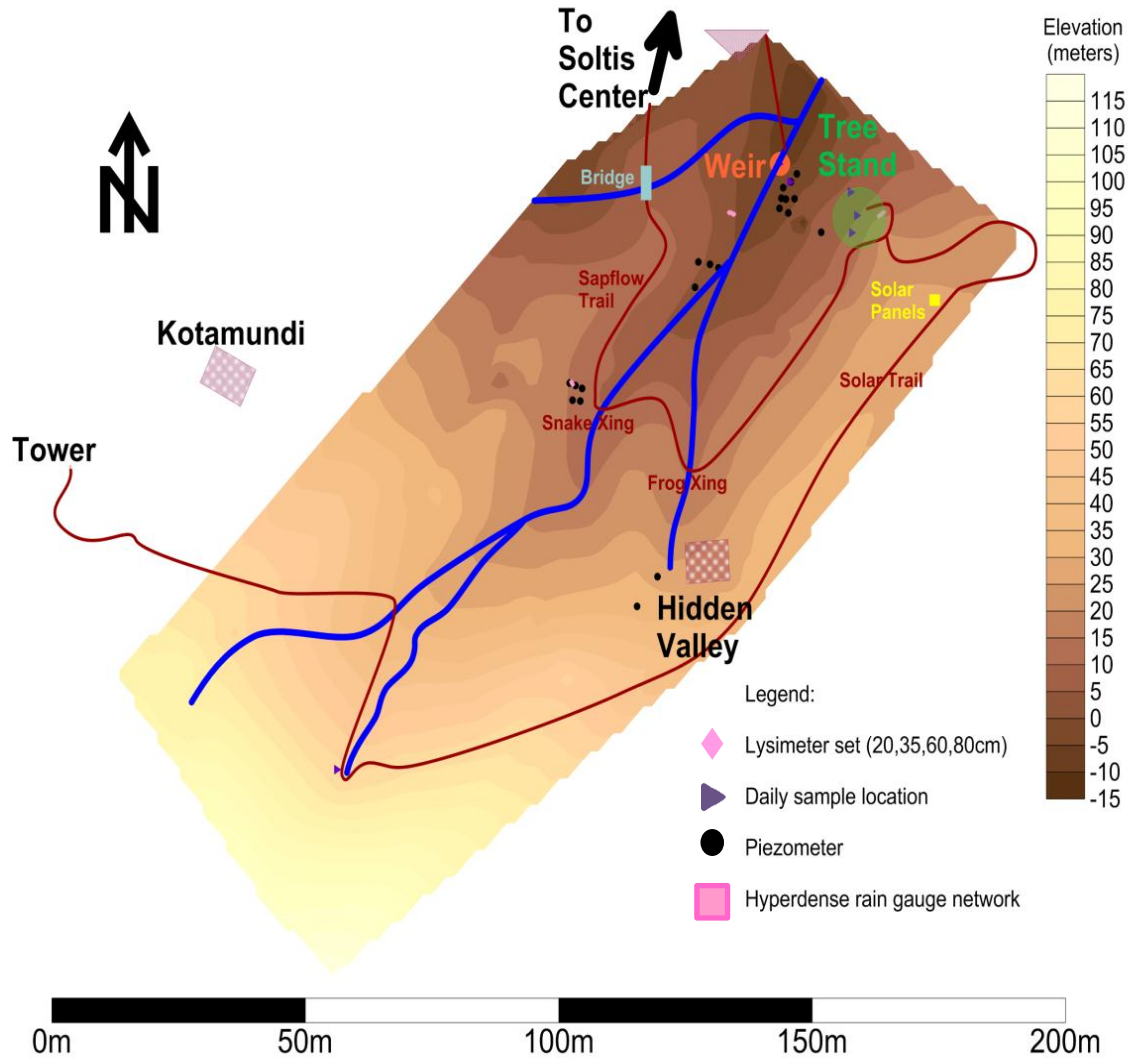
**Event 5 7/17/2013**



APPENDIX C  
PICTURE LOG



# Howler Hallows Field Map

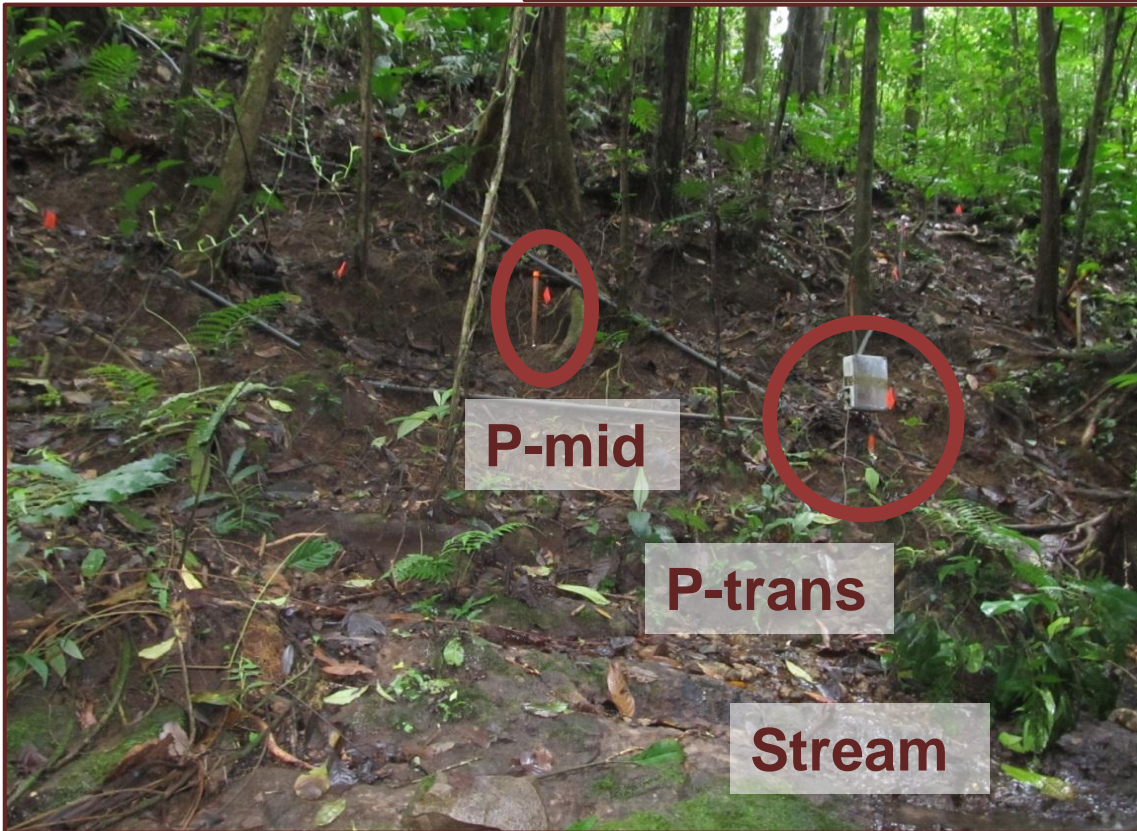


*Elevation contour map of studied watershed. Hyperdense rain gauge networks, Kotamundi and Hidden Valley, were installed by REU Students to test rain variability however they were not used in this study but are plotted for reference*

**Weir Site**

- Weir installed by students in REU 2011
- P-mid and P-trans piezometer installed by students in REU 2012
- Other piezometers installed by Leland Cohen, REU 2013

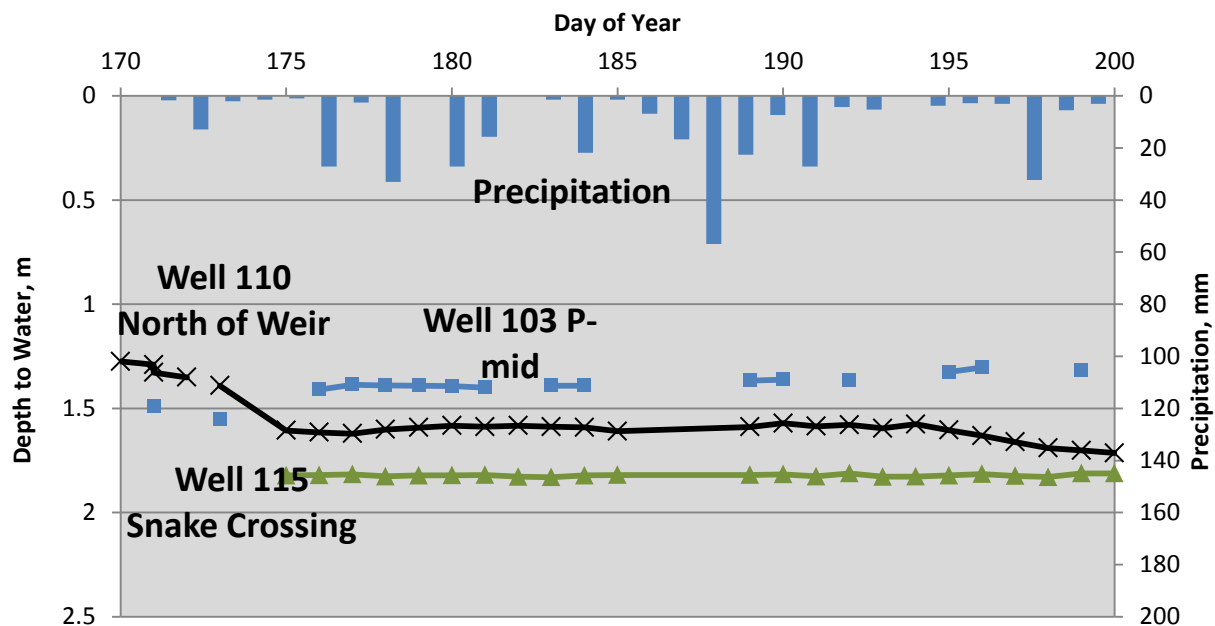
*Weir in main stream (right) and piezometers installed on the south side of the stream downhill of the tree stand (bottom)*



## ● Piezometers

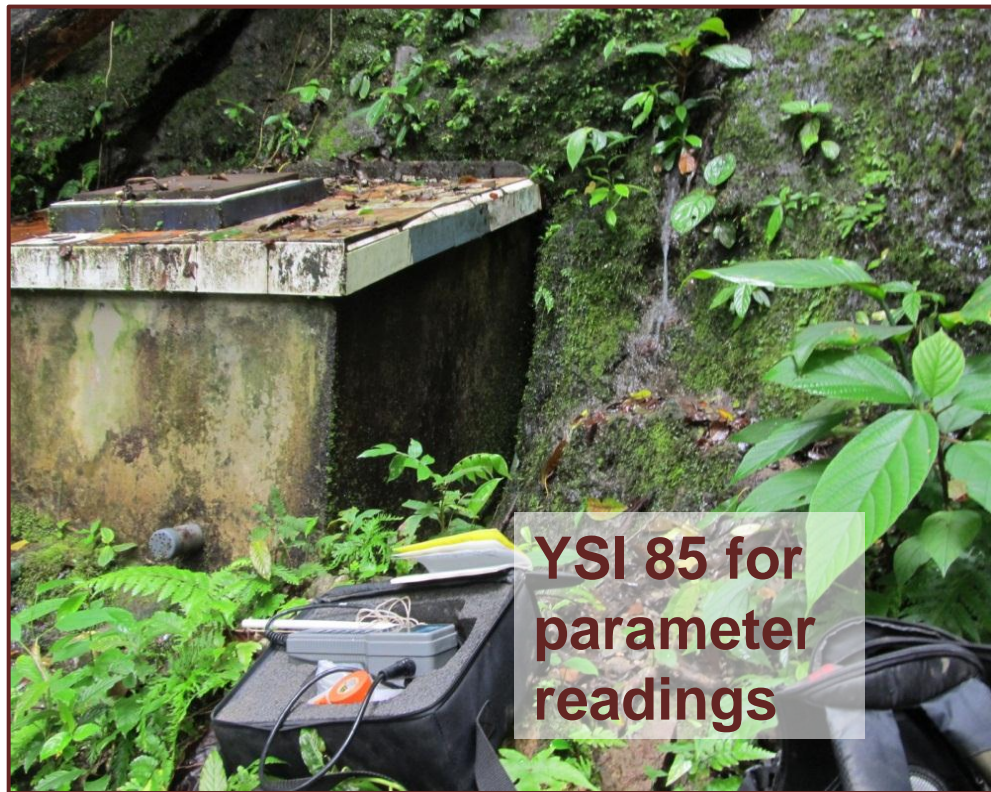
Supporting material from Leland Cohen, 2013 REU student

- *Groundwater velocity calculated at  $1.4 \times 10^{-6}$  m/s*
- *Gaining stream*
- *All wells in andisol clay with erratic saprolitic tuff*
- *Macropores due to fractures and vegetation disturbances*



► **Seeps**

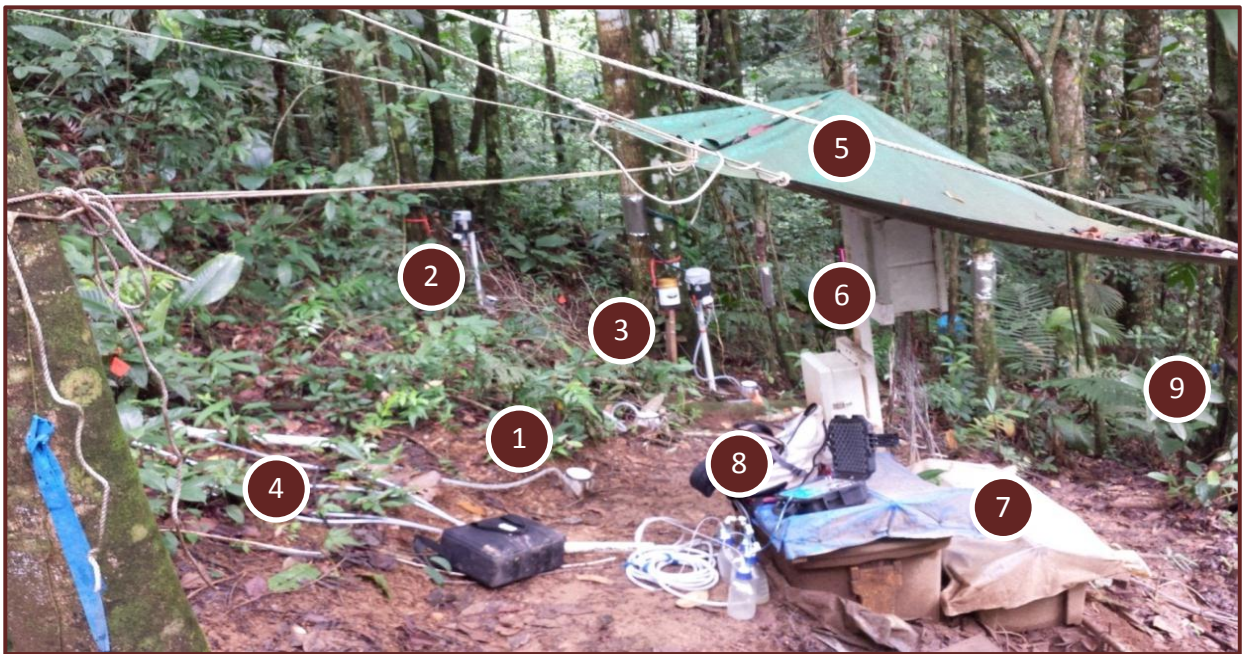
Location: near town  
cistern





## Tree Stand

Location: in stand



1. Litter water collectors ▶

2. Throughfall and stemflow-TOP ▶

3. Throughfall and stemflow-MID ▶

4. Soil water lysimeter set ◆

5. Rain cover

6. Datalogger enclosures

7. Battery Containers

8. Collection equipment

9. Throughfall and stemflow-BOT ▶

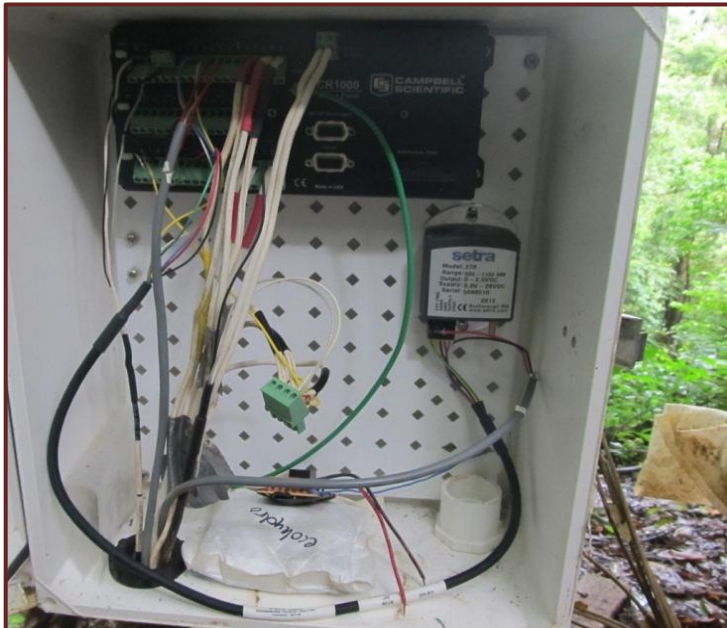


## Datalogger setup

Location: in stand

**Burgess** →

*Datalogger enclosures  
(3) and battery  
containers*

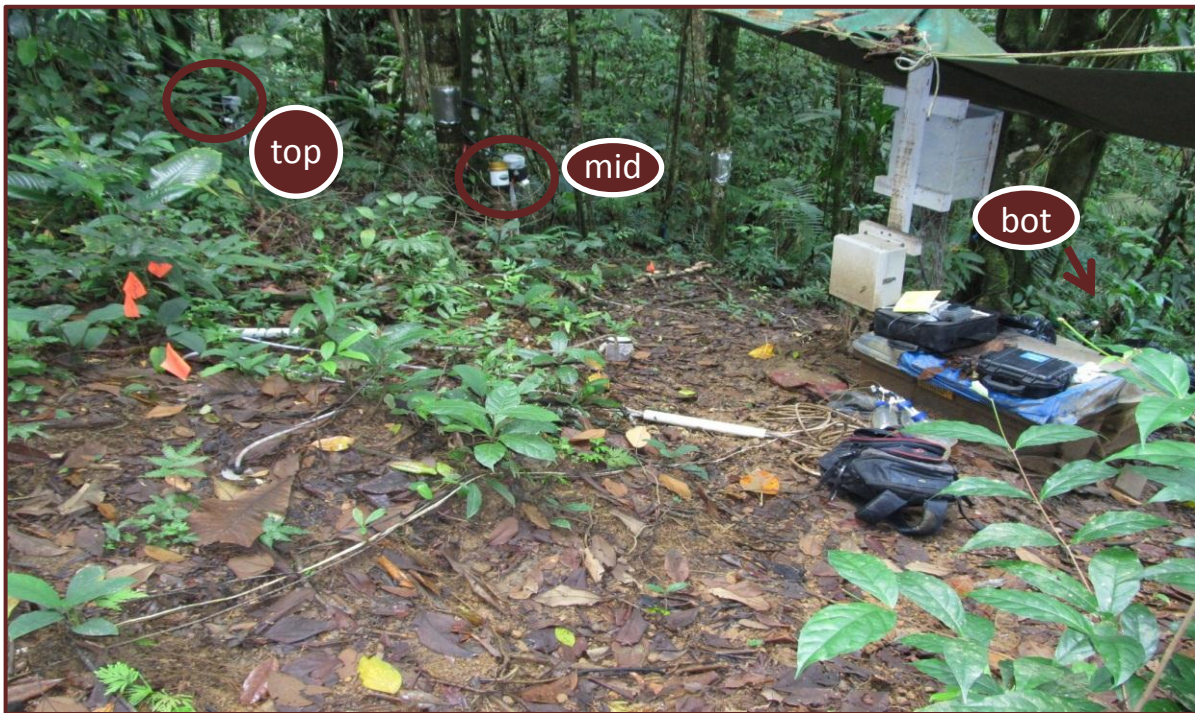


*Weir datalogger by  
Campbell Scientific*

► **Throughfall Collectors**

Location: in stand at top, mid, and bottom elevations  
Installed by students in REU 2011

*Rain gauge for 5 minute readings (right) and rain collector for samples (left)*



► **Stemflow Collectors**  
Location: in stand at top, mid, and bottom elevations next to TF gauges  
Installed by students in REU 2011  
Water flows down tube and into rain gauge, proceeds to collection container through funnels





► **Litter Collectors**

Location: in stand at datalogger location and uphill on south side of weir

*Litter layer water (runoff) flows through slots and end of PVC into tube and enclosed collector  
Shown at weir site next to p-mid piezometer*



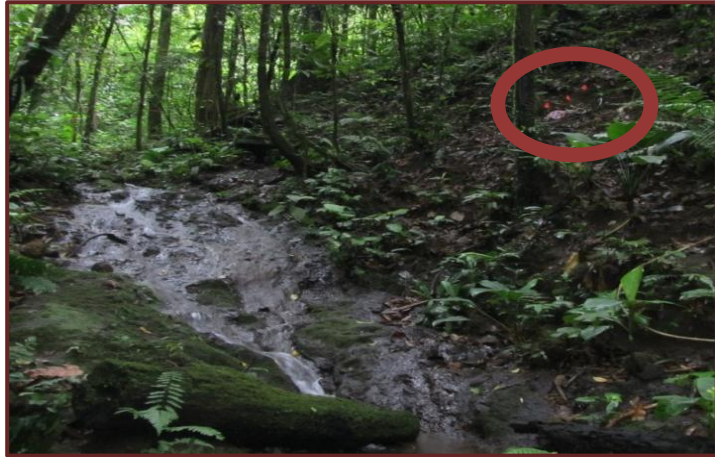
## ◆ Lysimeter Installation

Location: near stream

*Lysimeter auger*



*Installed at four depths  
20, 35, 60 and 80 cm  
corresponding to soil  
horizons; lysimeter  
tubes, bottles, and pump  
kept in black box for  
preservation from rain  
and mud*



*North side of stream*



## ◆ Lysimeter Installation

Location: in stand near litter water collector



◆ **Lysimeter Installation**

Location: near Snake Crossing next to 5 piezometer installations



## Tree 1-2

*Lacistemataceae Lozania pittieri*

Location: off sapflow path

Diameter: 4.7cm

Sapwood Area: 0.00047 m<sup>2</sup>

Water Use: 4.37 L/d



Supporting material from  
Gavin Miller, 2013 REU  
student

## Tree 2

*Asteraceae Koanophyllon hylonomum*

Location: in stand

Diameter: 6.8cm

Sapwood Area: 0.00068 m<sup>2</sup>

Water Use: 1.69 L/d

Tree tag  
Reflective covering  
over sapflow sensor



### Tree 3

*Phyllanthaceae Phyllanthus skutchii*

Location: in stand

Diameter: 4.2cm

Sapwood Area: 0.00042 m<sup>2</sup>

Water Use: 1.10 L/d



## Tree 5-1

*Pousandra trianae*

Location: off sapflow path

Diameter: 11.9 cm

Sapwood Area: 0.00119 m<sup>2</sup>

Water Use: 13.60 L/d





### Tree 8-1

*Myrtaceae Virola koschnii*

Location: off sapflow path

Diameter: 6.7 cm

Sapwood Area: 0.00067 m<sup>2</sup>

Water Use: 10.90 L/d



### Tree 10-Tower

*Meliaceae Carapa guianensis*

Location:  
branches hang  
onto tower

Water Use: 255.52  
L/d

No pictures  
available



**Tree 11-1 and 11-2**

*Rubiaceae Chomelia  
venulosa*

Location: off sapflow path  
Diameter: 6.7cm and 5.5 cm  
Sapwood Area: 0.00067 m<sup>2</sup>  
and 0.00055 m<sup>2</sup>  
Water Use: 57.84 L/d



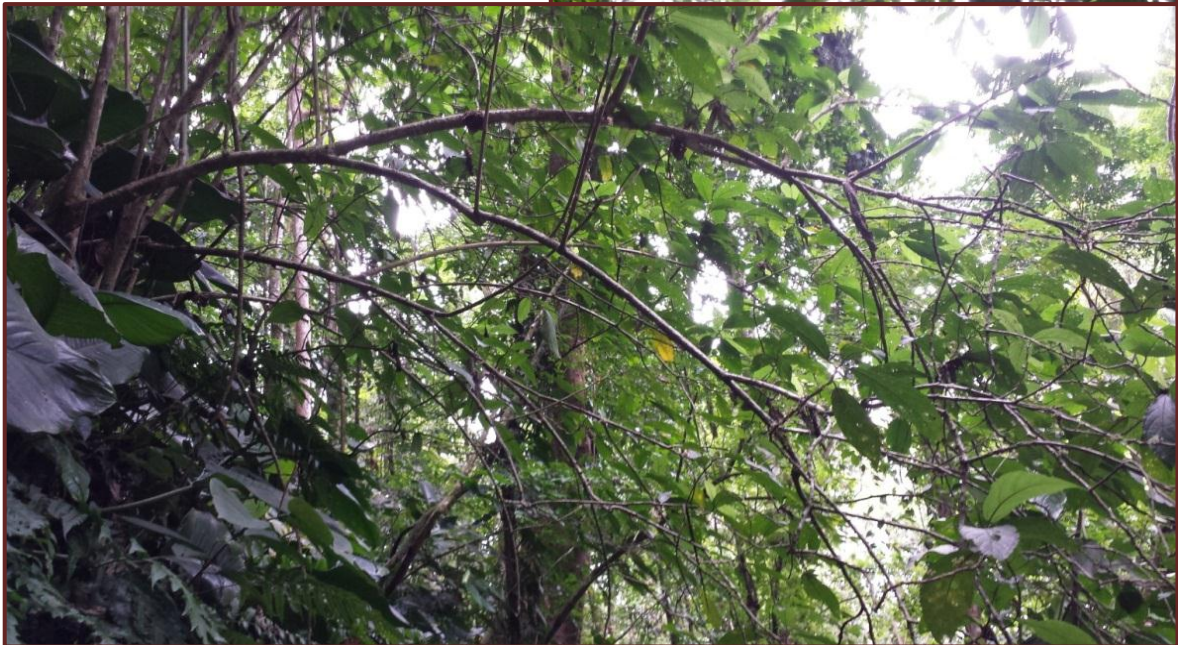
**Tree Seep-1**  
Species unknown  
Location: across trail  
from seeps



## **Tree Seep-2**

Species unknown

Location: on seep trail before  
crossing



## Data Tree

*Moraceae Ficus tonduzii*

Location: in stand, untagged



## Tree Stream South

*Meliaceae Carapa guianensis*

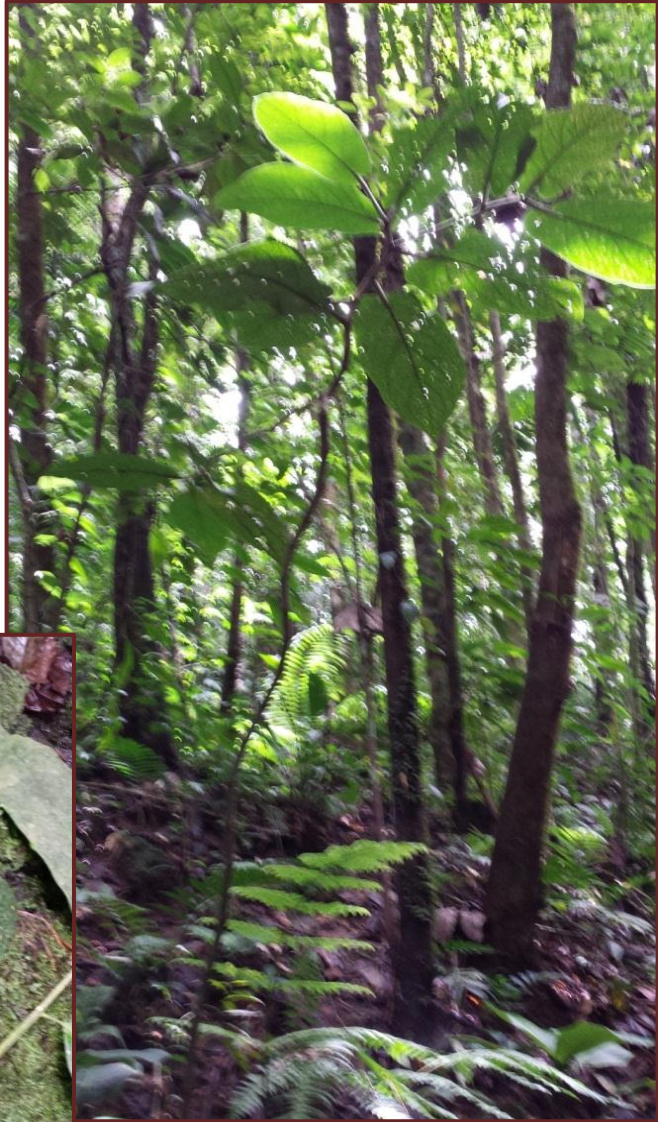
Location: south side of stream

Torn down between July and  
October



## **Tree Stream North**

Species unknown  
Location: north side of  
stream  
No woody parts left,  
stems are  
green and hollow



## Tree Stream North Downstream

Species unknown  
Location: north side of stream,  
downstream near weir





## Tree Snake

Species unknown

Location: at Snake Crossing

